Modeling and Concept Evaluation of a Hybrid Drivetrain System

BY

Aloke J Mascarenhas
B.E., Vishveshvaraya Technological University, 2007

THESIS

Submitted as partial fulfillment of the requirements
for the degree of Master of Science in Mechanical Engineering
in the Graduate College of the
University of Illinois at Chicago, 2012

Chicago, Illinois

Defence Committee :

Dr. Sabri Cetinkunt, Chair

Dr. Elisa Budyn

Dr. David He

This thesis is dedicated to my parents; the reason I am here.

ACKNOWLEDGEMENTS

I would like to take this opportunity to thank my academic advisor, Dr. Sabri Cetinkunt for giving me an opportunity to be a part of this research and for his constant support and guidance.

I would like to thank my thesis committee members Dr. Elisa Budyn and Dr. David He for their support and assistance during this thesis.

I would in particular like to express my gratitude to Aditya Bhandari for his guidance during my thesis. His technical experience and patience have been pivotal in obtaining the results of this thesis and in my understanding of MWL systems.

I would like to thank Caterpillar Inc. and all the staff I have interacted with, for their support during this thesis.

I would like to thank my colleagues Gurpreet Saini, Venkata Dandibhotla, Marilyn Worley, Keshav Sud, Omar Bennani and Mohammed Zaher, they have been patient and supportive during the writing of this thesis.

Last, I would like to thank my family, without their constant support, I would not be able to complete this research.

TABLE OF CONTENTS

LIST OF FIGURES

LIST OF FIGURES (Contd…)

LIST OF ABBREVIATIONS

CAT	Caterpillar Inc
MWL	Medium Wheel Loader
VPD	Virtual Product Development
DOE	Design of Experiments
TC	Torque Converter
R3D	Rocks3D
DOF	Degree of Freedom
UDF	User Defined Function
HE	Head End
RE	Rod End
ISG	Integrated Starter Generator
UC	Ultra capacitor
CVT	Continuously Varying Transmission
LUC	Lock Up Clutch
GDF	Generic Data file
ASCII	American Standard Code for Information Interchange
DAE	Differential Algebraic Equation
UHSF	Ultra High Speed Flywheel
SOC	State of Charge
KERS	Kinetic Energy Recovery System
LPT	Lower Powertrain
GUI	Graphical User Interface
ECM	Electronic Control Module
XMSN	Transmission
BSFC	Brake Specific Fuel Consumption

ABSTRACT

Energy efficiency and performance optimization are two important aspects in any construction and agricultural machine development. Most construction machines are designed for specific tasks and have repetitive work cycles.

Analyzing these work cycles from a component level, it is possible to identify various opportunities in a cycle to capture energy that would otherwise have been wasted. This research focuses on strategies to develop a regenerative energy capture system to harness this otherwise wasted energy.

1. INTRODUCTION

The first chapter introduces the basic concept, motivation and structure of the thesis. Here we define the scope of the research to be carried out and provide a brief insight into the wheel loader, the flow of power through the transmission and the general cycles against which it is commonly evaluated. There is also a description of the various hybrid systems that have potential to be used in such a machine.

1.1 Motivation

Earthmoving machines are versatile equipment that can perform a large number of operations on a worksite. Machines can be run continuously up to 8 hours a day with typical work cycle being 4 minutes long. As fuel efficiency is a growing concern in today's world, the focus shifts towards maximum utilization of a machine's capability by identifying opportunities in a work cycle for optimizing fuel consumption, integrated over an 8 hour shift it would result in a significant fuel savings. There would be two possible ways to proceed with the analysis:

1) optimize or improve the combustion process,
2) optimize the utilization of the available energy from the engine to improve overall fuel efficiency.

Combustion efficiency optimization is not in the scope of this discussion, we focus on using non conventional methods of energy utilization so as to maximize the overall efficiency of the machine. To do this, we have to intimately understand the work cycle, identify conditions which results in energy wastage in phases of the cycle and devise a method to capture this energy to be used later in the work cycle.

We proceed to understand some core concepts about the wheel loader that can help us analyze the losses, the work cycle and the methodology to go about improving the energy utilization.

1.2 Wheel Loader Dig Cycles

The wheel loader is a very important machine in the construction industry. The loading cycles for this machine can be divided as 'the digging cycle' and 'the load and carry cycle'. The bucket can be manipulated with the help of two hydraulic cylinders that perform the bucket lift and tilt functions.

The digging cycle shown in fig 1.1 and can be described as below:

- *Moving forward to the pile:* Lift cylinder retracted, tilt cylinder retracted, wheel loader moves in the forward direction towards the pile. The vehicle speed plays an important role here in describing the momentum of the machine.
- *Penetration in the pile:* In this phase, the machine pushes deeper into the pile. This is done by the operator shifting to a lower gear and increasing the tilt lever command such that there is an optimum bucket angle for smooth material flow into the bucket
- *Initial lift:* Lift lever command goes from 0 to 50%. Pressure builds up in lift cylinder head end.
- *Rack and lift:* Tilt lever at 100% while maintaining the lift lever command at 50-100%
- *Exit from the pile:* Lift lever at 100%, reverse direction from the pile.

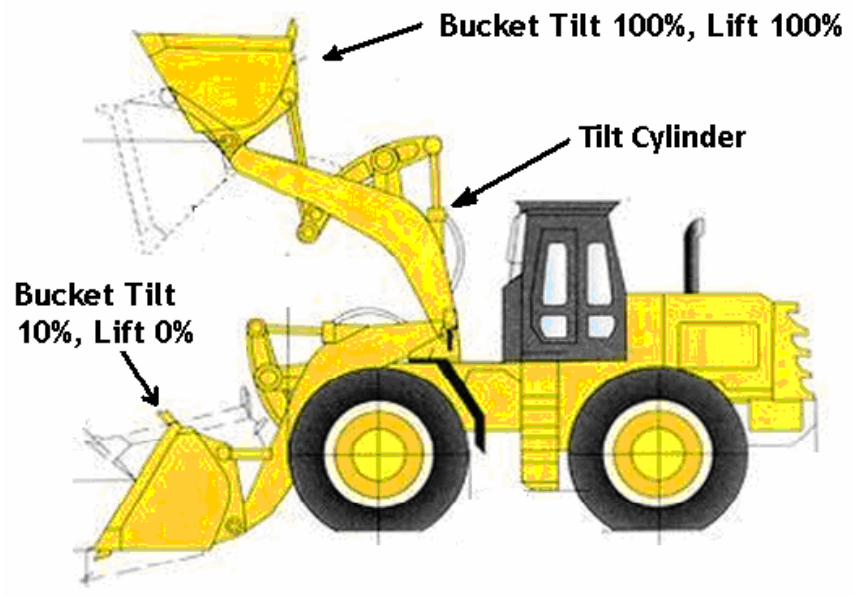

Fig 1.1 Basic wheel loader with linkage configuration positions. [8]

The load and carry cycle can be described with respect to figure 1.2:

- *Bucket filling :* the wheel loader enters the bank at (1) and starts the bucket filling
- *Leaving bank :* then reversing towards (2)
- *Retardation*
- *Towards load receiver:* changing the direction at (2) and starts to accelerate again towards (3).
- *Bucket emptying:* At (3) the wheel loader will empty the bucket to the receiver.
- *Leaving load receiver, retardation and reversing:* After the load is dumped the wheel loader will reverse towards (2) again.
- *Towards bank and Retardation at bank:* At (2) the wheel loader will change direction and move forward towards (1) again.

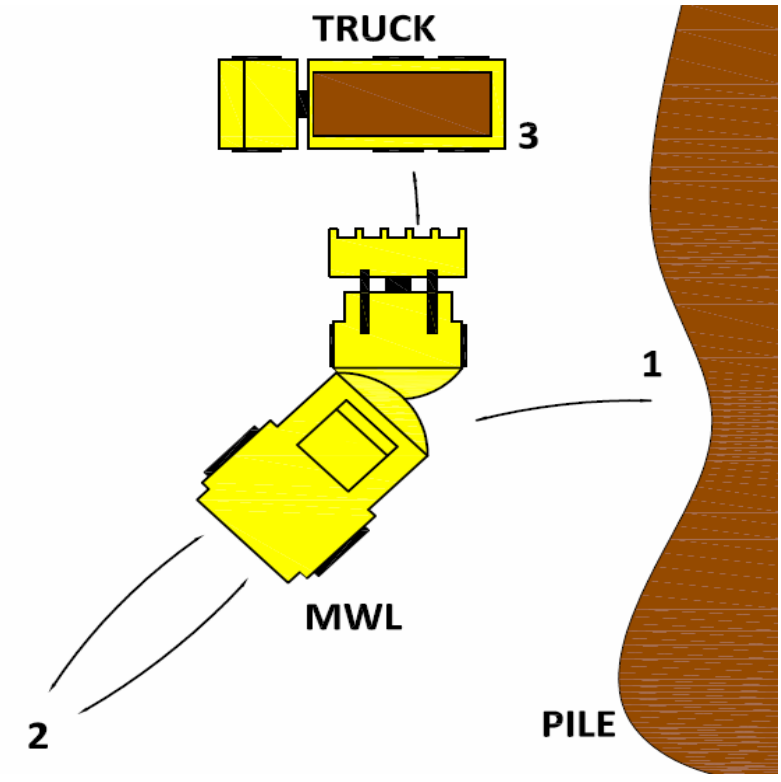

Fig 1.2 Load and carry cycle

1.3 Power Flow for the Wheel Loader

The aim of this research is to capture unutilized energy in the system. This can only be accomplished by analyzing the flow of power through the system. The schematic 1.3 clearly illustrates the same.

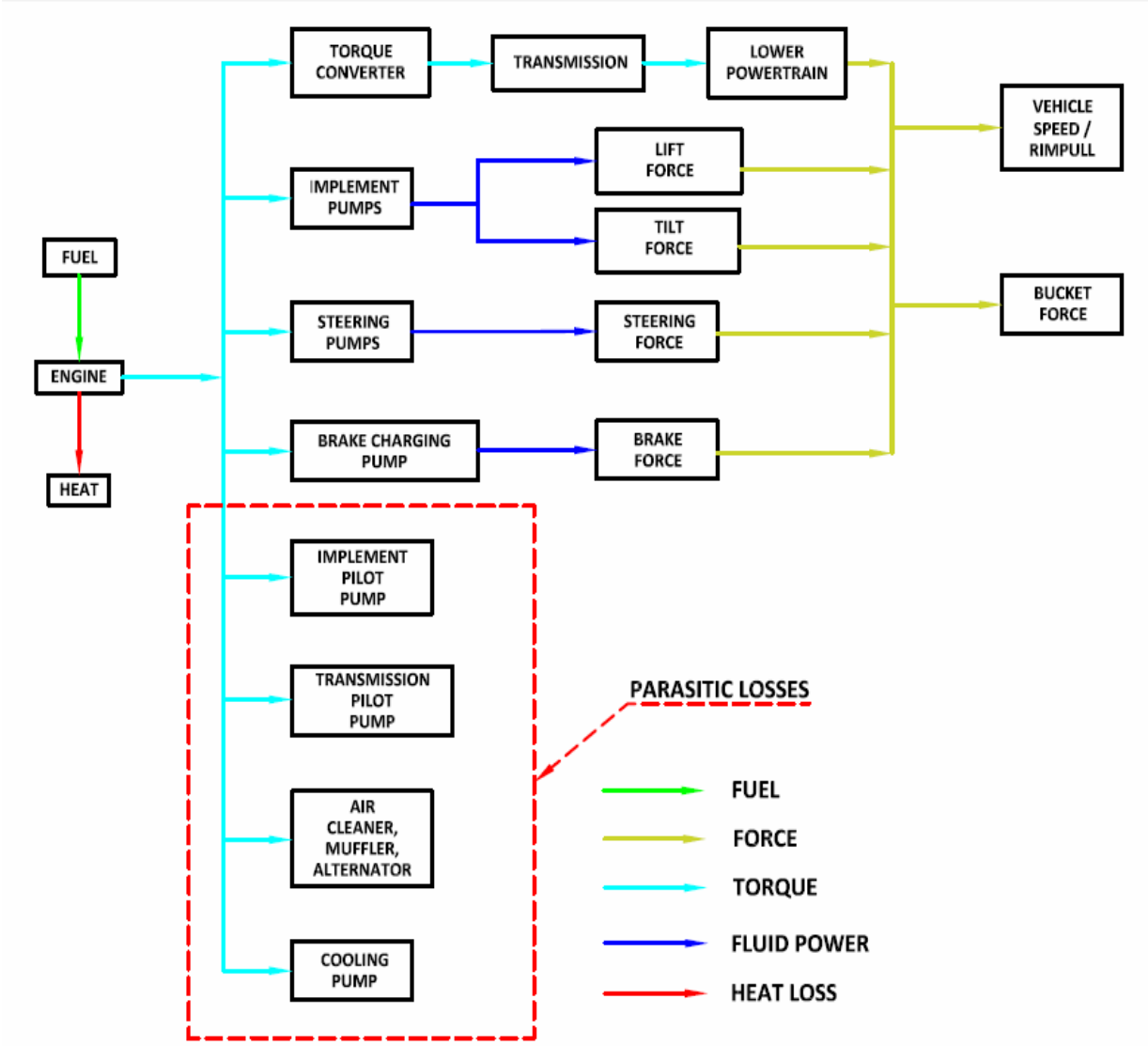

Fig 1.3 Energy / Power flow in a Wheel Loader system [7]

Fuel into the engine block is the key component for power generation. This is converted into rotational power at the output of the drive shaft and heat. This useful energy, by means of a torque converter, hydraulic circuit and brake pumps are converted into rimpull, bucket tilt and rack, steering force and braking force.

1.4 Hybrid System

Hybrid systems can be defined as those which have more than one flow path for energy. In general, hybrid systems have two states, where the hybrid system or alternative flow path is active and when it is not. These states are governed by a control logic that analyses discrete variables in the cycle and ensures the correct transition between normal and hybrid operation of the system.

It is important to understand when there is an opportunity to capture energy in a normal work cycle. Fig 1.4 illustrates how one can judge (by rule of thumb) if a system can produce regenerative energy by analyzing the state of speed or torque of the system (rotary system).

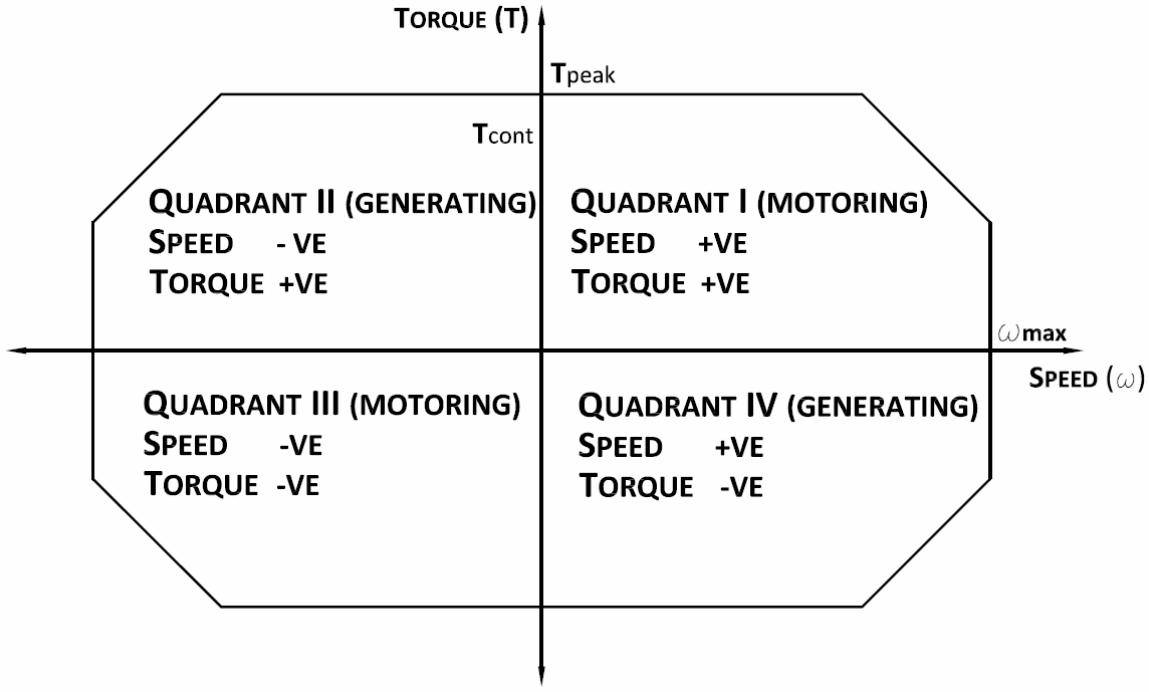

Fig 1.4 Map to analyze regenerative energy capture possibilities in a mechanical moving system [1]

This epitomizes the basic principle of the hybrid drivetrain, which aims to utilize the energy at the driveshaft at negative speed or negative torque and converts it into stored energy by means of mechanical or electrical gains. Hybrid systems are classified on the basis of configuration of the auxiliary system with respect to the main drive of the vehicle. There are two basic configurations as shown by Fig 1.5.1 and 1.5.2

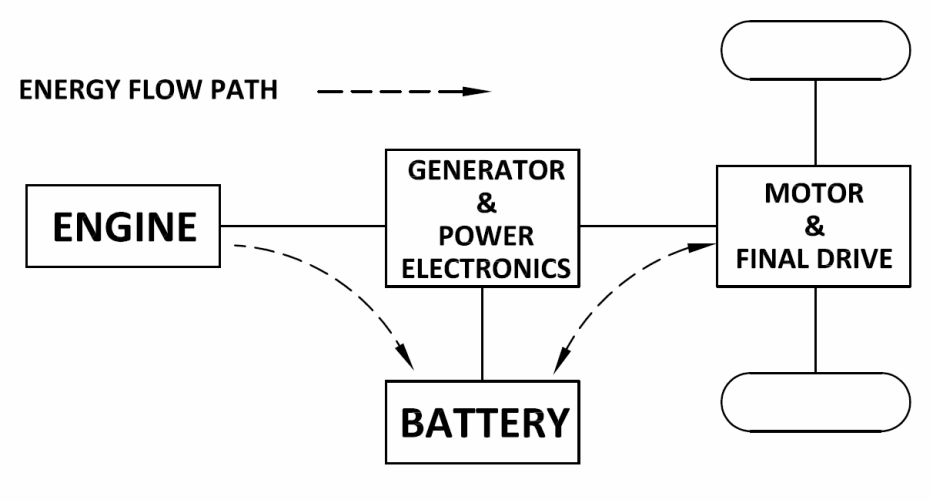

Fig 1.5.1 Series hybrid system [3]

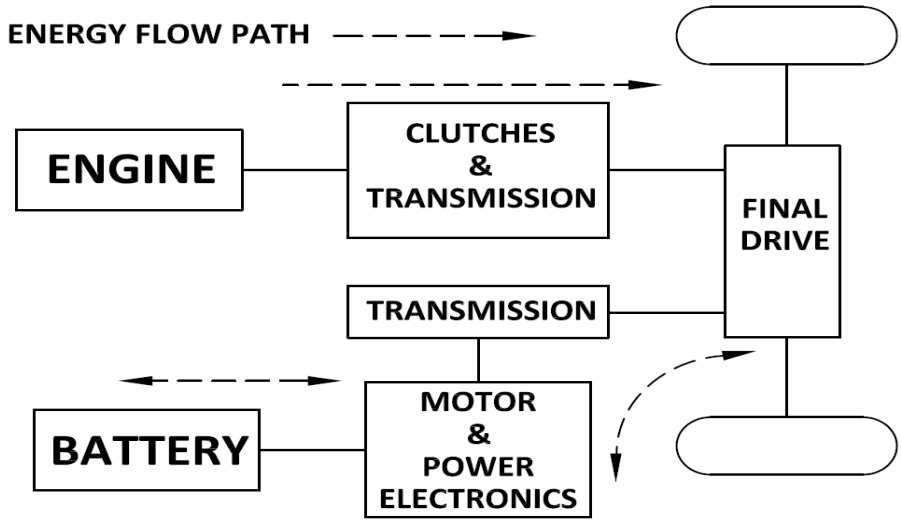

Fig 1.5.2 Parallel hybrid system [3]

In this review we analyze a series hybrid system and try to understand what the savings are available using a load and carry work cycle such that all possible inertial energy can be utilized during braking. The main sources of energy conversion and storage that exist are as below:

i. Integrated Starter Generator

ii. Ultra Capacitor Storage

iii. Battery Storage

iv. Ultra High Speed Flywheel

However in the scope of this thesis we will only discuss the flywheel and battery storage systems.

1.5 Thesis Outline

In this analysis we study the CAT 966D wheel loader. We can however generalize this analysis to other machines that have similar potential to use regenerative braking to assist the capture of otherwise spent energy and similar cycles of operation. The brief descriptions of the chapters to follow are as below:

Chapter 2

Chapter 2 goes into a description of the various systems in the wheel loader and breaks down the torque distribution from the engine to the implements. It concentrates on the formulation of the basic mathematical equations and allows for the understanding of the various subsystems in the vehicle.

Chapter 3

Chapter 3 gives a brief discussion and an overview on the software used to model and test this concept on the wheel loader. This chapter aims to give a better understanding on how various systems are modeled and how the governing equations are taken into account to achieve an accurate simulation of the wheel loader in the load and carry cycle. Dynasty is propriety software of Caterpillar Inc.

Chapter 4

Chapter 4 discusses about the hybrid systems that are studied in this thesis, the mathematical formulation of the torque generated, sizing guidelines, the design procedure that can be followed in sizing the storages and the methods of interfacing it with the existing drivetrain on the system. It also outlines various control strategies that can be leveraged for this concept

Chapter 5

Chapter 5 discusses the underlying control strategy that will govern the capture and release of energy into the storage devices. It discusses how the controller will oversee the energy capacity, the algorithms that will be used and important concepts that govern the threshold for charge and discharge in storage devices.

Chapter 6

Chapter 6 describes the operator model used to simulate the standard work cycle and mimic real world operator actions for given cycles. The modification of this work cycle is out of the scope of this thesis however it is important that the reader has a brief overview to understand the basic event based logic modeled in the controls.

Chapter 7

Chapter 7 discusses the modeling of the hybrid systems and their integration into the wheel loader. It also discusses the problems faced in modeling and how these were overcome to get the required results. It discusses the results of the energy utilization, efficiency and fuel consumption with and without the hybrid systems on the machine so as to provide a level ground for analysis of the overall improvement of machine characteristics.

Chapter 8

Chapter 8 discusses the conclusions of this thesis, the difficulties faced and suggestions that could improve the fidelity of the model but require in depth analysis of the cycle, a design of experiments and more time than that available for this study.

1.6 Literature Review

This research can be divided into three distinct parts. The first part comprises of the basic machine description, power flow analysis and overall concepts of the system. This material has been adapted from training material from courses taught at Caterpillar and rough outline has been adapted from [7], the introduction to regenerative braking was obtained from [1], the introduction to the hydraulic system and functioning of the torque converter was obtained from [2].

Second section is the hybrid system, the analysis of the existing systems and how the underlying concepts can be harnessed in the analysis and modeling of the KERS system. [3], [5] and [6] have been good resources in this regard and provide a good overview of these systems.

The third section is the virtual modeling section and the setting up of the algorithms for the controls logic. The VPD basic training modules available as a part of Caterpillar's internal documentation system were a major help in this concept evaluation and modeling of the system. Reference [4] has been a very important reference source in this regard.

2. MACHINE DESCRIPTION

We can, on analysis of the machine, breakdown the power flow from the engine to three main areas.

1. Implement system,
2. Powertrain system,
3. Steering circuit.

The implement system consists of the tilt and lift cylinders and auxiliary functions. This powers the linkage motion as per commands from the operator. The powertrain system is used to power the linear motion of the machine and the momentum generated plays an important role in the digging work cycle. The steering circuit is important in changing the direction of the machine but it is used for about 10% or less in a regular work cycle. Figure 2.1 shows the different power paths of the system.

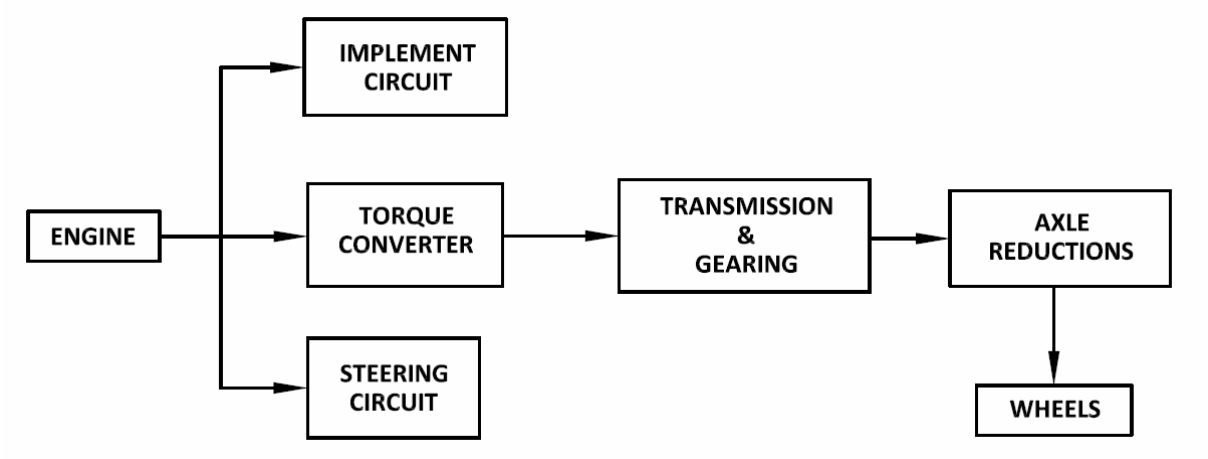

Fig 2.1 Main components of a wheel loader

These components are described individually in the following chapter. Due to the nature of our analysis being on a system level, not too much detail has been provided. However an effort has been made to convey the basic idea and functioning of the machine so as to allow for a better understanding of analysis to follow. Fig 2.2 gives us a basic idea of how the torque absorption takes place in the system from engine down to the lower powertrain.

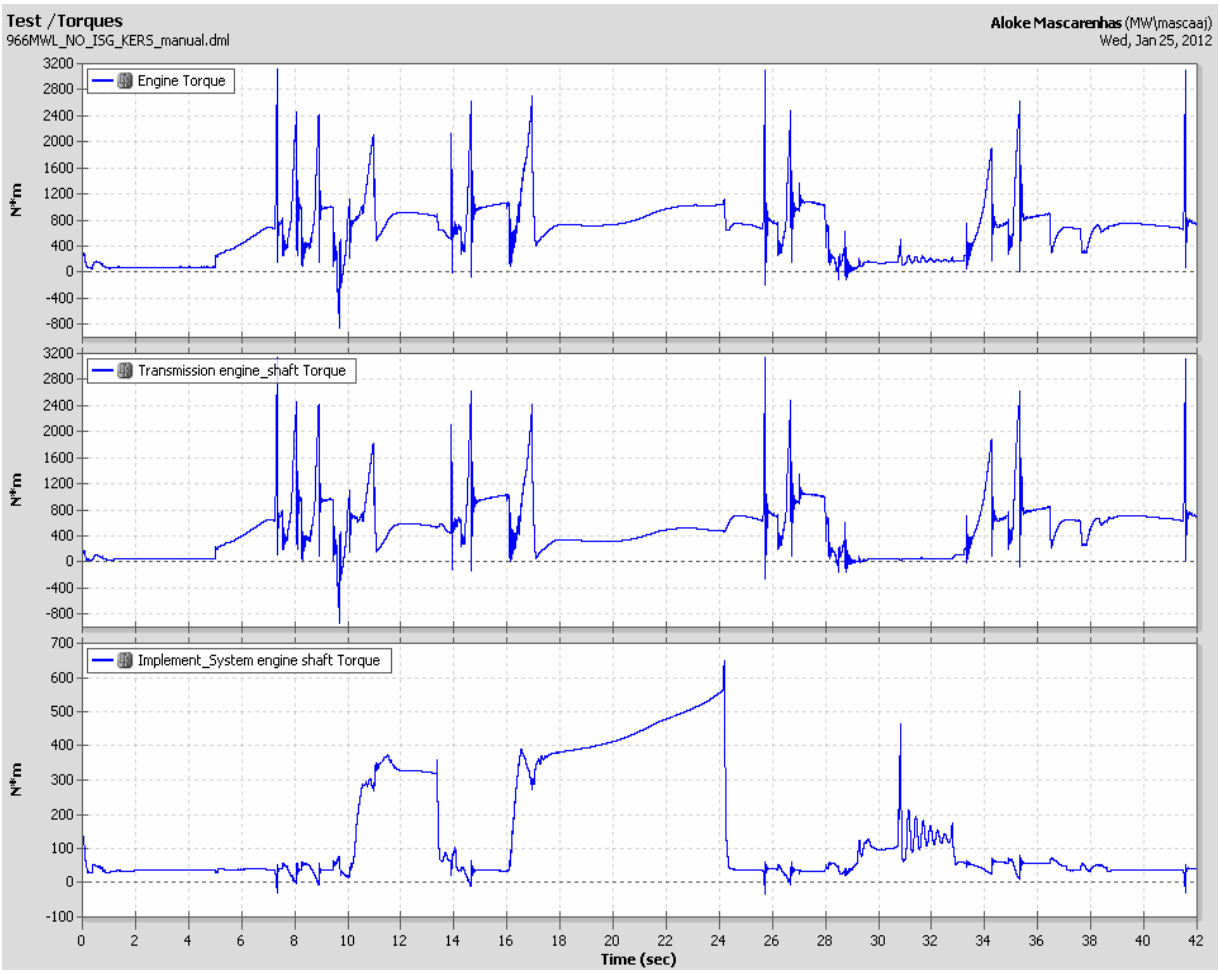

Fig 2.2 Plot of torque output at engine output, torque converter and lower powertrain.

2.1 Engine

The engine is the prime mover responsible for the generation of energy for the operation of the machine. Engines are classified based on the power, capacity, load response time and torque at rated engine speeds. This implies the power and torque available at the driveshaft before the parasitic losses like alternator, fan losses, turbocharger inertias etc. The first strip in Fig. 2.2 is the torque available at the output of the driveshaft through the cycle.

Any engine can also be described by a lug curve. A lug curve can be best described as the torque output of an engine for a speed sweep over its given operating range. It is a slow test and can be called a steady state test. In order to standardize the configurations, most engine tests occur at full

throttle and the output lug curve thus signifies the maximum torque available at the engine at any particular speed. A lug curve can be best described by the Fig 2.3

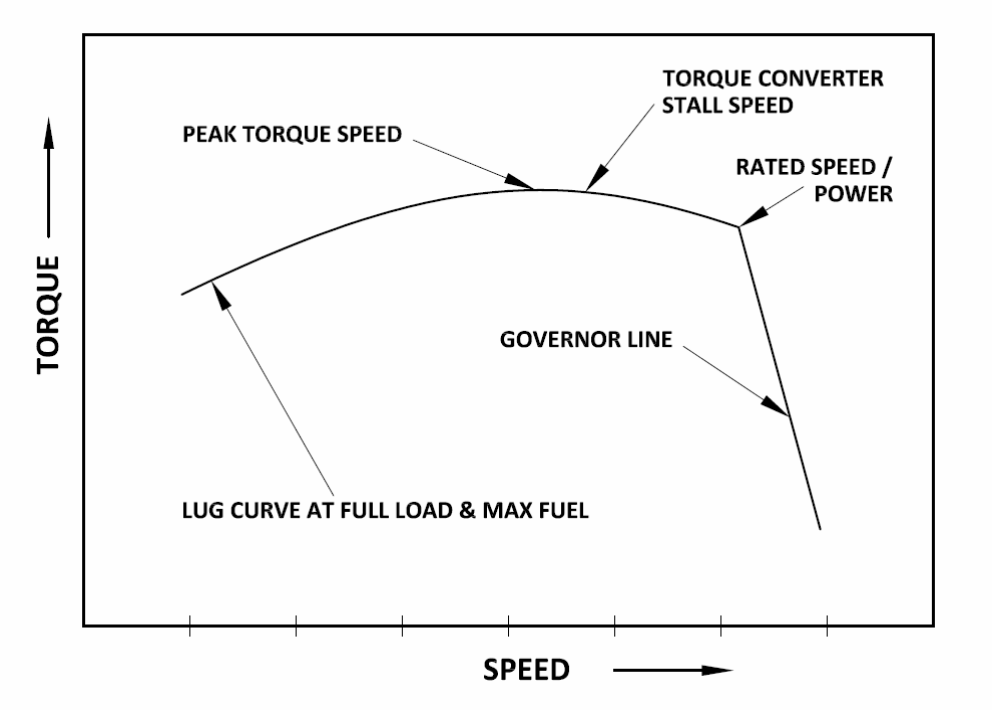

Fig 2.3 Lug curve [2]

In order to get a complete picture of how the various losses affect engine performance we define a few parameters:

- Gross lug curve represents the max torque out of the Engine (indicated by blue line in fig 2.4)
- Net lug curve represents the actual energy available at the powertrain after parasitic losses (Fig 1.3) are taken into account (indicated by red line in Fig 2.4)
- Engine speed
- Brake specific fuel consumption (BSFC) represents the fuel consumed per unit power produced at the drive shaft
- Engine efficiency represents the ratio between the energy produced at the output of the driveshaft to the maximum energy that can be produced with the fuel used for that cycle.

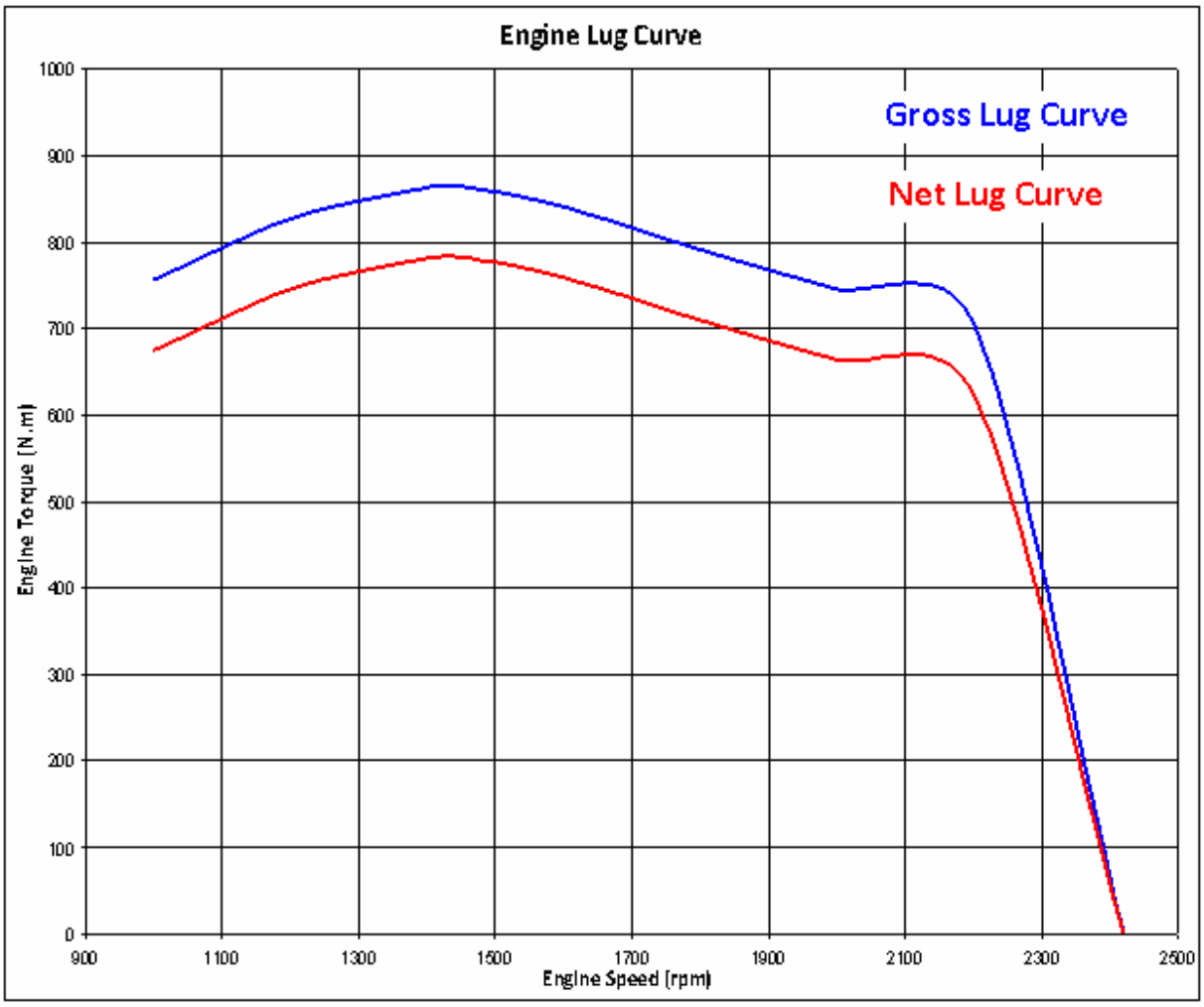

Fig 2.4 Typical Wheel Loader lug curve

2.2 Powertrain

The powertrain subsystem is responsible for the motion of the machine. It is composed of:

- Torque converter;
- Transmission and gearing;
- Axle reductions;
- Wheels.

It acts as a medium through which the engine transmits torque to the wheels and allows for the machine to gather enough of momentum to move through the cycle. Due to the gearing, speed reduction and torque multiplication is seen through the drive system ending with the high torque generated at the tire at low speed.

2.2.1 Torque Converter

Torque converter is a fluid coupling that is used to transfer rotating power from an engine to a rotating driven load. Like a basic fluid coupling, the torque converter normally takes the place of a mechanical clutch, allowing the load to be separated from the power source. However, a torque converter is able to multiply torque when there is a substantial difference between input and output rotational speed, thus providing the equivalent of a reduction gear. There are four main components inside the housing of the torque converter:

- Pump
- Turbine
- Stator
- Transmission fluid

The housing of the torque converter is bolted to the flywheel of the engine (in a conventional setup), which allows for it to rotate at the same speed as that of the engine output shaft. The fins that make up the pump of the torque converter are attached to the housing, so they also turn at the same speed as the input shaft. Fig 2.5 shows the construction / assembly of a torque converter.

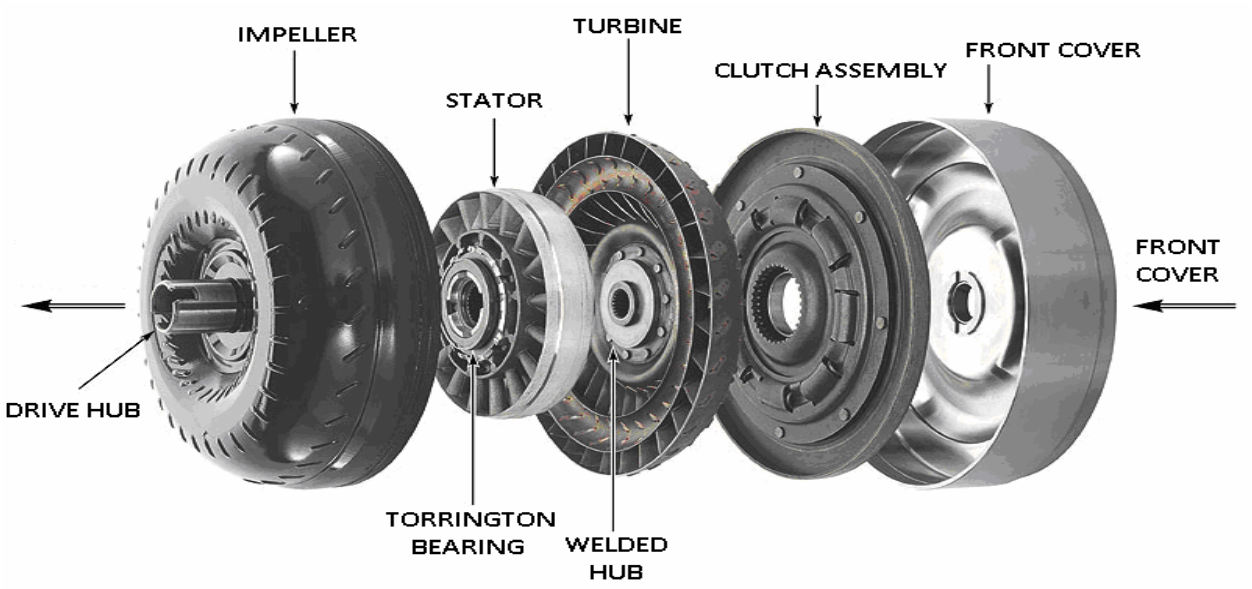

Fig 2.5 Torque converter construction [9]

A torque converter has three stages of operation:

- **Stall**: The prime mover is applying power to the impeller but the turbine cannot rotate. The stall phase actually lasts for a brief period when the load initially starts to move, as there will be a very large difference between pump and turbine speed.
- **Acceleration**: The load is accelerating but there still is a relatively large difference between impeller and turbine speed. Under this condition, the converter will produce torque multiplication that depends upon the actual difference between pump and turbine speed.
- **Coupling**: The turbine has reached approximately 90 percent of the speed of the impeller. Torque multiplication has essentially ceased and the torque converter is behaving in a manner similar to a simple fluid coupling. In modern automotive applications, it is usually at this stage of operation where the lock-up clutch is applied, a procedure that tends to improve fuel efficiency.

The efficiency of the torque converter is related by two main parameters:

- Speed Ratio (S_r): The ratio between output speed and input speed.
- Torque Ratio (T_r): The ratio between the output torque and input torque.

As mentioned earlier, when the speed of the input and output shafts are almost similar, the lock-up clutch is actuated which is effectively a bypass system. This allows the coupling to take place as a rigid member such that T_r, and $S_r = 1$, therefore also $\eta \approx 1$ (accounting for clutch losses).

2.2.2 Transmission and Gearing

The engagement of the torque converter leads to torque being transmitted to the transmission before it is converted into useful force by the machine. The operator manually controls the gear ratios based on the torque and rimpull required by the work cycle. The applied gear ratio then modifies the input speed and torque before it transfers it to the lower powertrain. This is implemented by discontinuous clutches used in conjunction with planetary gearing to meet the high values of torque for the cycle. Therefore for a range of gear ratios, a typical gearbox is constituted by several sets of internal planetary gears, like the one shown in Fig. 2.7.

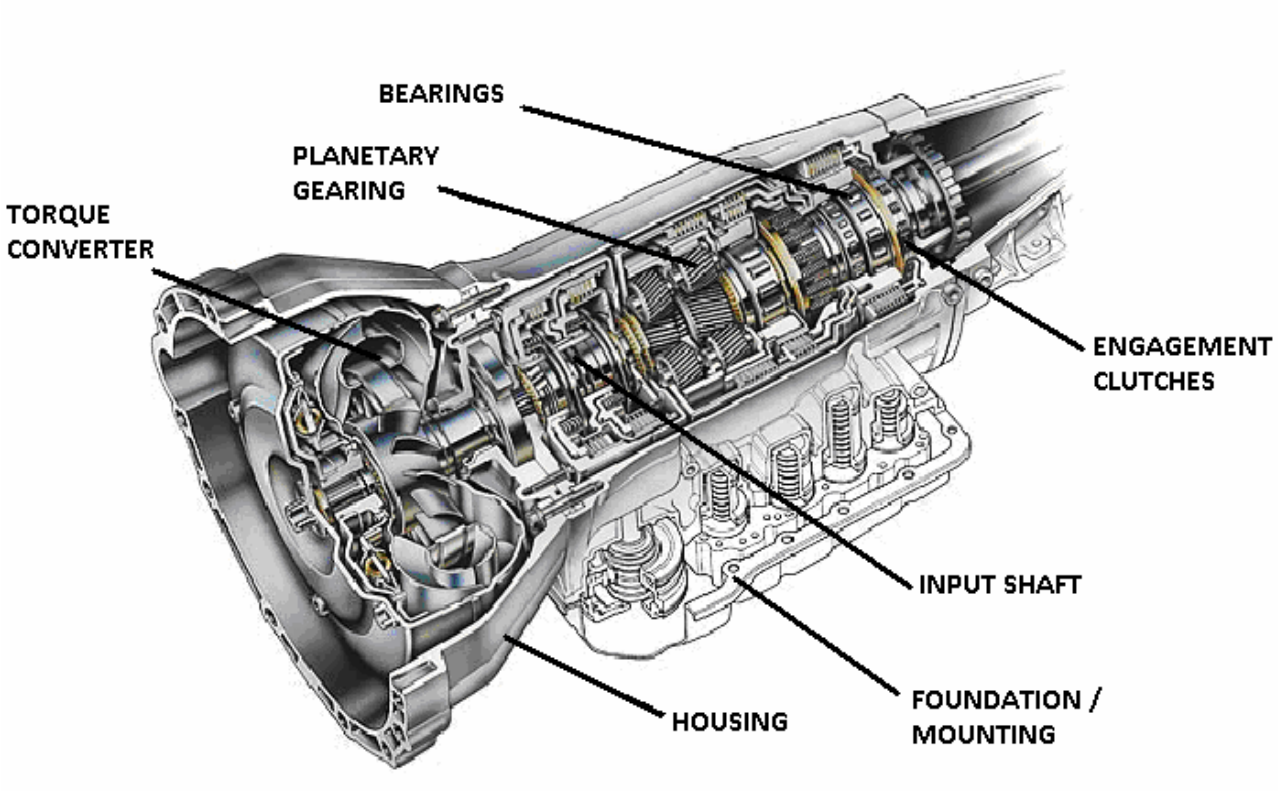

Fig 2.6 Gearbox housing [11]

This kind of planetary gearing or epicyclic gearing offers great flexibility and a range of gear ratio based on the configurations in which it is loaded and utilized.

The basic components of the epicyclical gear are:

- *Sun*: The central gear
- *Planet carrier*: Holds one or more peripheral planet gears, all of the same size, meshed with the sun gear
- *Ring Gear*: An outer ring with inward-facing teeth that mesh with the planet gear or gears
- *Planetary gear* or *idler gear*

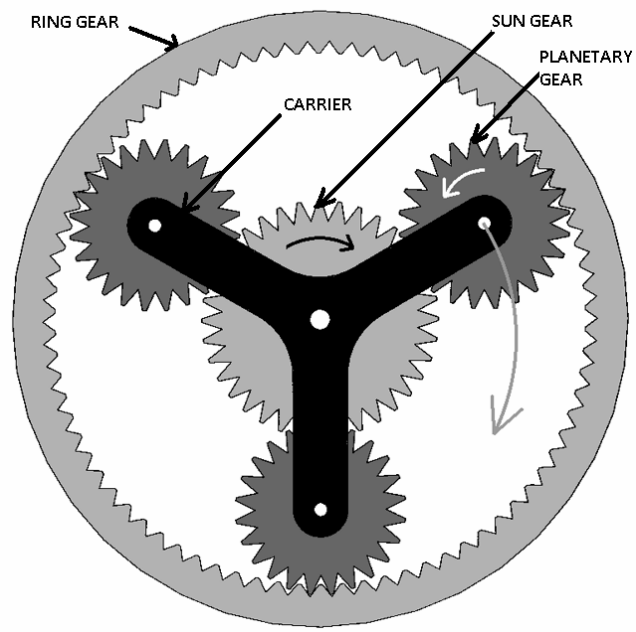

Fig 2.7 Planetary gearing system [12]

We can understand a few of these configurations by setting one gear as an input, one as an output and one stationary. The configurations produce different speed and torque ratios that can be utilized at different points in the machine operation.

Based on the construction, we can define three modes of operation for planetary systems in general based on which gear is the input and which one is the output:

Case A: The planetary carrier is stationary, sun gear is the input, planetary gears are idling, ring gear is the output. The direction of the output is opposite to the input. The torque multiplication and the speed reduction can be obtained from the individual ratios.

Number of Sun gear teeth: N_s

Number of planetary gear teeth: N_p

First mesh sun: Planetary gear ratio: N_s/N_p

Number of ring gear teeth: N_a

Second mesh planetary: Ring gear ratio: N_p/N_a

The final gear ratio can thus be given by: N_s / N_a

Case B: The ring gear is stationary, the planetary gear carrier is the input and the sun gear is the output. The direction of the output is the same direction as the input. The final gear ratio is $1+N_a/N_s$.

Case C: The ring gear is stationary, the sun gear is the Input and the planetary carrier is the output. The direction of the output will be in the direction of the input. The gear ratio in this case will be $1/(1+N_a/N_s)$. This configuration is the lowest possible speed reduction available for this planetary gear setup.

By monitoring the input torque values to the transmission from the torque converter and the requested torque by the lower powertrain based on a torque requirement calculator, we can vary the configuration using a series of clutches and planetary gearing mapped at specific shift points to obtain the optimum speed and torque at output of the transmission.

2.2.3 Axle Reductions

The torque from the gearbox has to be divided and sent to the tires. The output from the gearbox is transferred to the differential by means of the rear and front axles. The differential then divides the torque and sends it to the left and right tires. The differential is composed of bevel gears and is just a means of changing the direction of the torque and splitting it, no torque multiplication takes place here. It allows for the same quantity of torque to be provided to each of the wheels while allowing for a different angular speed. The tires are sized based on the payload requirements, the type of work site and application such that the machine has maximum rimpull capability. Mathematically

$$T_{o,gearbox} = T_{i,Front\text{-}diff} + T_{i,Rear\text{-}diff}$$

$$T_{i,Front\text{-}diff} \neq T_{i,Rear\text{-}diff} \tag{2.1}$$

$$T_{o,Rear\text{-}diff} = T_{i,R,\ Rear\text{-}wheel} + T_{i,L,\ Rear\text{-}wheel}$$

$$T_{i,R,\ Rear\text{-}wheel} = T_{i,L,\ Rear\text{-}wheel} = T_{o,Rear\text{-}diff}/2$$

There is another speed reduction just before the wheel called the final drive. This is done with planetary gearing such that the output speeds and torque generated meet the rimpull design requirements for the machine.

2.2.4 Rimpull Curves

Rimpull is the ability of a machine to pull load at a given speed; it is also a measure of machine grade-ability and is an important criterion for transmission design. The amount of rimpull a machine is capable of is a function of the machine speed and the gear ratio of the machine or the speed / torque available at the wheel. We can calculate the rimpull for any machine by working through the torque multiplication through the various gear drives and the speed ratio reduction as we move down the driveshaft. The final rimpull calculation is done knowing the radius of the wheel and the torque at the wheel shaft, calculating the moment generated by the wheel during the wheel ground interaction.

We know the gear reduction ratios at each point along the drivetrain. Individually calculating these values we arrive at the torque at the wheel. For a single gear ratio, the torque converter can output a range of torques. Using the radius of the wheel, we can calculate rimpull for every value of torque for a given gear ratio in the transmission. When plotted versus the vehicle speed we obtain a versatile curve which indicates the rimpull of the machine for every machine speed value and gear ratio.

Let R_{wheel} = Radius of the wheel

T_{wheel} = *Torque* available at the wheel

V_x = Machine Linear Speed

Then the equation for rimpull and machine velocity can be given by equations

$$F_x = \frac{T_{wheel}}{R_{wheel}}$$
$$V_x = R_{wheel} \cdot N_{wheel} \tag{2.2}$$

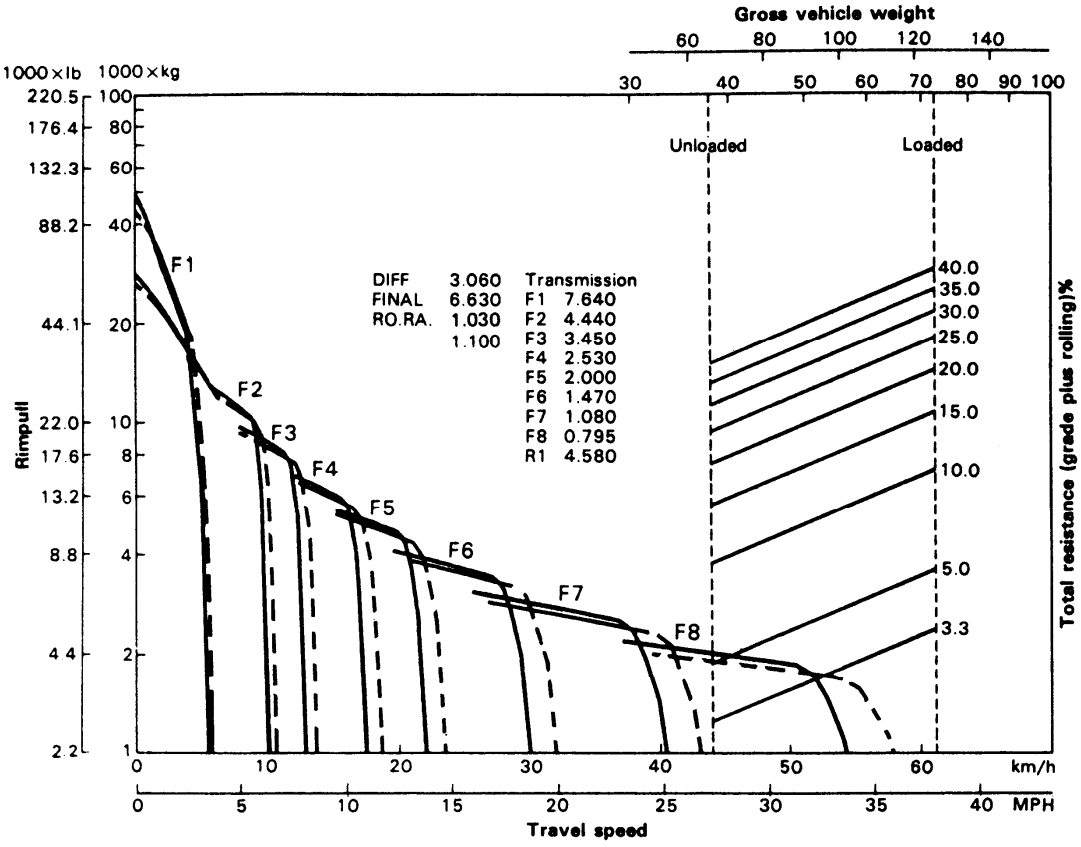

2.8 Typical machine rimpull curve [13]

2.3 Hydraulic Circuit

The implement system in the CAT 966D, like most of the wheel loader systems, has closed-center hydraulics. Implement actuation is done through a pilot system which is initiated by in-cab lever commands.

The pump implemented in wheel loaders is a load-sensing pump Fig 2.12. The load sensing system is an important part of hydro-mechanical pump control as it acts effectively as a comparator between cylinder pressures and the pump delivery pressure in case of a loaded condition and cylinder pressures to a tank pressure incase of no load. This allows the pump to stroke up or down and meet system requirement at any point of time during the machine operation thus improving efficiency.

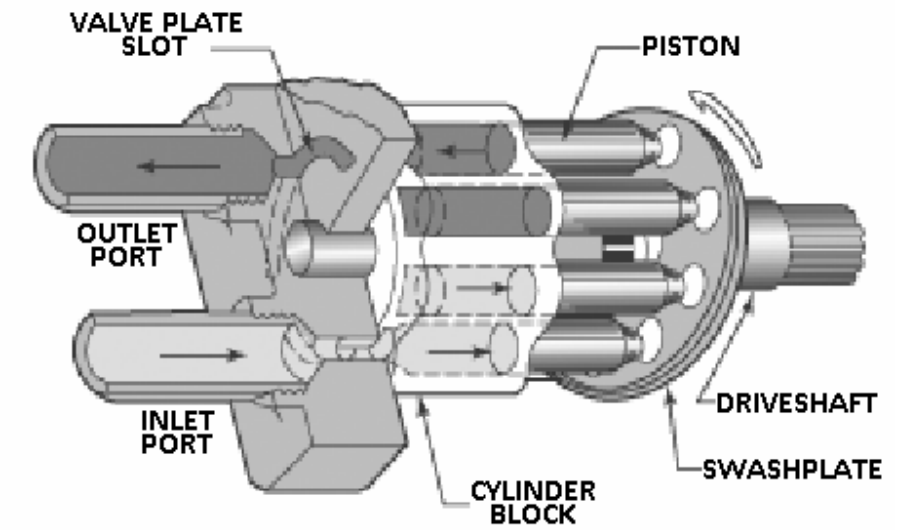

Fig. 2.9 Axial piston pump half section [2]

The shuttle valve in the system senses the higher of the pressures between the two implements and sends this signal as a pilot pressure back to the load sensing comparator. Comparing this pressure to the pump discharge pressure, the swash plate piston changes the angle of the swash plate to increase or decrease the flow, factoring in pump margin pressure. The comparator has a 'max-win' pressure setting for the system and only the highest of the pressures is the feedback given to the pump such that it can output the maximum flow requirement for the system at that time instant.

A pressure limiting compensator is placed in the feedback loop to ensure the system pressure does not exceed the design pressure and ensure safety of the system.

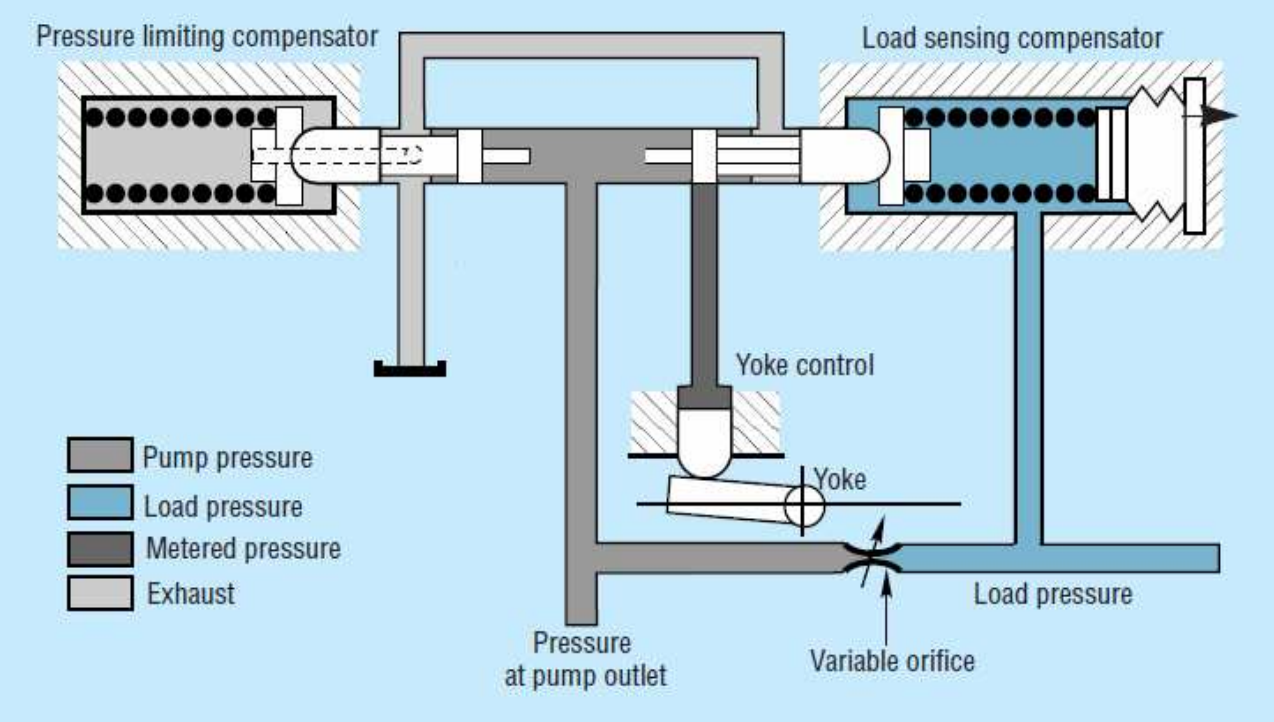

Fig 2.10 Load sensing circuit [15]

The load sensing system allows for proper flow sharing to take place between implements such that priority between implements is maintained, actuator speed is consistent and the machine does not waste energy by supplying flow to a low pressure circuit and blowing main relief to tank or lose power due to a high pressure differential across a small modulated valve spool area. The load sensing system allows for the pump to predict and supply flow based on requirement and is an efficient trend in MWL.

2.4 Linkage Description

The linkage design in wheel loaders is very important so that the operator can leverage as much of useful energy out form the machine as possible. This is done by an arrangement of levers and cylinders that when actuated can perform a variety of functions and configurations for the required work cycle. Most wheel loaders use the 'Z-Bar' linkage, called so because of the orientation of the links and cylinders in the system. The cylinders, through the operator commands, generate a pressure in the cylinders that is converted to linear force.

The frame of the MWL has 2 main components separated by a pivot pin.

1. Non Engine Frame (NEEF)
2. Engine Frame (EEF)

The schematic of the linkage is as shown in Fig 2.13

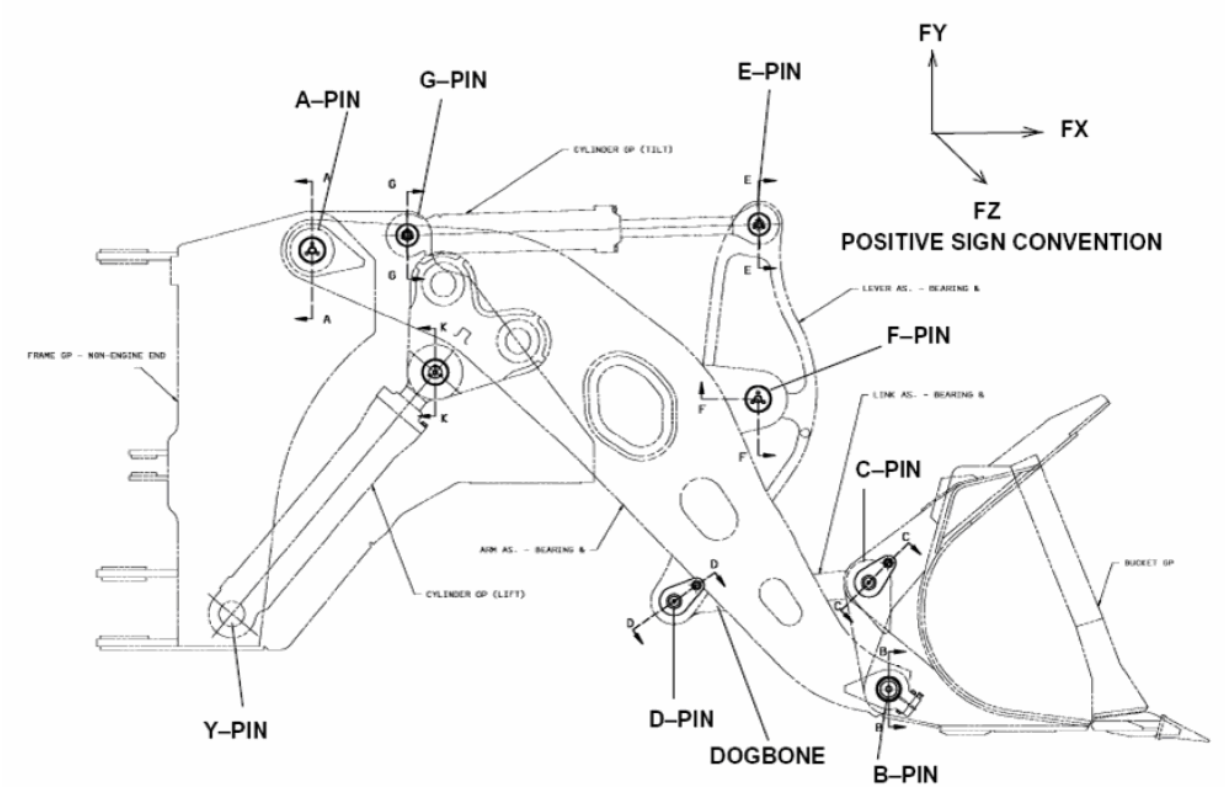

Fig 2.11 Z-bar linkage description [7]

The tilt cylinder is connected to the bucket by a series of pins and linkages that allow it to get the maximum mechanical advantage for the given configuration. The bucket has 2 pin connections, the B-Pin which is the pivot pin and the C-Pin. The C-pin is connected to the D-Pin through the idler dog-bone linkage. The D-pin connects to the E-pin through the lever which is pivoted at the F-Pin. The tilt cylinder connects to the lever at the E-Pin. The tilt cylinder is pivoted to the NEEF at the G-Pin. By means of the linkages and the pivot B-pin, the bucket is able to maintain a circular motion and optimum design of the links allows for the best mechanical advantage.

The lift cylinder has a simpler configuration. It is pivoted to the NEEF with the Y-Pin and is connected directly to the cast boom at an angle that allows for maximum mechanical advantage for the bucket in max reach position. The boom or lift arm, is pivoted to the NEEF by the A-Pin. The configuration of the lift arm is such that when the bucket is stationary and the lift cylinders are extended, the tip of the bucket will trace an imaginary circular path.

3. VIRTUAL MODEL

This chapter describes in brief how we used Virtual Product Development to model a complex machine and how we can through simple physics based equations model components that will mimic real world characteristic behavior. The following are the steps used in VPD modeling:

- Develop machine model - component upwards.
- Correlate component within machine model (engine, pump etc) using test data.
- Correlate machine model transient response to represent physical hardware.
- Simulate work cycle to represent physical operator on machine.
- Validate VPD machine model to improve its fidelity.

These models save time and resources as they help in evaluation of new concepts without physically procuring and testing the parts, it also helps understand how the machine will behave with these new changes and in failure prediction. In this study, we use two different types of software, Dynasty – Caterpillar Inc. proprietary software which helps us model the physical components from already pre-modeled blocks using basic equations, connected through a GUI. Matlab Simulink from Mathworks is used to design and simulate the controls for the machine. Using a specially designed 'Co-sim' block, dynasty can run in conjunction with simulink to have proper real world simulation.

3.1 Dynasty Overview

Dynasty is an integrated, general-purpose, dynamic modeling simulation tool used to aid in the design and analysis of physical systems. It is widely used to predict the transient and steady-state behavior of vehicle systems. Dynasty contains over 350 pre-defined components (e.g., torque converters, springs) which can be graphically connected to build a mathematical model of the physical system. User code may also be integrated into the model.

The model may consist of a sub-system (e.g., hydraulic system) or an entire vehicle or engine system. Dynasty's patented, state-of-the-art solver uses the model to simulate the dynamic response and presents the results in the form of plots, gauges, and tables in a native Windows interface.

It integrates numerous engineering technologies, including

- hydraulics,
- drivelines,
- mass-elastics,
- linkages,
- controls,
- electronics,
- cooling,
- 2-D and 3-D rigid bodies,
- 3-D flexible bodies

to perform transient-dynamic, performance, and linear system analysis. It also incorporates many features to enhance ease of use and productivity, including

- an interactive, graphical model builder;
- a predefined component library;
- parameter optimization;
- a user-customizable plotting package;
- animation;
- ASCII and binary Generic Data File (GDF) data file creation;
- linkage to user-written and external software

3.1.1 Solver Overview

Dynasty was built from the ground up to make modeling and simulation of physical systems as fast, easy, and flexible as possible for the user. A major factor affecting these features is the design of Dynasty's solver. The solver influences nearly every aspect of the program, including how the components are described, how models are assembled, and how simulations are set up and run. But the underlying idea is that the solver should allow you to focus on the modeling of the physical system, not on the mathematics or how to make the equations fit the solvers limitations. Dynasty makes the solver fit the model, not the other way around.

In general, models in Dynasty are described as components connected together to form a physical system. The act of putting components in a model adds equations to the system. Connecting components together adds connection equations that tie the component equations together into a coupled system.

3.1.2 The Solution Method and Benefits

Dynasty uses a Differential-Algebraic Equation (DAE) solver to numerically solve the resulting system of equations. The DAE solver accepts both ordinary differential equations and algebraic equations. This allows component equations to be formulated directly from the basic physical equations (in other words, textbook equations) without the additional rearrangement needed to eliminate the algebraic equations. The rearrangement may result in less meaningful variables than in the original formulation and, in some cases, rearrangement may not be possible without modifying the modeling approach. Thus, a DAE solver is the most general solver that can handle the widest range of model types.

Dynasty's equation solver is both explicit and implicit. Prior to simulation, Dynasty assembles and processes the model equations to explicitly solve as many equations as possible by symbolically sorting and rearranging them. The equations that cannot be solved explicitly are then solved during simulation numerically, by guessing variable values and iterating on those values until equation errors are within a specified tolerance. Contrast that with the more common explicit-only methods which often have problems with algebraic loops, sets of simultaneous equations that cannot be solved directly by simple algebraic rearrangement. Because Dynasty can handle algebraic loops automatically, the solver allows it to simulate tightly coupled systems without requiring the user to manually break the algebraic loops by adding springs, control volumes, delays, or other artifacts that are not part of the desired physical model.

Boundary conditions (constraints) can be easily moved around to any physically reasonable area in the model, without having to manually rebuild the entire model because you have changed the input/output relationship. This allows the model to be easily reused for different simulation objectives. Also, initial conditions can be set on higher derivatives, such as acceleration, a seemingly obvious feature that most other simulation programs lack.

In Dynasty, a numeric nonlinear equation solution technique (such as Newton-Raphson) is used to move the variables toward a solution when iterating. The initial set of guesses for variable values can be automatically specified by Dynasty for many models and modified by the user for more challenging models. If Dynasty has difficulty in finding an initial condition solution, it will automatically switch to a multi-pass approach where subsets of the system equations are solved in each pass.

The passes are as follows:

- Pass 1 - Equations that are only differentiated
- Pass 2 - Integrated and differentiated (and Pass 1) equations
- Pass 3 - Equations that are only integrated (and Pass 2) equations
- Pass 4 - All equations

Dynasty's solver and integration techniques give flexibility to easily model and solve integrated system models containing components from many different engineering disciplines. The ability to handle implicit loops helps to decouple the modeling process from the underlying numerical method. You are free to create models the way you want to, not the way the underlying solver requires. [4]

3.2 Energy Flow Sign Convention and Nomenclature

Knowledge of sign convention is very important in Dynasty. It plays a crucial role in result analysis and the interpretation of data from result files. Most components have an input and output port which can be connected to physical inputs and outputs or signal inputs and outputs based on they type of component it is. The figure 3.1 below illustrates the general sign convention of the components in Dynasty

Fig 3.1 Dynasty sign convention

The general convention is that physical energy into the system can be considered positive and physical energy out of a system can be compared to energy lost or given out and is considered negative.

Sign convention is especially significant in the later sections where the development of the controls logic and the interpretation of the results are dependent on energy flow to and from the system.

3.3 Control System Overview

Simulink is the software that provides an environment for modeling, analysis and optimization of multi domain systems. It allows the user to design, simulate and implement various real world scenarios and check system stability. It is very important in the field of controls and signal processing as it allows simulation of time varying systems. Simulink can be used to design controls and verified on the workstation, but it also has a unique feature of being able to, in conjunction with xPC Target, simulate and test the controls on the physical system.

A block diagram consists of two main components, blocks and signal lines. These blocks in Simulink, represent real world systems and connected to other blocks can represent the dynamic system that is required to be modeled. We can describe two states in a model, discrete and continuous. Simulink allows the user to model both types of systems in the form of simple and complex ordinary differential equations (ODE). Simulink has inbuilt solvers using numerical methods that allow for mathematical integrations and computerized algorithms of ODE equations. The accuracy of a solution is dependent on the performance output of the system on which it has to be run. Simulink allows the user to modify the time steps of integration in order to preset the level of accuracy required in the system for the requirement of the analysis.

Simulink also has a capability that allows users to embed matlab code into the Simulink using an ‘embedded code block’ which is a good feature for concept evaluation for quick and iterative trials of a concept with out having to restructure the controls. When used with Dynasty, Simulink must have a ‘co-sim’ block that allows it to connect and exchange signals calculated, to Dynasty and vice versa.

4. HYBRID SYSTEM ANALYSIS

As defined earlier, any system that uses more than one flow path for energy may be termed as a hybrid system. This is an open scope definition and in this thesis we limit our selves to the discussion of two specific types:

1) Ultra High Speed Flywheel (UHSF) (capture energy)
2) Battery Storage (steady state storage)

These two are the most important as they are the concepts upon which the virtual model and its control methodology are developed.

4.1 Ultra High Speed Flywheel

A flywheel is a rotating mechanical device that is used to store rotational energy. Flywheels have a significant moment of inertia, and thus resist changes in their rotational speed. Energy is added to a flywheel by applying torque to it, thereby causing its rotational speed to increase. Conversely, its rotational speed decreases as it releases its stored energy. Flywheels have been used in automobiles and heavy machinery in order to provide continuous energy in systems where the energy source is not continuous. In such cases, the flywheel stores energy when torque is applied by the energy source and it releases stored energy when the energy source is not applying torque to it.

A flywheel may also be used to supply un-sustained pulses of energy at energy transfer rates that exceed the capabilities of its energy source. By accumulating potential (rotational) energy in the flywheel over a period of time, at a rate that is compatible with the energy source, and then releasing that energy at a much higher rate over a relatively short time. For general applications, flywheels generally have a higher mass and lower speed in accordance with the governing equations to maintain a constant reserve of energy (for the required application).

However in non standard applications such as hybrid flywheel systems, the weight and speed can be varied in a constant ratio to obtain a system which can store energy and dissipate it when required with a much higher rate, the advanced flywheel is a lightweight composite rotor with a lower weight and speeds in the order of ten thousands of rpm; it is the so-called ultra-high-speed flywheel.

As a hybrid system, the UHSF has many advantages:

- specific energy
- high specific power
- long cycle life
- high energy efficiency
- quick recharge
- maintenance-free characteristics
- cost effectiveness
- environmental friendliness.

A rotating flywheel stores energy in the kinetic form as

$$E_f = \frac{1}{2} m.(r.\omega_f)^2 = \frac{1}{2} m.r^2.\omega_f^2 = \frac{1}{2} J_f.\omega_f^2 \quad (4.1)$$

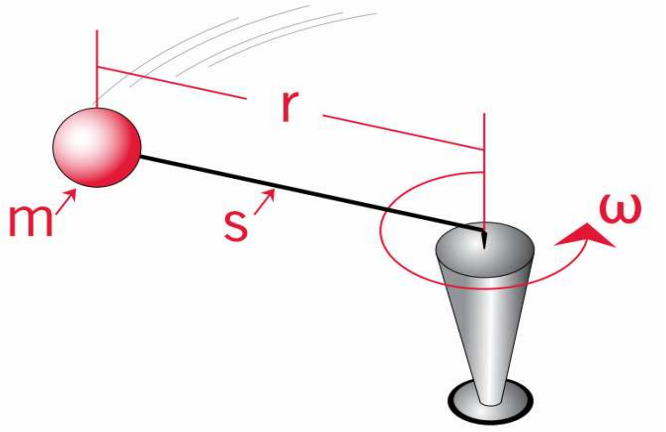

Fig 4.1 Simple flywheel [6]

J_f is the moment of inertia of the flywheel in kg.m^2/s and ω_f is the angular velocity of the flywheel in rad/s. Equation (4.1) indicates that enhancing the angular velocity of the flywheel is the key technique to increasing its energy capacity and reducing its weight and volume.

The level of current technology allows us to conceive a vehicle that can propel itself with the use of energy stored in a flywheel based on changes to its motion state and continuously varying transmissions. In this thesis however we shall limit ourselves to the study of the commonly used approach of coupling an electric machine to the flywheel directly or through a transmission to constitute a so-called mechanical battery. The electric machine, functioning as the energy input and output port, converts the mechanical energy into electric energy or vice versa, as shown in Figure 4.2

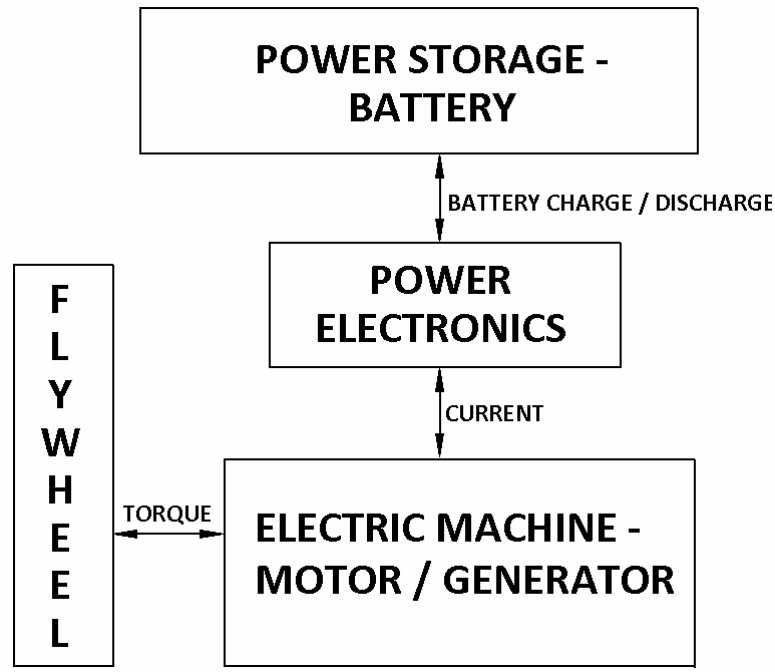

Fig 4.2 Flywheel based integrated starter generator [3]

Equation (4.1) indicates that the energy stored in a flywheel is proportional to the moment of inertia of the flywheel and flywheel rotating speed squared. A lightweight flywheel should be designed to achieve a large moment of inertia per unit mass and per unit volume by properly designing its geometric shape. This can be shown by the figure 4.3

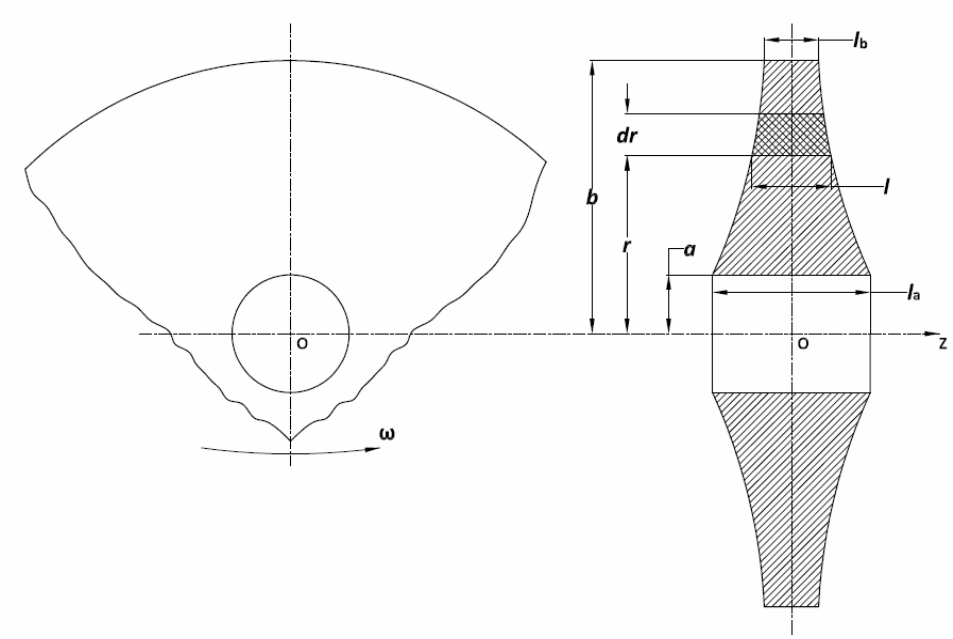

Fig 4.3 Flywheel cross-section. [16]

The moment of inertia of a flywheel can be calculated by

$$J_f = 2\pi\rho\int_a^b l_r r^3 dr \tag{4.2}$$

Where ρ is the density of the material $l_{(r)}$ is the width of the flywheel as a function of the radius. The mass of the flywheel can be calculated as

$$M_f = 2\pi\rho\int_a^b l_r r dr \tag{4.3}$$

Thus the specific mass moment of inertia can be defined as the moment of inertia per unit mass and can be given by the equation

$$J_{fs} = \frac{\int_a^b l_r r^3 dr}{\int_a^b l_r r dr} \tag{4.4}$$

Equation (4.4) indicates that the specific moment of inertia of a flywheel is independent of its material mass density and dependent solely on its geometric shape $l_{(r)}$. We can also understand how material properties play an important role in reduction of the size of the flywheel.

Consider the volume of the flywheel:

$$V_f = 2\pi \int_a^b l_r r dr \tag{4.5}$$

We can thus define the Volume density of the moment of inertia of the flywheel as the moment of inertia per unit volume. Mathematically from equation (4.2) and (4.5) we have

$$J_{fv} = \frac{\rho \int_a^b l_r r^3 dr}{\int_a^b l_r r dr} \tag{4.6}$$

For a flywheel with constant width along the radius (b-a), the equation (4.6) would then reduce to

$$J_{fv} = \rho\left(b^2 + a^2\right) \tag{4.7}$$

which indicates that heavy material can, indeed, reduce the volume of the flywheel with a given moment of inertia. The torque of a flywheel can be given by the product of the mass moment of inertia and the change in angular velocity (angular acceleration). Mathematically this can be written

$$T_f = J_f . \frac{d\omega_f}{dt} = J_f \alpha_f \tag{4.8}$$

Now power can be defined by the change in flywheel energy with respect to time. Mathematically:

$$P_f = \frac{dE_f}{dt} \tag{4.9}$$

Differentiating Equation 4.1 with respect to time and substituting it in equation 4.9 we get:

$$P_f = J_f . \omega_f \frac{d\omega_f}{dt} = J_f . \alpha_f . \omega_f = T_f \omega_f \tag{4.10}$$

4.2.3 Existing Hybrid Control Strategies

Consider for simplicity that the flywheel was connected to an electric machine on one side of the through shaft and to a torque load on the other side. From equation (4.8) we can understand that the torque T_f is torque acting on the flywheel from/to the electric machine based on the mode at which the flywheel is acting in (generating / motoring). When the flywheel discharges energy, the electric machine acts like a generator by converting rotational mechanical energy to electric energy and when the flywheel requires torque, the electric machine acts as a motor and converts electric energy to mechanical energy. From the equation (4.10), we can understand that the sizing of the flywheel with respect to power is a factor of torque and angular velocity. Varying these parameters we can obtain a characteristic curve for the motor shown by Fig 4.4

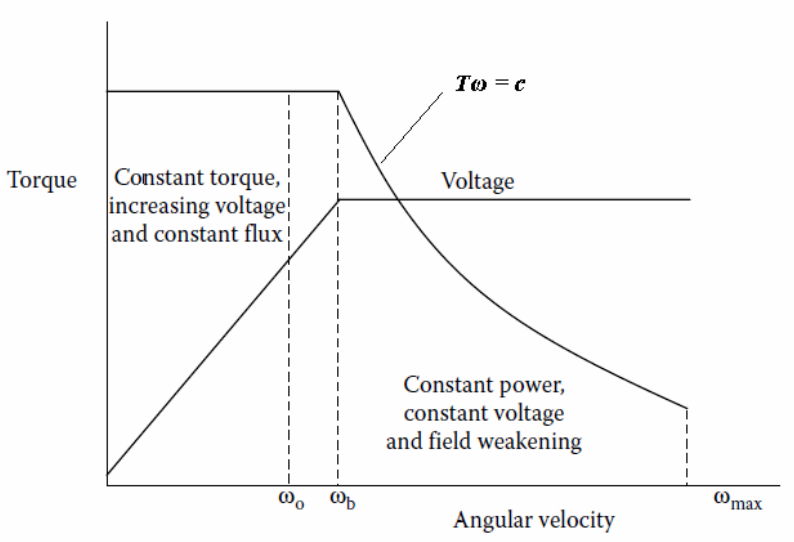

Fig 4.4 Integrated starter generator speed v/s state of charge plot [3]

Here we define 3 parameters:

- ω_{max} = Max speed of the ISG / SRM
- ω_b = Base speed of the motor / Corner speed if the motor (Maximum Power)
- ω_o = Bottom speed of the flywheel connected to the motor

If the motor was charging the flywheel, it would be an important consideration to note that the base bottom speed of the flywheel and the base speed of the motor should be close together in order to effect efficient conversion of energy and smaller more compact motor design.

Consider the equation (4.8), integrating it within the limits ω_0 to ω_{max} we can obtain a time for which the motor reaches the maximum power.

$$t = \int_{\omega_0}^{\omega_{max}} \frac{J_f}{T_m} d\omega = \int_{\omega_0}^{\omega_b} \frac{J_f}{P_m \omega_b} d\omega + \int_{\omega_b}^{\omega_{max}} \frac{J_f}{P_m \omega} d\omega \qquad (4.10)$$

Integrating and re-arranging:

$$P_m = \frac{J_f}{2t}\left(\omega_b{}^2 - 2\omega_b\omega_0 + \omega_{max}{}^2\right) \qquad (4.11)$$

Which puts the design of an ISG (during charging) down to the following design considerations:

- Moment of inertia of the UHSF
- Acceleration time of the flywheel
- Base speed of the motor
- Bottom speed of the flywheel

As ω_0 moves closer to ω_b, the effective bottom speed of the flywheel and the base speed of the motor coincide, the equation (4.11) can be reduced to

$$P_m = \frac{J_f}{2t}\left(\omega_{max}{}^2 - \omega_0{}^2\right) \qquad (4.12)$$

As we move closer to this condition it can be seen from the Fig 4.4, that the voltage along this constant power region is constant, this would help to make the controls simpler and reduce the transient response of the power electronics.

4.2 Battery Storage

Battery storage also known as electrochemical storage works to convert electrical energy to chemical and vice versa during charging and discharging cycles. It is one of the most commonly used portable energy storage mechanisms in the world. Batteries generally consist of electrodes (positive and negative) and an electrolyte solution.

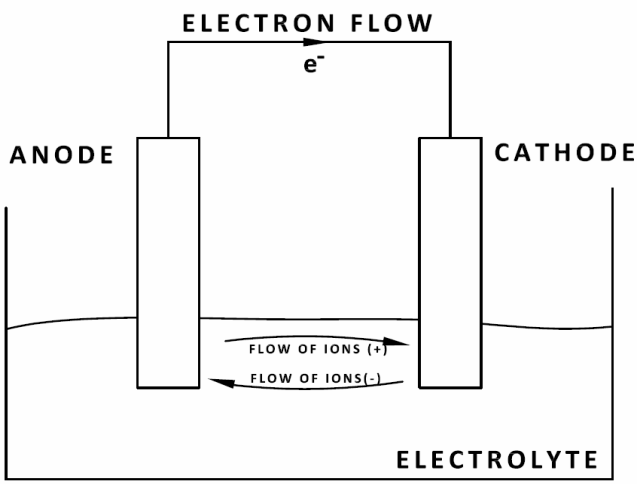

Fig 4.5 Battery construction [28]

Most batteries are rated on an Ampere-Hr basis along with the current discharge rate. From this it is possible to calculate the average current discharge (Amps). State of Charge (SOC) is a very important parameter that governs all rechargeable battery design and control algorithms. It is defined as the ratio of remaining capacity to fully charged capacity. Generally from a control perspective the SOC is what defines the charging, discharging and inactivity of the battery. This can be seen by Fig 4.6

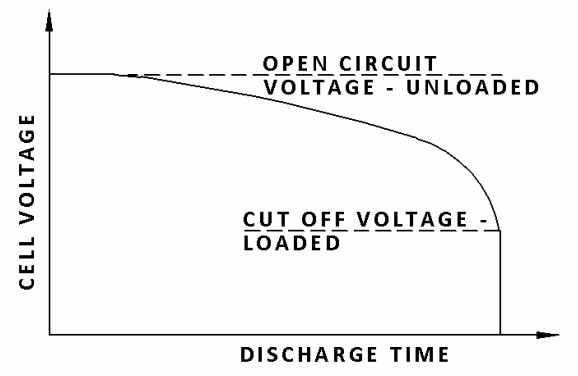

Fig 4.6 State of Charge / Charging and discharging curve [3]

Mathematically, SOC change over a time interval dt, with discharging or charging current *i* can be expressed as:

$$\Delta SOC = \frac{i.dt}{Q_{(i)}} \tag{4.13}$$

Where $Q_{(i)}$ is the Ampere-hour capacity of the battery at the current rate *i*. Thus SOC can be defined as

$$SOC = SOC_0 - \int \frac{i.dt}{Q_{(i)}} \tag{4.14}$$

The energy delivered from the battery can be expressed as:

$$E_C = \int_0^t V_{(i,SOC)} i_{(t)} dt \tag{4.15}$$

where $V_{(i, SOC)}$ is the voltage at the battery terminals, which is a function of battery current and SOC. The energy or power losses during battery discharging and charging appear in the form of voltage loss. Thus the efficiency of the battery during discharging and charging can be defined at any operating point as the ratio of the cell operating voltage to the thermodynamic voltage, that is, during discharging:

$$\eta = \frac{V}{V_0} \tag{4.16}$$

During charging:

$$\eta = \frac{V_0}{V} \tag{4.17}$$

The terminal voltage, as a function of battery current and energy stored in it or SOC is lower in discharging and higher in charging than the electrical potential produced by chemical reaction. Figure 4.7 shows the efficiency of and electrochemical battery during discharging and charging. The

battery has a high discharging efficiency with high SOC and a high charging efficiency with low SOC. The net cycle efficiency has a maximum in the middle range of the SOC. Therefore, the battery operation control unit should ensure that the battery SOC is in its middle range so as to enhance the operating efficiency and depress the temperature rise caused by energy loss as high temperature would damage the battery.

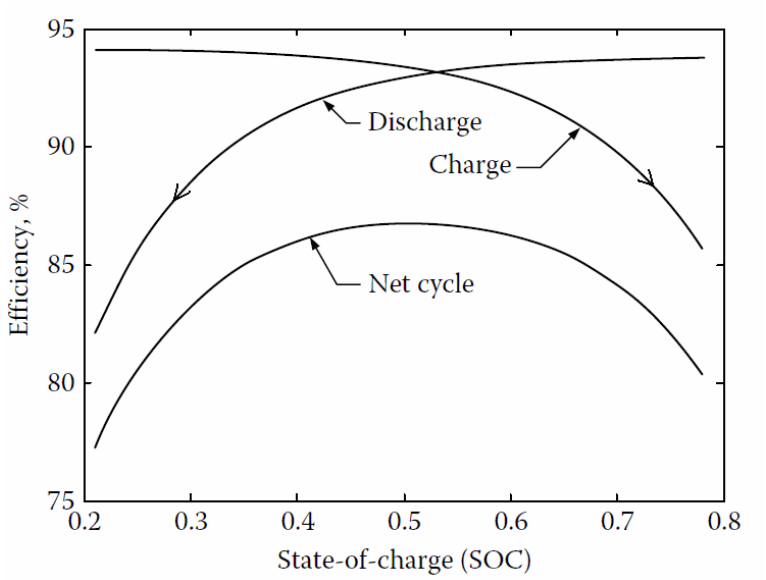

Fig 4.7 Charging and discharging plot [3]

Thus in summary, battery design depends broadly on the following parameters:

- Average amperage required during discharge (i)
- Ampere-Hour capacity for the battery ($Q_{(i)}$)
- SOC cut off voltage
- Voltage across the terminals of the battery.

Remarks

Using the data in the hybrid section, we can not only understand how the systems in general are designed but also uncover very important design parameters that would allow us a proper control over the system. The few points to take away from the chapter in the form of implementation are:

- ISG design for power based on flywheel speed (power available at the output of a flywheel shaft).
- State of charge for battery operated systems and how it could affect the KERS system.
- High speed flywheel design parameters, angular deceleration and how it plays an important role in flywheel design.
- Predictive methods and how to implement using a torque system requirement strategy.
- Efficiency monitoring over the cycle.
- How the application of test data can be used to correlate the VPD model in the future.

5. CONTROL STRATEGY

5.1 Control Variables

Based on the position of the KERS we can define control variables that can be sensed from the Wheel Loader during the work cycle and be used to engage and disengage the KERS system. The control variables to be used for this model are:

a) Torque variable at proposed KERS interface

b) Engine speed

c) State of charge (SOC)

d) Desired engine speed

5.2 Control Strategy

Using the regenerative braking method for energy capture, we can obtain the following control points based on the magnitude and the direction of the variables we can define specific engagement and disengagement points in our control strategy

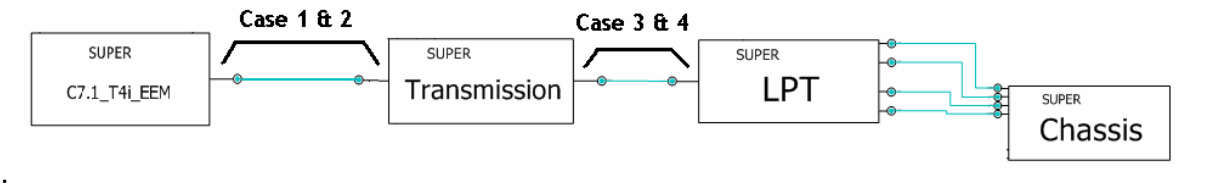

.

Fig 5.1 Points of KERS Analysis

Case1: Engine to Transmission Driveline. Engagement for capture condition (charge logic):

Actual Engine speed > Desired Engine Speed @ Engine output shaft

Torque at input to Torque converter <= 0 [Torque given back to the system]

Clutch Engagement Flag = High [KERS Capture active]

Case2: Engine to Transmission Driveline. Engagement for discharge condition:

Actual Engine speed < Desired Engine Speed @ Engine output shaft

Torque at input to Torque converter > 0 [Torque demand in the system]

SOC > 0.1 [threshold set by initialization]

Clutch engagement flag = High [KERS discharge active]

Case 3: Transmission to Lower Powertrain. Engagement for capture condition (charge logic):

Actual Engine speed > Desired Engine Speed @ Engine output shaft

Torque at input to Torque converter <= 0 [Torque given back to the system]

Clutch Engagement Flag = High [KERS Capture active]

Case 4: Transmission to Lower Powertrain. Engagement for discharge condition:

Actual Engine speed < Desired Engine Speed @ Engine output shaft

Torque at input to Torque converter > 0 [Torque demand in the system]

SOC > 0.1 [Threshold set by initialization]

Clutch engagement flag = High [KERS discharge active]

5.3 Control Logic and Control Code:

Actual Speed = N_{ACT}

Desired Speed = N_{DES}

$N_{DIFF} = N_{Des} - N_{ACT}$

Lower powertrain torque = T_{LPT}

Transmission input torque = T_{XMSN}

Flywheel speed = N_{FLY}

Safe Rated High Speed (Flywheel) = N_{SRHS}

SOC = N_{FLY} / N_{SRHS}

If $T_{LPT/XMSN} <= 0$, $N_{DIFF} <= 0$, SOC<0.4

$F_{TRQ} = 1$

elseif $T_{LPT/XMSN} > 0$, $N_{DIFF} > 0$

$F_{TRQ} = 1$

else

$F_{TRQ} = 0$

Where F_{TRQ} is the Torque status flag that indicates torque requirement by the system.

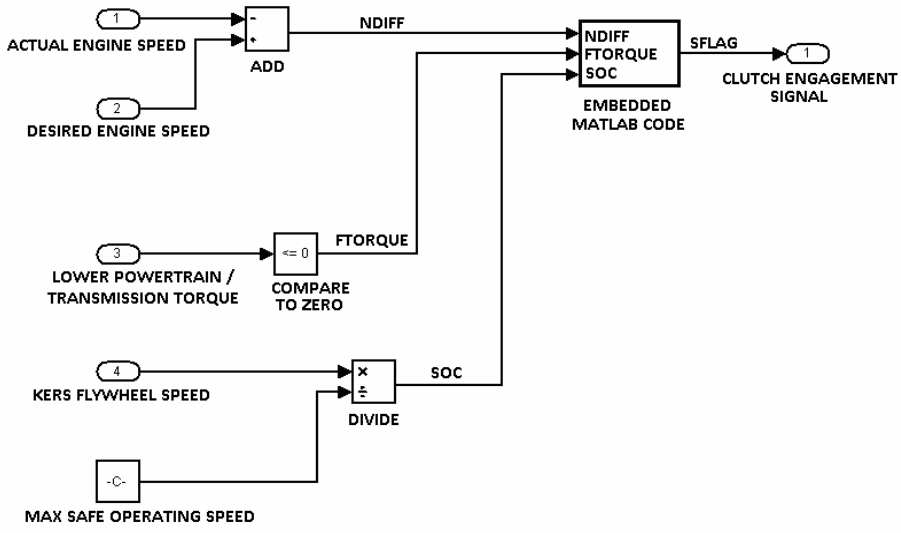

Fig 5.2 Controls for KERS

Controls System design & matlab function block code

```
function sflag = fcn(Ndiff, Tlpt, SOC)

%#eml

%% Ndiff = Ndes - Nact , if Ndiff <0 == Overshoot from desired engine speed.

%% if Tlpt =1, torque is negative (less than zero based on logic) i.e. torque being fed back into the system

        if (Ndiff<=0 && Tlpt==1)

         sflag = 1;

%% Ndiff = Ndes - Nact , if Ndiff >0 == droop from desired engine speed.

%% if Tlpt = 0, torque is positive (greater than zero based on logic)i.e. torque being fed back into the system

                elseif (Ndiff>0 && Tlpt==0 && SOC>0.1)

                sflag = 1;

        else

        sflag = 0;

end

end
```

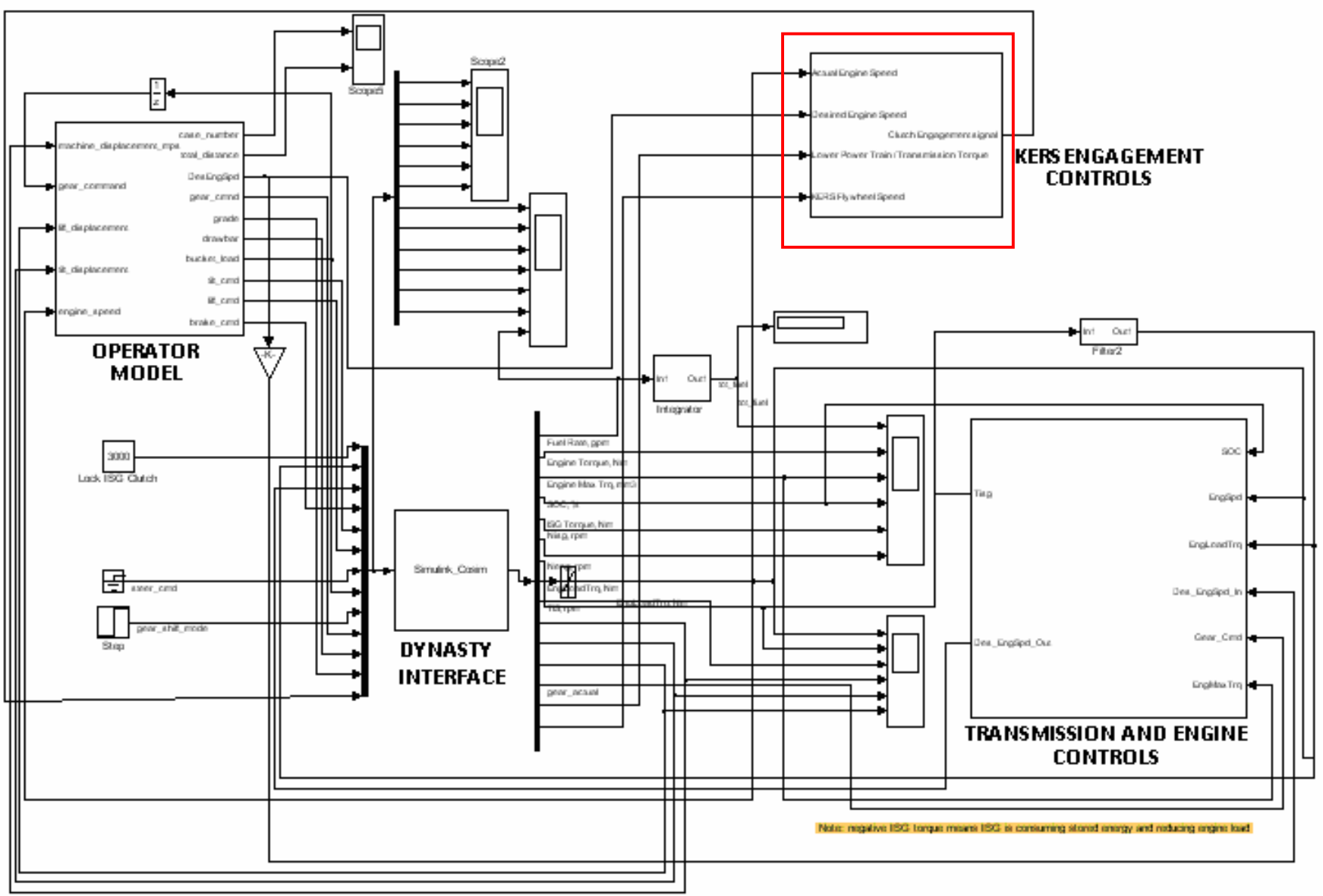

Fig 5.3 Control systems overview MWL

6. OPERATOR FOR DIGGING CYCLE

The operator model plays an important part in the analysis that follows. The work cycle in the real or virtual world is governed by an operator and how he gives the appropriate lever commands using the feedback from the machine. Data from the real world operators are collected over hours of operation and on analysis a pattern for lever commands are generated that are typical of a standard work cycle.

In the VPD world this can be modeled in two ways, a dynasty operator and a Simulink logic based operator. The dynasty operator is simplistic and is modeled as a truth table that takes the values from the machine signals, compares them to a predefined threshold value and outputs a value indicative of a lever command. The other method is to use logic modeled in Simulink to evaluate machine parameters and based on a fixed logic, calculates commands per time step of the simulation. The operator model for this study is in Simulink and though modeling it is not in the scope of this thesis, it will be explained in brief so the reader has an idea as to how the commands for the cycle are generated.

The work cycle is broken down into segments based on time and linear displacement of the machine.

Total distance covered: Gear position (1F, 2F, 1R, 2R, etc.) and machine speed (m/s), we can understand the direction of the machine. Integrating the machine speed as a function of time we obtain the total distance covered for that time instant.

Segment : The segment can be defined as the part of the standard cycle the machine is at a particular time instant. This can be determined by comparing values of time (sec), distance covered (m), engine speed (rpm) and the gear commands for to preset values for a standard cycle. The output is a number between 1 to n, where n is the maximum number of segments in the cycle.

The segment value can be passed through an ‘if block’ which outputs to an else action subsystem. If the required subsystem has been activated by the segment decision block, the lever commands are

then decided by 1 Dimensional maps that have preset data mapped to total distance covered and/ or cycle time at that instant. The tilt and lift segments have hard coded stops such that if the cylinder reaches the end of stroke, the lever command will go to zero.

The outputs of the operator subsystem in Simulink are as below:

1. Desired Speed
2. Gear Command
3. Grade
4. Drawbar Position
5. Payload
6. Tilt Command
7. Lift Command
8. Brake Command

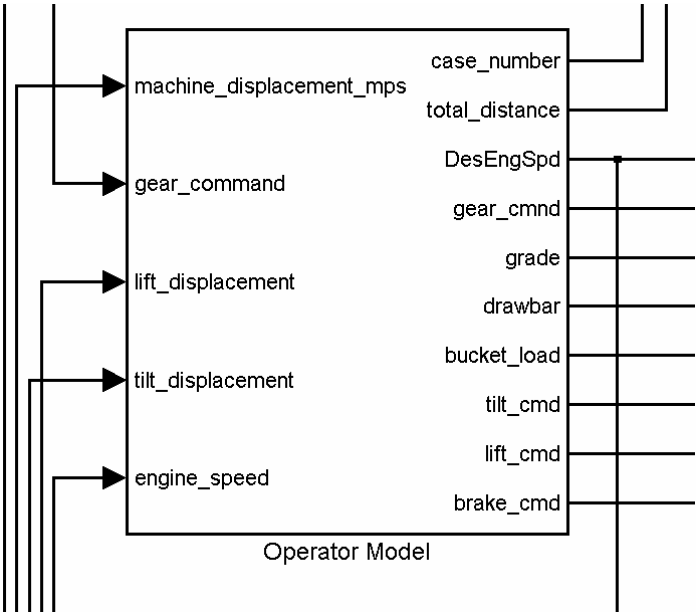

6.1 Top level view of the Simulink Operator Model

7. MODELLING / VPD & RESULTS

7.1 High speed flywheel model (KERS)

The flybrid model could be modeled mathematically in Simulink. However since the machine model on which this concept has to be evaluated is Dynasty, it can be modeled in dynasty using pre-existing component that would mimic the behavior of the real world system. To do so we have to understand the basic construction of the real world system to be tested / modeled.

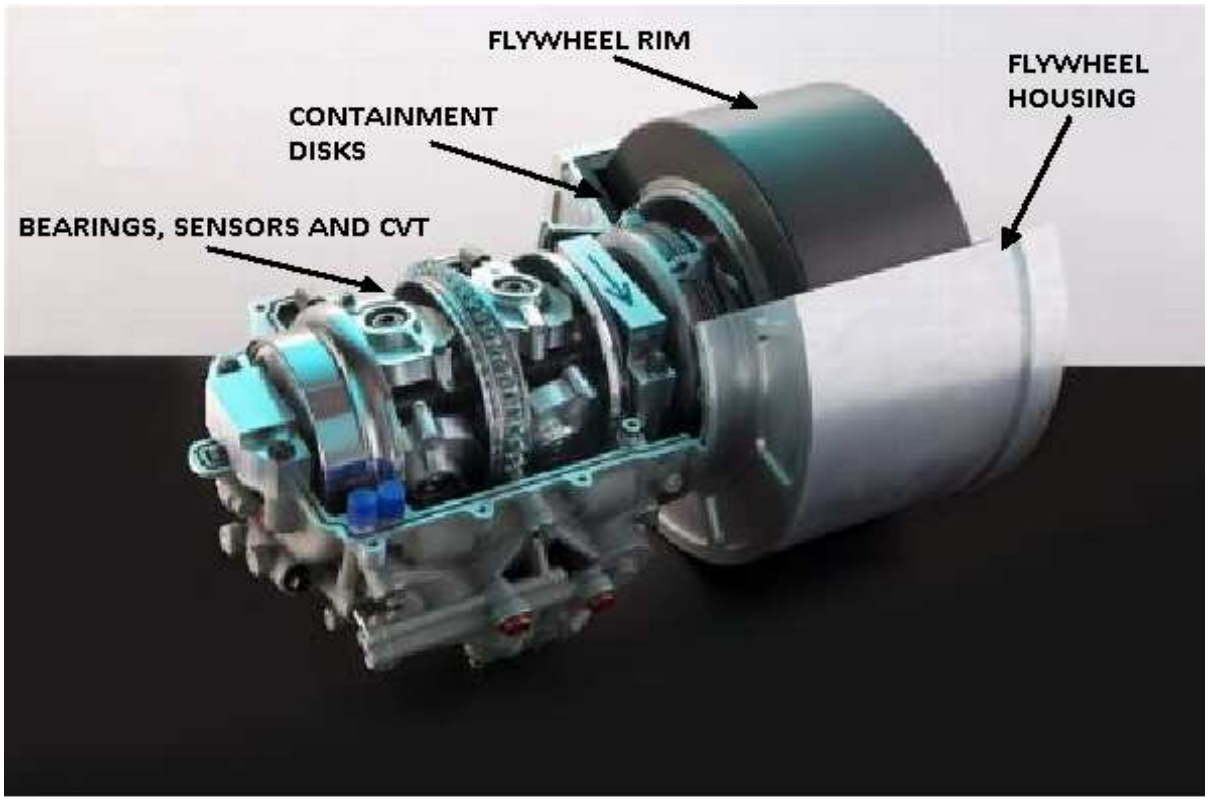

Fig 7.1 KERS system [14]

From this system and design specs we can approximate the basic working of the KERS system. When broken down into a block diagram form it can be represented simplistically, as below:

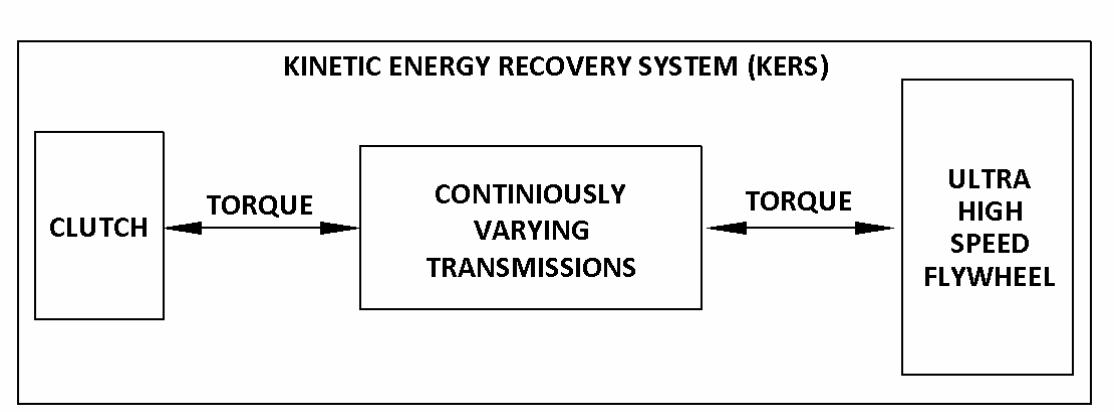

Fig 7.2.1 Simplistic high speed flywheel component break up

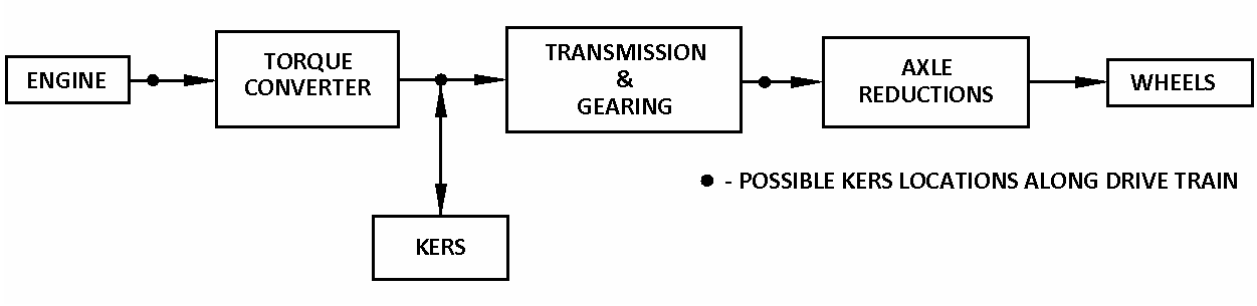

Fig 7.2.2 Possible KERS locations along the drivetrain

The above system can be modeled for performance analysis at a system level in the virtual world using the dynasty software. This is done by converting inertial components into single components using physics based equations and obtaining a high fidelity model mimicking the real world system. Using this system in the virtual machine model and running a standard work cycle is how we can evaluate the improvements using the KERS. The work cycle will be explained in depth in the later sections of this chapter. From the fig 7.1 we can devise a simplistic system as shown in fig 7.2 which breaks the components down into its subsystem levels.

The three basic subsystems in the KERS system are:

1) *Drive subsystem:* The drive subsystem contains the inertial components such as the flywheel, the CVT and the engagement clutch.
2) *Clutch pressure subsystem:* The clutch pressure subsystem contains a simple pressure model to interpret the engagement signal based of the control logic and convert that signal into a continuous output pressure signal.
3) *Shift logic subsystem:* The drive subsystem has a CVT, the inputs to which are dependent on the speeds of the input shaft to the engagement clutch. This logic is monitored and taken care of by the shift logic subsystem.

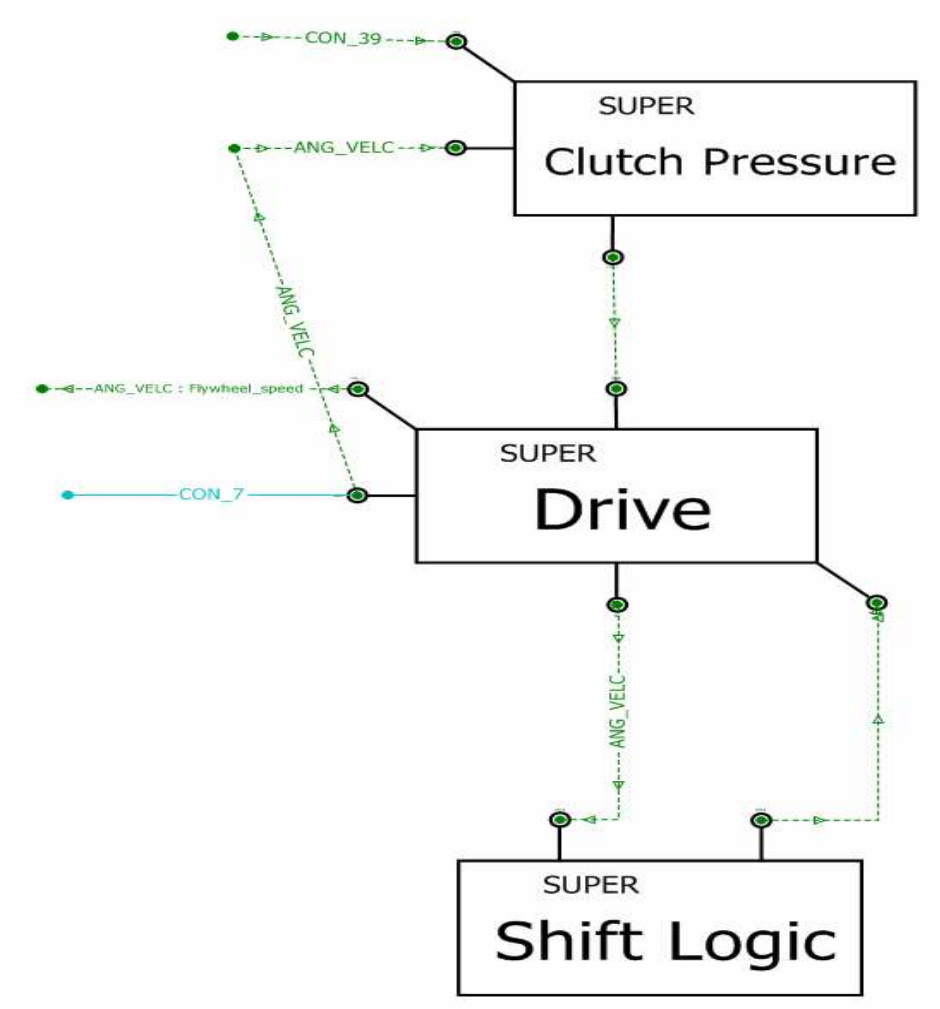

Fig 7.3 Modeled KERS system

7.1.1 Drive Subsystem

The drive subsystem has three basic components as shown in fig 7.4

A) An engagement clutch that allows for the torque to flow to and from the high speed flywheel. The clutch is designed so as to obtain maximum amount of torque transfer without allowing for slippage and power loss.

B) Continuously Variable Transmission that allows for a non-discrete speed ratio changes based on shift logic and input shaft speed to the flybrid system. This system is a low inertia system and thus allows for the transfer of the torque at a higher speed with minimal losses.

C) The flywheel is designed to have a low moment of inertia based on the principles explained in equations (4.1) to (4.12). The flywheel has a Moment of inertia 0.02375 kg.m^2 as per the current design from the OEM supplier.

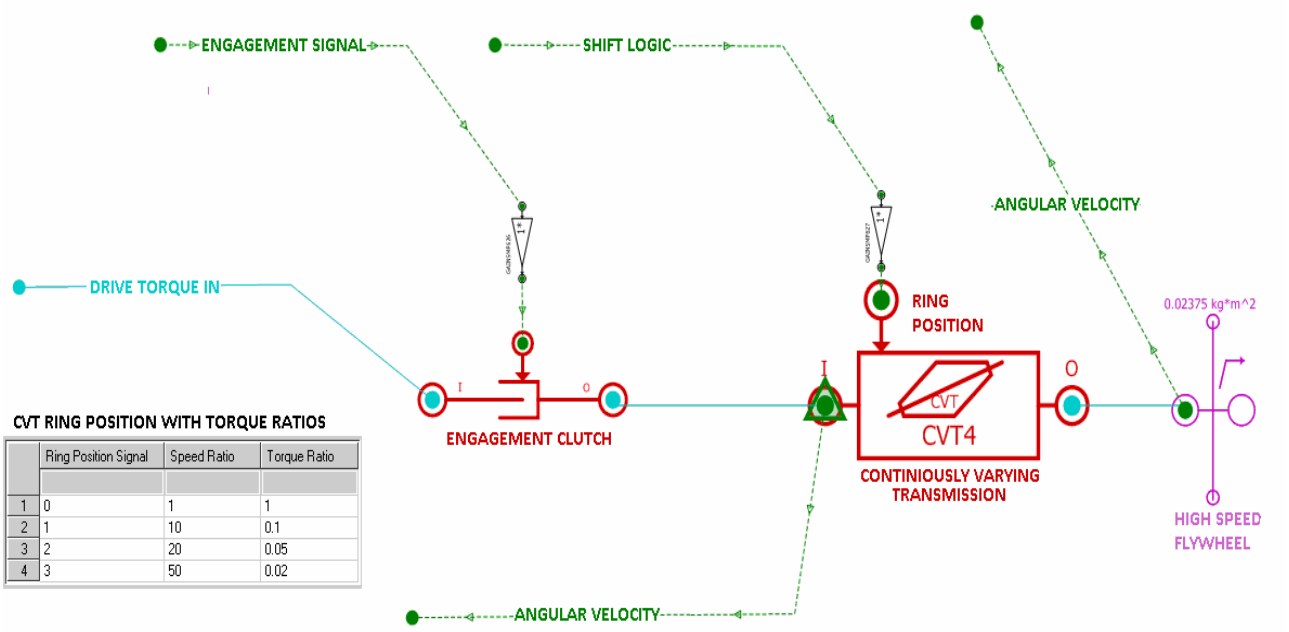

	Ring Position Signal	Speed Ratio	Torque Ratio
1	0	1	1
2	1	10	0.1
3	2	20	0.05
4	3	50	0.02

Fig 7.4 Modeled KERS drive system

7.1.2 Clutch Pressure Subsystem

The engagement and disengagement clutch in the drive subsystem requires a signal pressure as an input. This pressure can be generated by various methods like a pilot line of the hydraulic system or an electrical input given from the ECM through the alternator or battery bank.

In this model, in order to maintain a simplistic configuration and to avoid making too many changes in the existing machine implement line, the modeling is done to allow a flow from a hydraulic flow (generating source) sink to tank. By regulating the restriction on a control valve, we can accurately develop a high pressure upstream when the valve is closed and by setting up a stiff check valve downstream we can ensure the system pressure is high overall. Due to a requirement of quick convergence, no hydraulic lines and orifice areas have been modeled. The input to the control area is the control signal from the ECM (simulink controls) indicating the KERS engagement for the charging and discharging of the flywheel. The pressure signal from downstream of the control area will generate high pressure when the valve is open. This signal is filtered for high frequency content using an 18 Hz first order filter and for frequency content lower than 8Hz (based on iteration and the response of the clutch to high frequency content) first order filter so as to allow the smooth transition between engagement and disengagement of the clutch.

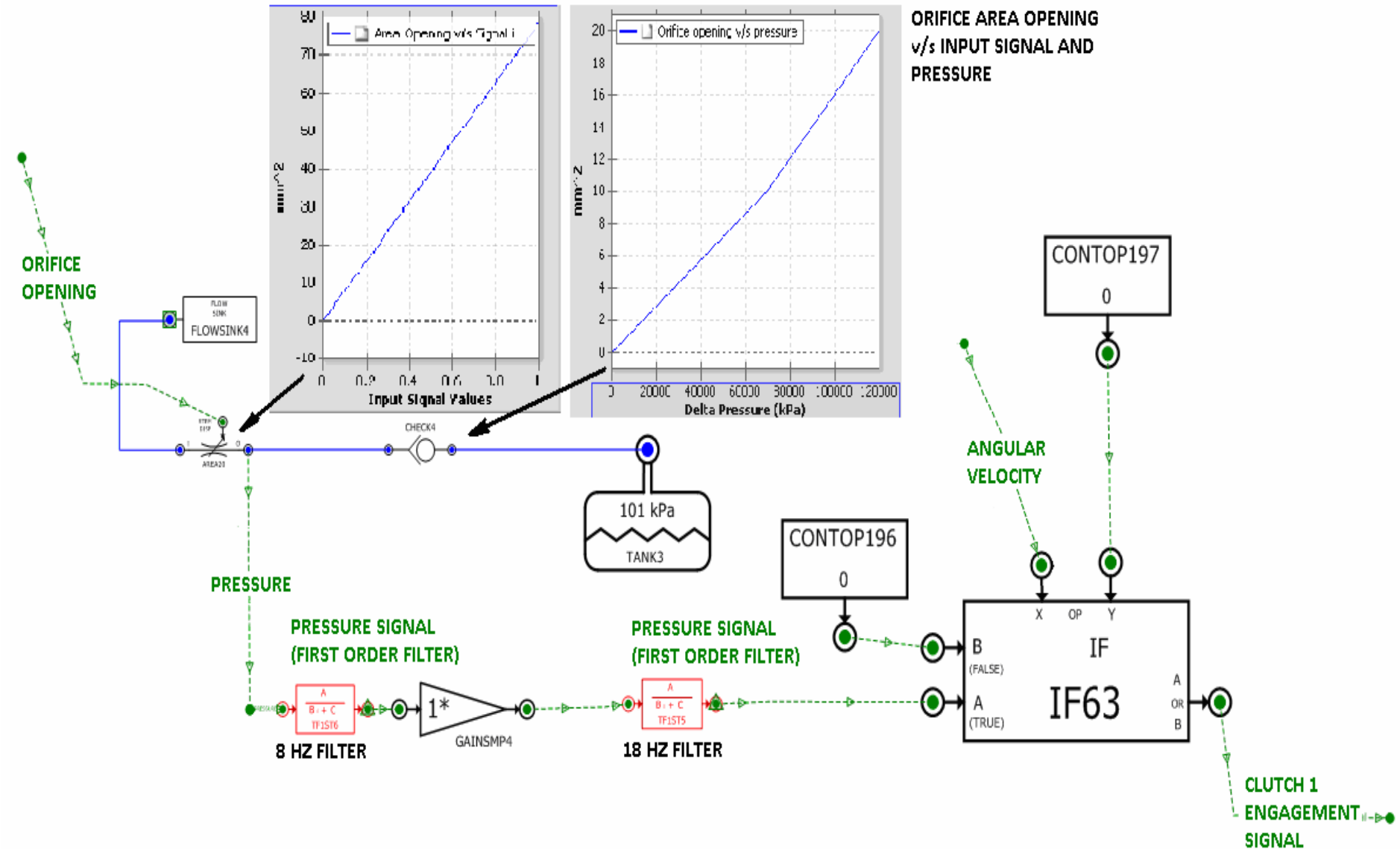

Fig 7.5 Modeled KERS clutch pressure system

7.1.3 Shift Control Logic

The shift control logic block is a simplistic system that determines the value of the input speed and adjusts the ring value for the CVT based on preset thresholds. This component allows for the compensation and hystersis of the input speeds such that switching has a slight overlap and the simulation does not crash because a point of discontinuity. Other components allow for the output from the transmission controller block to be in the form of discrete signals.

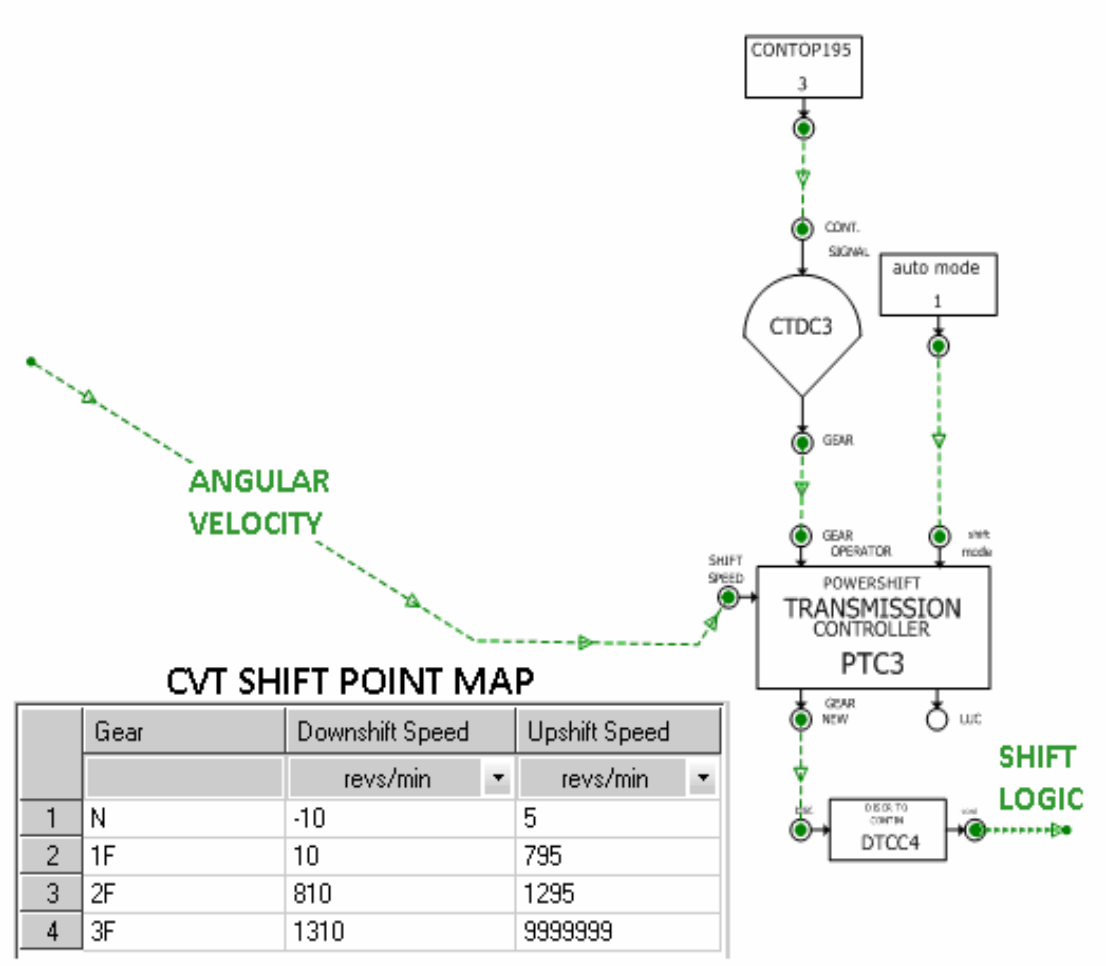

CVT SHIFT POINT MAP

	Gear	Downshift Speed	Upshift Speed
		revs/min	revs/min
1	N	-10	5
2	1F	10	795
3	2F	810	1295
4	3F	1310	9999999

Fig 7.6 Modeled KERS shift points system

7.2 Outline of Control System and Model

From Fig 5.2 we have an output from the controls ‘sflag’ which can have an output of 1 or 0 based on the state required. This is a direct input to the control area which determines the pressure on the output side of the valve. Closing this valve would result in a low pressure and opening it would result in a high pressure.

The pressure signal is an input to the clutch and the input source and the selection of the check valve cracking pressure is dependant on the pressure required to engage the clutch plates with out slippage. This pressure signal is passed through a first order filter to smooth any high frequency content and then engages / disengages the clutch.

7.3 Work cycle without Hybrid Drivetrain

In order to have a reference to monitor and measure the improvements / short comings of the suggested hybrid system, it is important to set up the baseline model. This model is will run exactly the same (event based) work cycle and in comparing these cycles to each other we can understand the improvements based on cycle time (productivity) and fuel efficiency (fuel burnt for the completion of the same events) . The figures will illustrate the various signals used to understand the work cycle and how it has potential areas in which we can design the controls to engage and disengage the KERS.

Figure 7.8 explains the truck loading cycle in a snapshot. The graphs are time based and they represent all the important variables that play an important part in the truck loading cycle. The variables represented are as below:

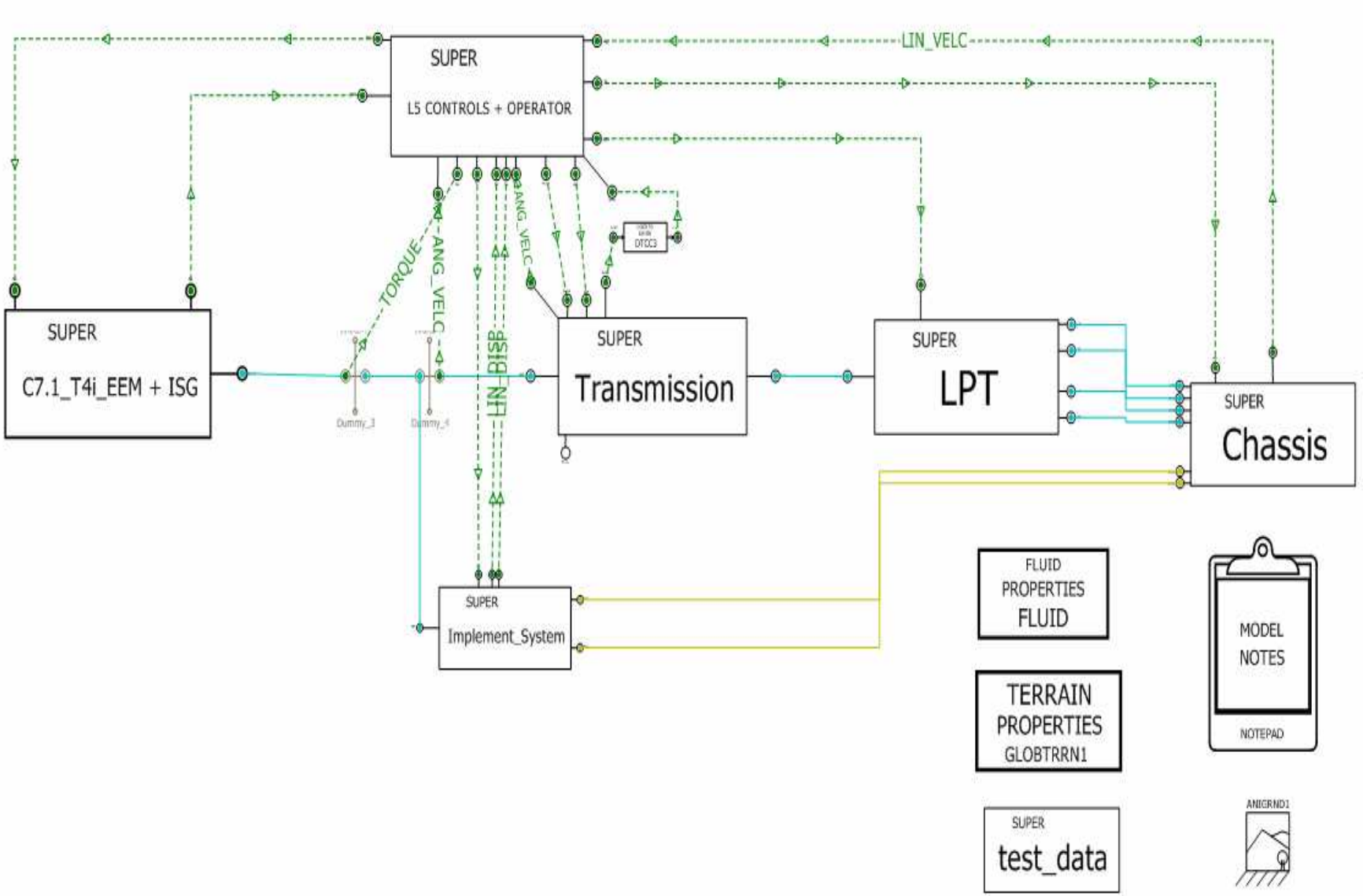

Fig 7.7 MWL VPD model – No KERS – Baseline

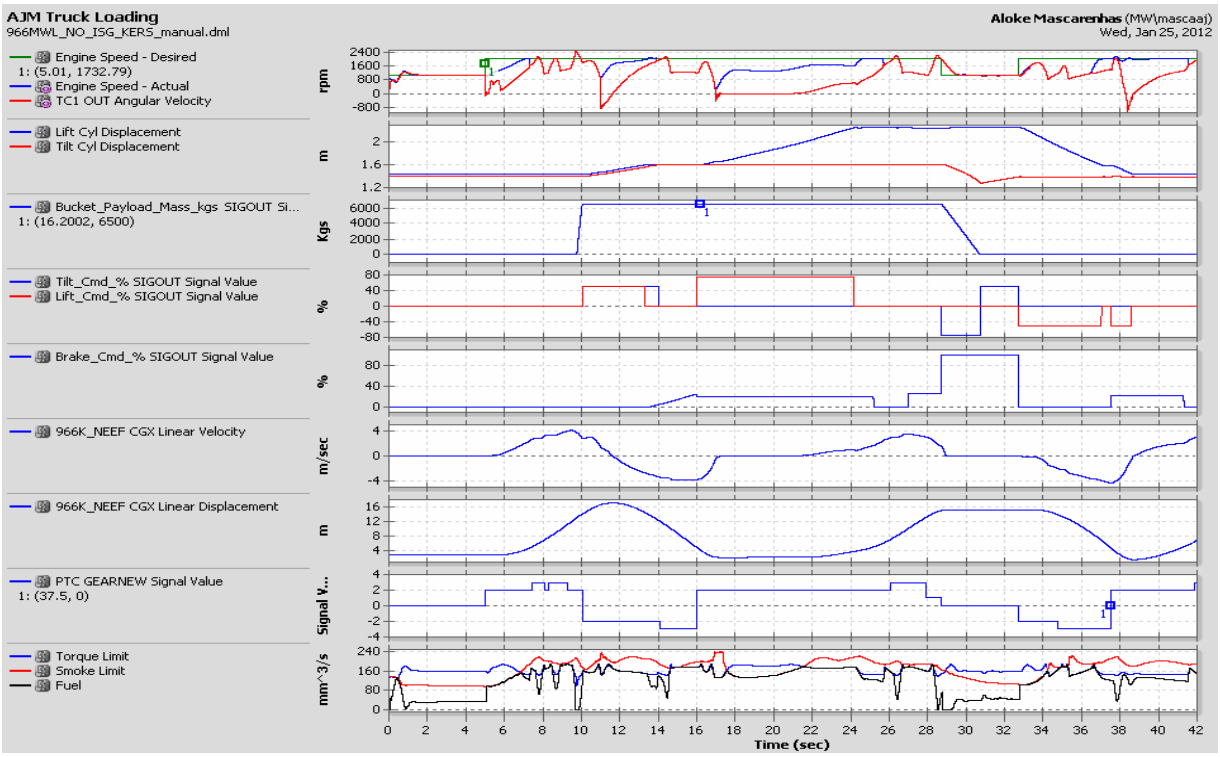

Fig 7.8 MWL Hybrid truck loading cycle plot – No KERS

1. Shaft speed
    - Actual engine output
    - Desired engine output
    - Torque converter output

2. Cylinder displacement
    - Lift Cylinder
    - Tilt Cylinder
3. Bucket Payload
4. Operator Lever Commands
    - Tilt Cylinder
    - Lift Cylinder
5. Brake command % value (operator command)

6. Vehicle linear velocity – NEEF
7. Vehicle linear displacement – NEEF
8. Gear position
9. Fuel Values
    - Torque Limit
    - Smoke limit
    - Actual Fueling

There are 2 points marked on the graph. These indicate the start and end of the cycle respectively. The first five seconds of the cycle are engine warm up, the first point indicates the same.

The end of cycle is identified by the point at which the payload is zero, the cylinders come to minimum position, the engine speed almost reached desired engine speed and the gear signal goes from negative to positive implying the machine moving towards the pile indicated as the second point on the graph.

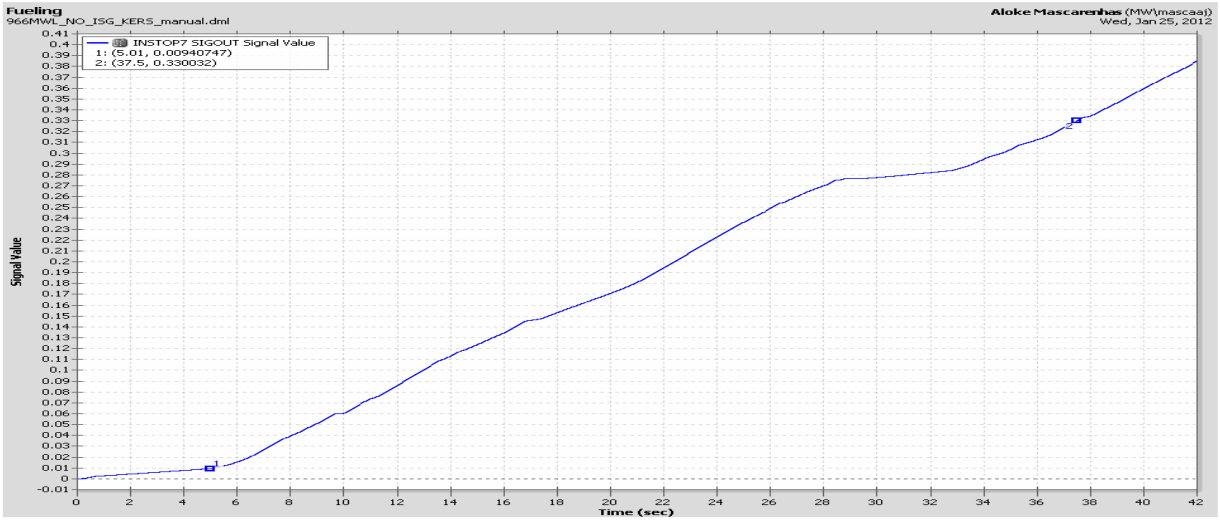

Fig 7.9 Fueling plot truck loading cycle – No KERS

The fig 7.9 indicates the summation of fuel as a function of time. By marking the points at which the cycle starts and ends we can obtain the cumulative fuel used in the cycle and measure fuel. Figure 7.10 shows the flow of torque to and from the engine, transmission and implement system. In later sections torque to the KERS System will also be shown.

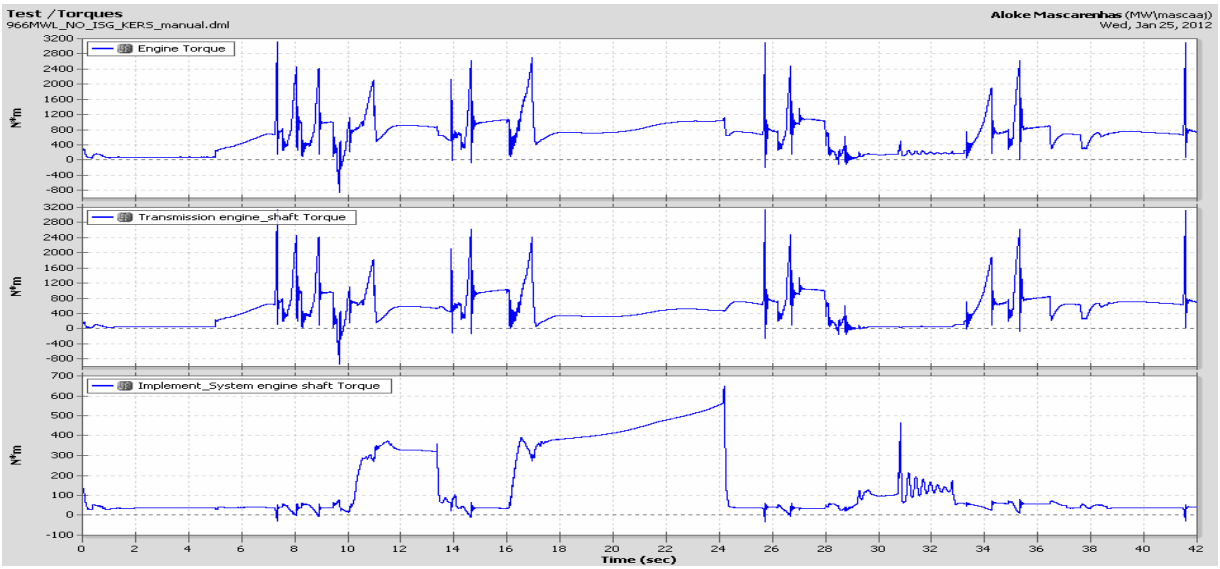

Fig 7.10 Torque plot truck loading cycle – No KERS

7.4 Work cycle with Hybrid Drivetrain

As discussed earlier, the modeled flywheel hybrid system has to be tested at various points along the transmission in order for us to understand how it reacts to the torque fluctuations in the truck loading cycle. In this section we can understand how the KERS reacts at all points along the drivetrain

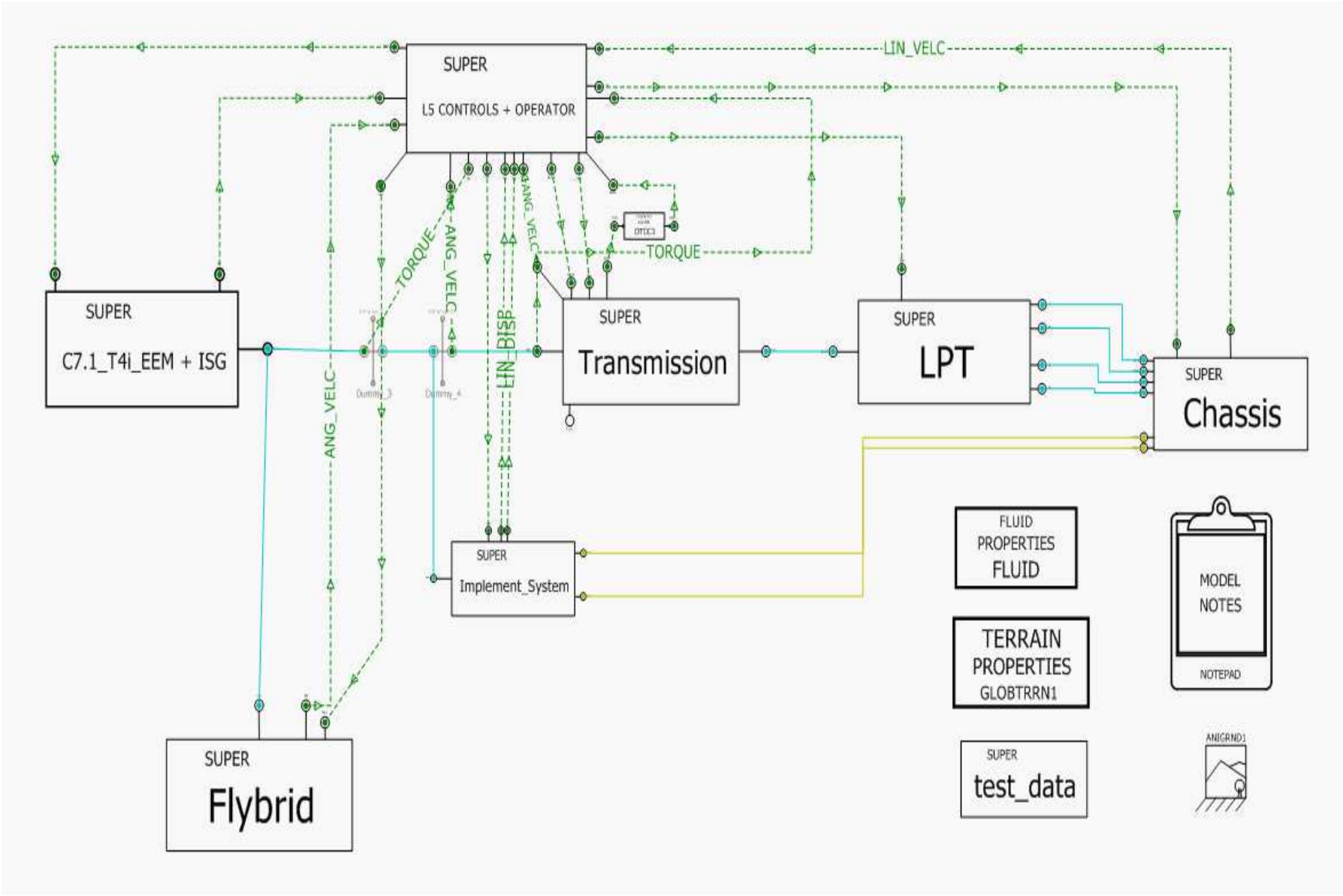

Fig 7.11 MWL VPD model –KERS active

Figure 7.11 illustrates the arrangement of the KERS System with respect to the drivetrain. The truck loading variables for a general system are as shown in figure 7.12.

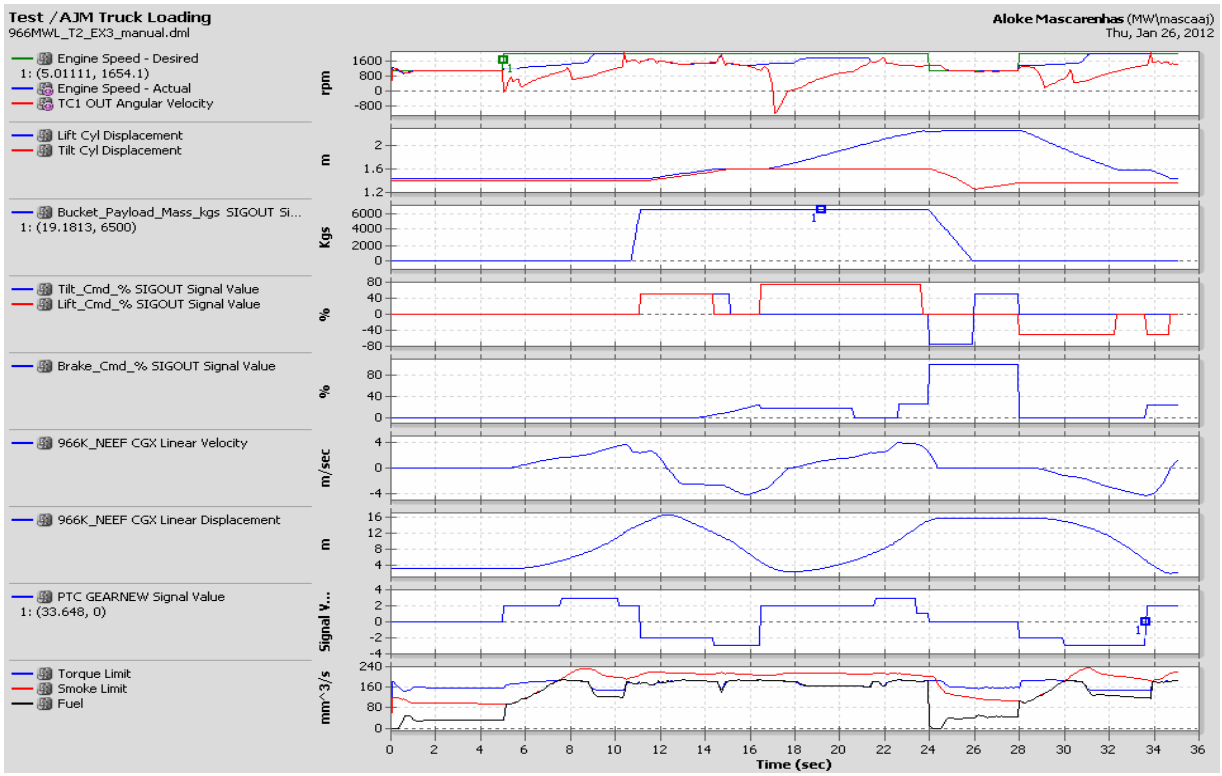

Fig 7.12 MWL Hybrid truck loading cycle plot – KERS active

Figure 7.13 represents the Fuel numbers that are indicative of cycle efficiency.

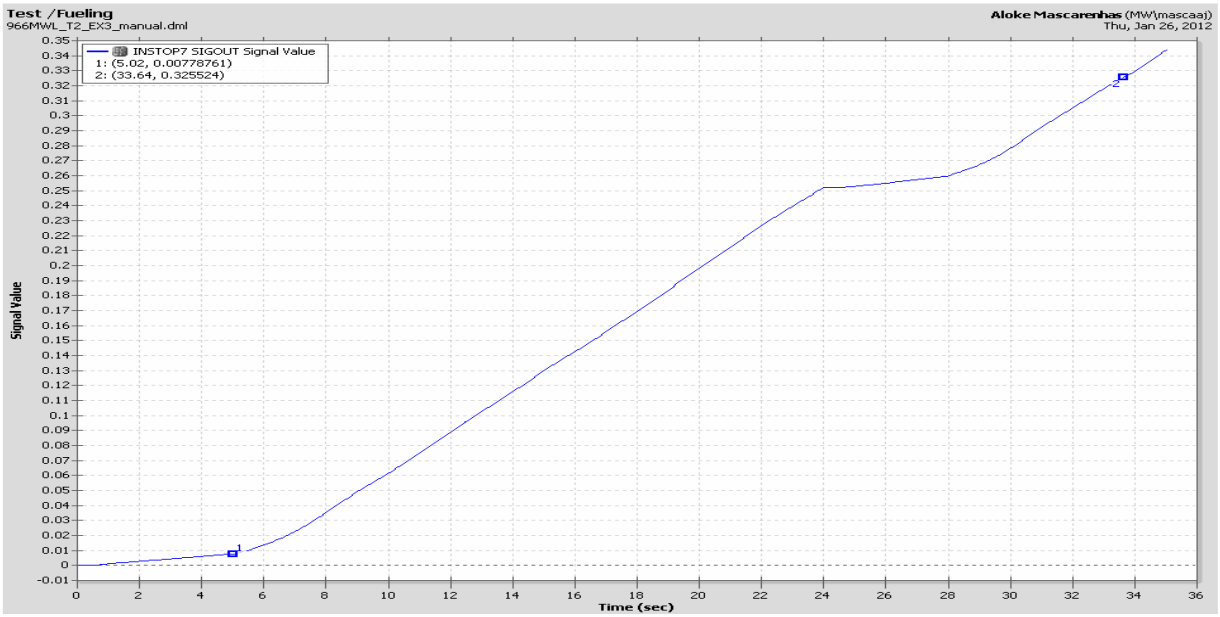

Fig 7.13 Fueling plot truck loading cycle – KERS active

Figure 7.14 represents torque at the Engine, Transmission, Implement system and torque to and from the KERS. Sign convention implies that positive torque is torque into the system.

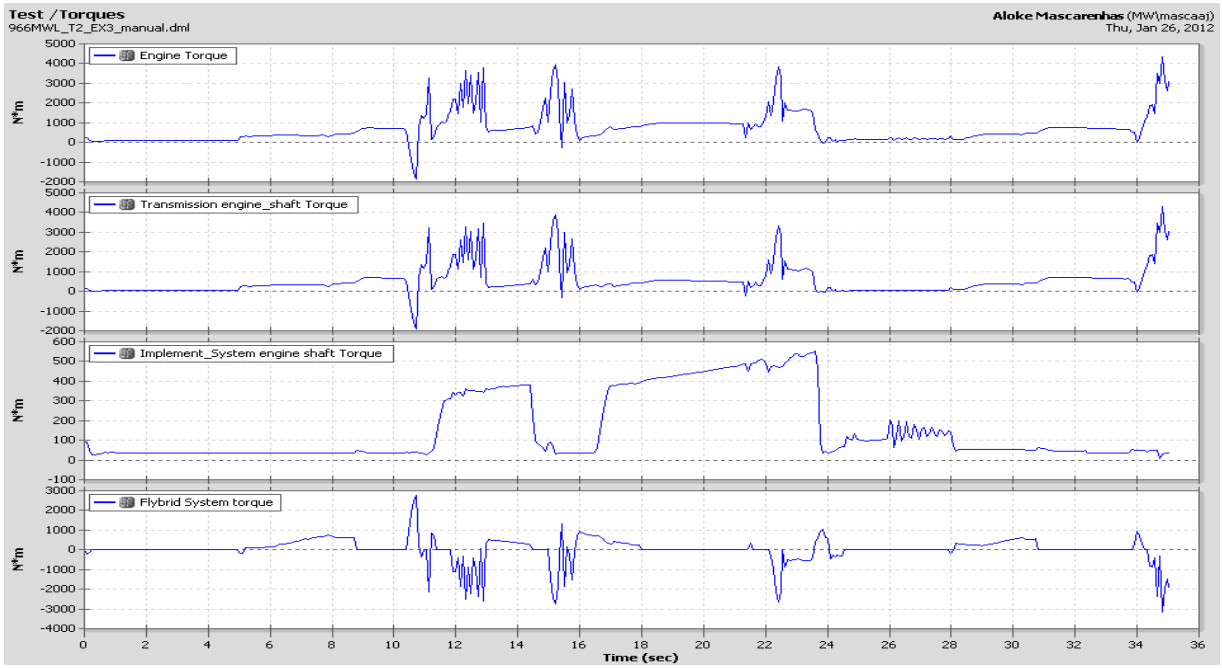

Fig 7.14 Torque plot truck loading cycle – KERS active

Figure 7.15 represents the capture and discharge signals from the controls, the CVT ring position and the flywheel speed for the entire cycle. Note that the flywheel speed is within 10 percent of the speed at the beginning of the cycle indicating that no extra energy has been given to the system.

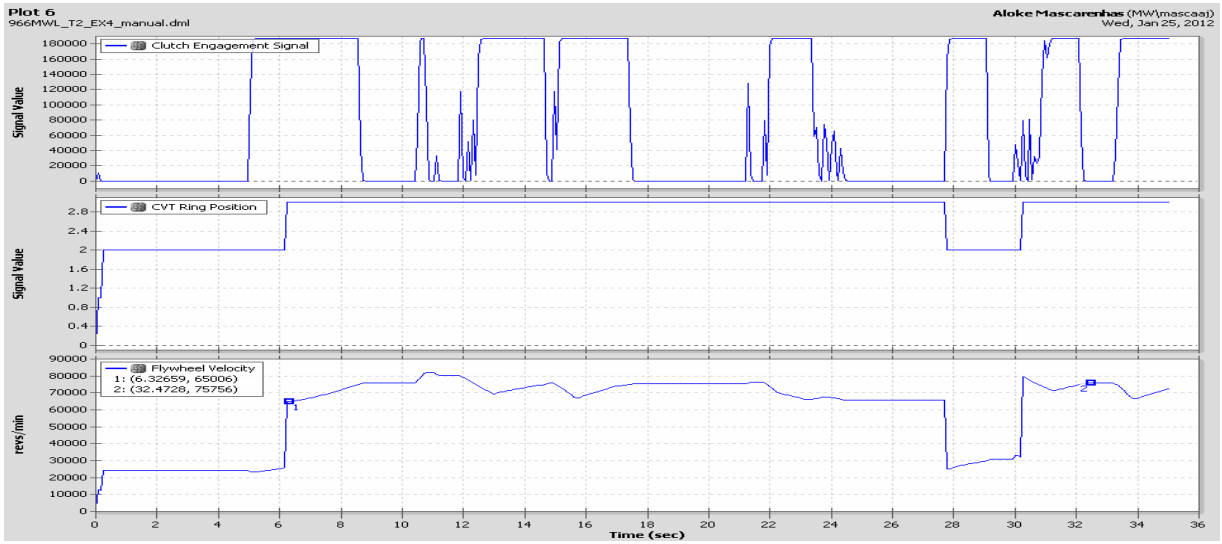

Fig 7.15 Active KERS parameters

7.5 Comparison of Results

In order to discuss and document the results at all points efficiently, various important parameters that have to be monitored across simulations have been plotted versus the position on the flybrid system on the drivetrain. This will give us a clear indication as to how the systems stack up to each others on a work cycle level. We can define three parameters that will allow us to quantify if the system developed works better than our baseline concept. They are:

1. Productivity - Number of tons of payload the machine can move in one hour
2. Fuel Consumption – Number of liters of fuel required per hour
3. Fuel Efficiency – Number of tons of payload that can be moved per liter of fuel consumed.

Analyzing the data from the graphs in the previous sub section and the remaining work cycles we can generate the following plots.

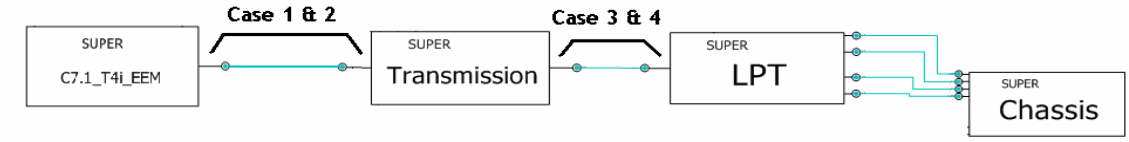

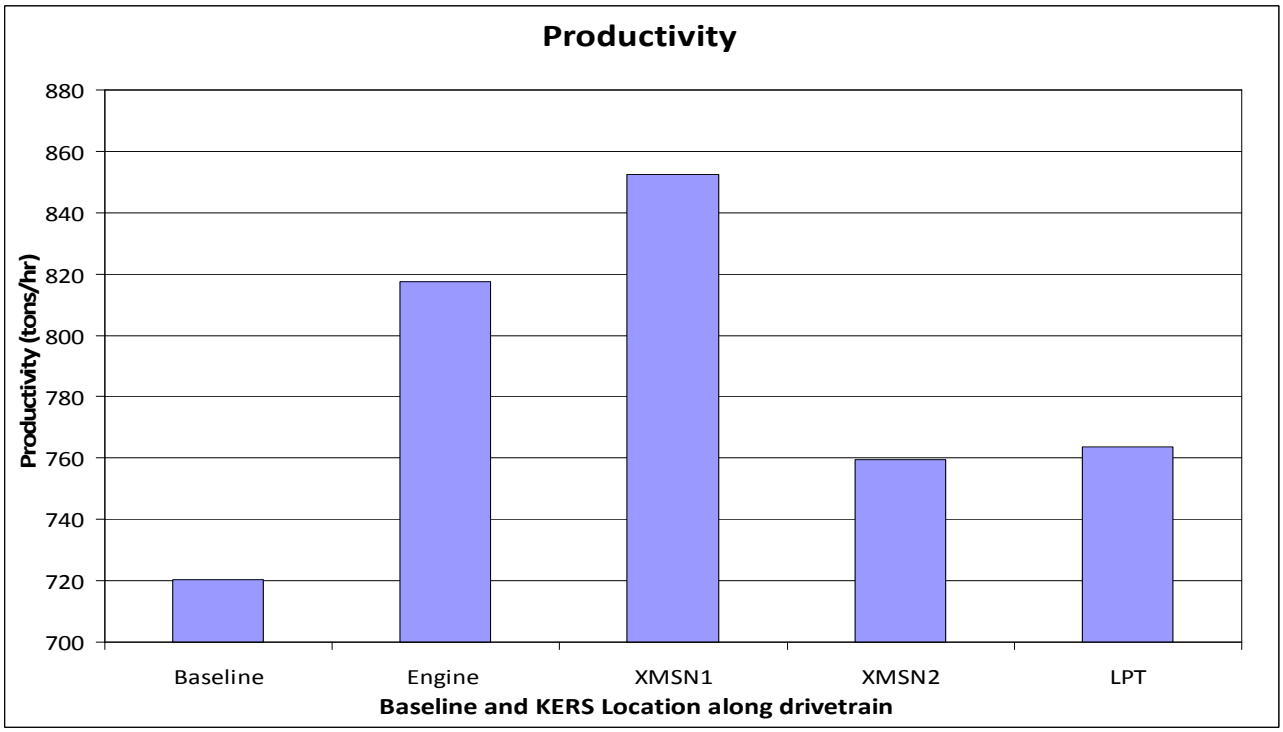

7.16.1 Productivity comparison of KERS System along the Drivetrain

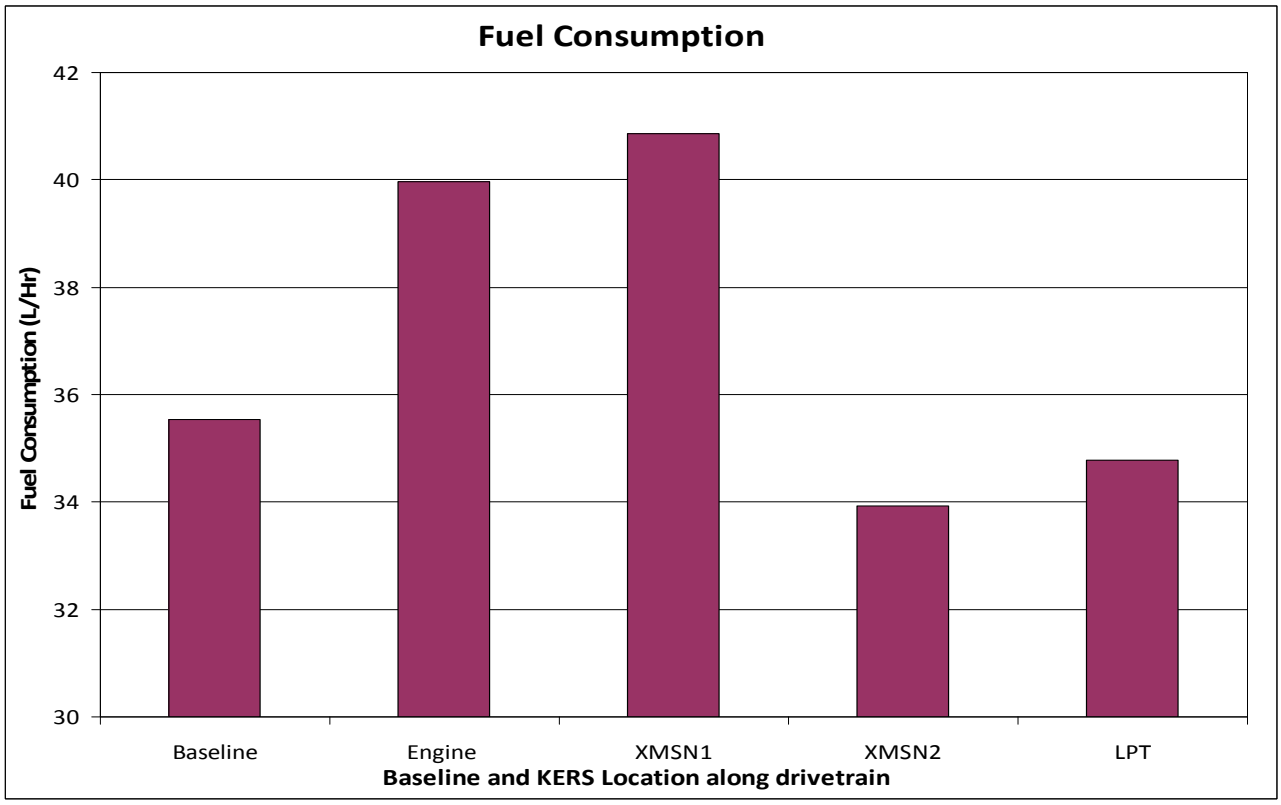

7.16.2 Fuel Consumption comparison of KERS System along the Drivetrain

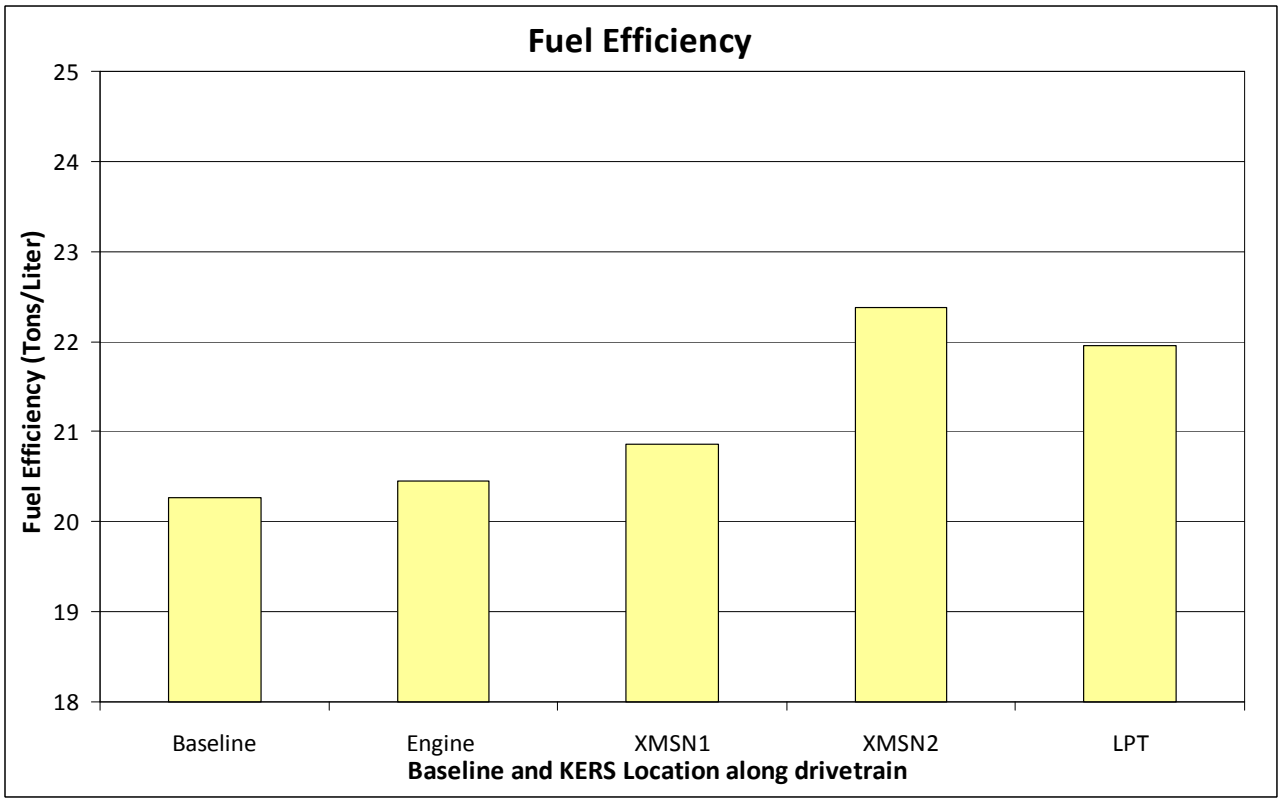

7.16.3 Fuel Efficiency comparison of KERS System along Drivetrain

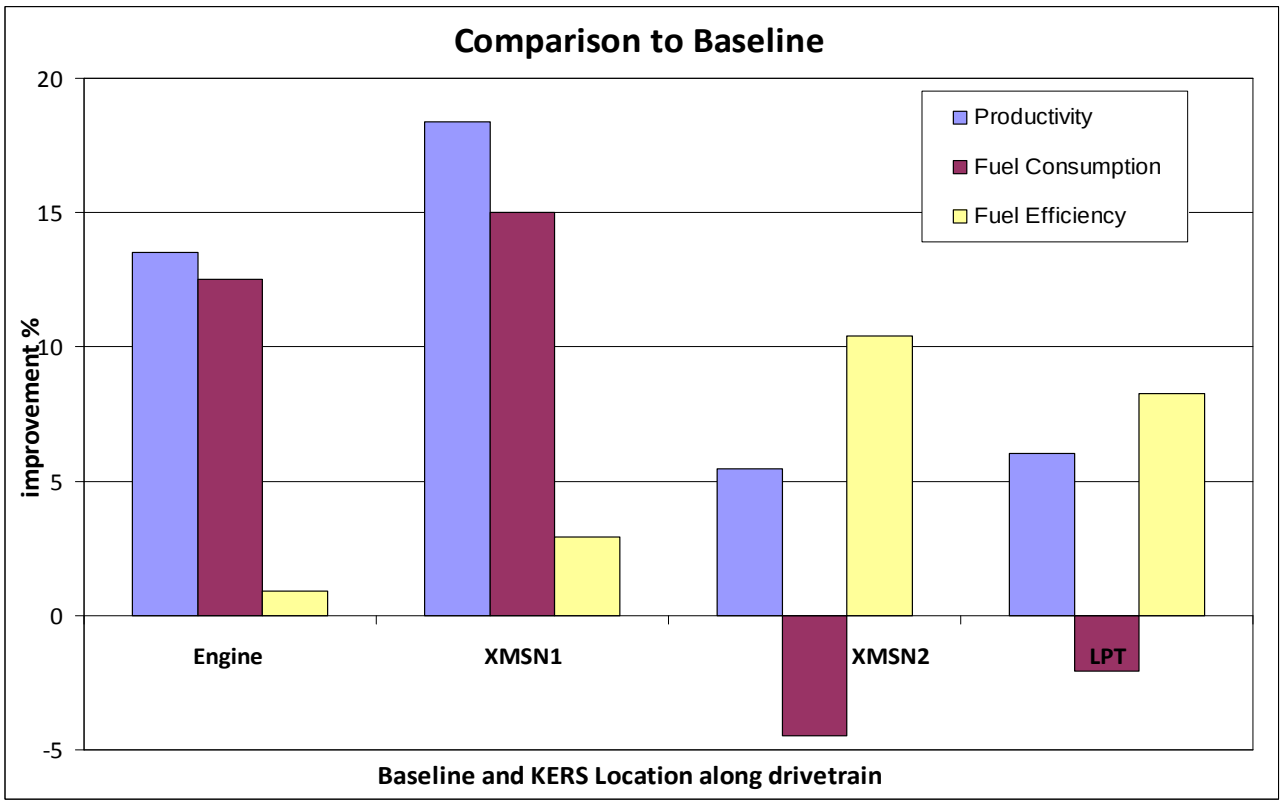

7.16.4 Comparison of Productivity, Fuel Consumption and Fuel Efficiency with respect to Baseline with KERS Active along Drivetrain

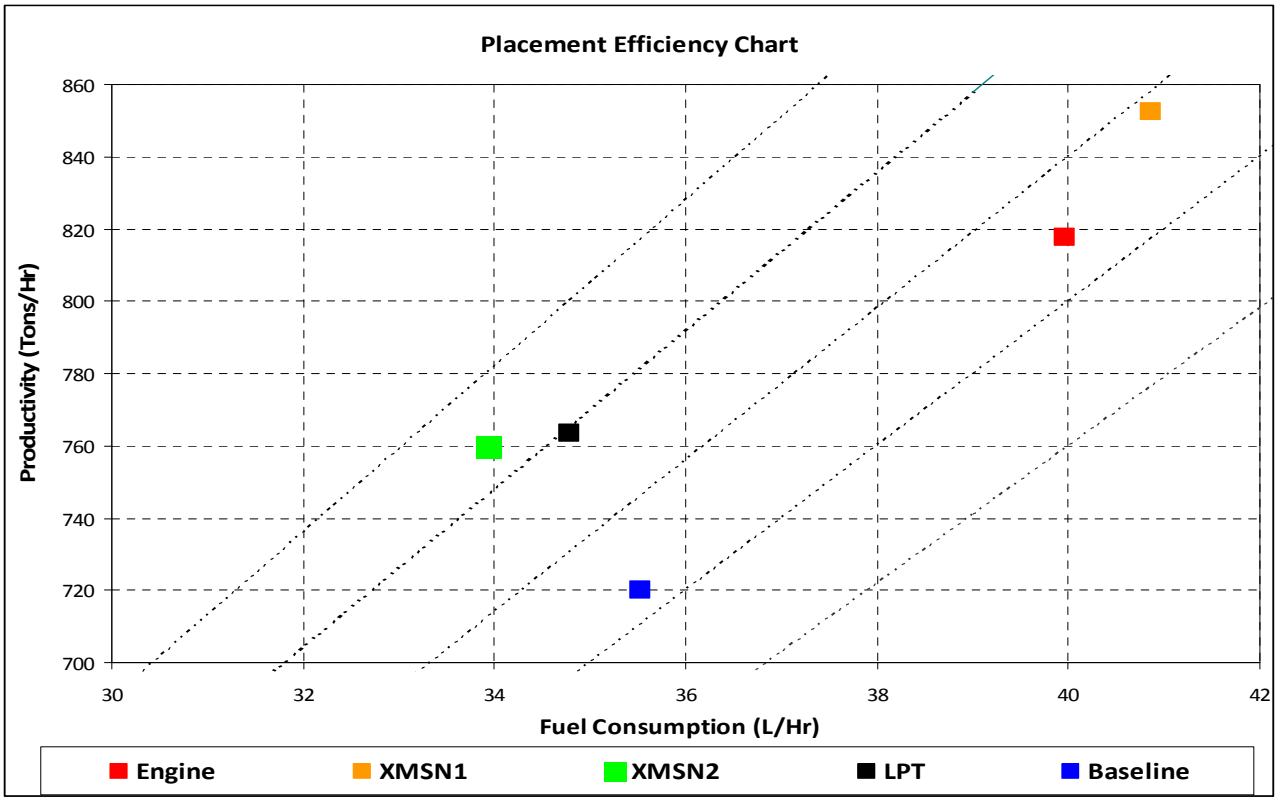

7.16.5 Placement Efficiency Chart

Refining the model and improving model confidence

On analyzing the results from the LPT (cases 3 and 4) more closely, we find there is a problem faced by the KERS in absorbing and discharging energy in when the vehicle moves in the reverse direction. The KERS engages when it meets the requirements for torque and speed as per the control criterion set, but due to the LPT drive shaft angular rotational direction being reversed, the energy stored up in the flywheel over the course of the cycle is discharged instantaneously. This is confirmed as a problem on the physical system as well. As a means to tackle this problem, it is suggested to model solutions in the virtual world to address this problem; we will explore two possible solutions.

1. Generate a new predictive control strategy using feed forward controls.
2. Modify the system hardware to react to changes in the direction of positive energy flow.

The previous control strategy, though effective in the forward part of the Drivetrain, faced 2 main problems with capture and discharge of torque downstream from the transmission. They are:

1. The discharge of torque from the flywheel is faster than the controls minimum time step, causing the flywheel energy to go below the designated SOC level.
2. The speeds downstream of the flywheel are inherently low and even though it is more efficient, it is at the limitation of the CVT as the optimum functioning of the flywheel depends on the maximum capture.

In order to address these problems we can compare the torque required at the LPT and the torque available at the KERS output. Knowing the time constant for discharge, it is easy to calculate the time for discharge and compare it with the minimum time step for the KERS controls to receive a feedback signal form the machine.

This torque estimator requires the following parameters:

1. CVT Shift Points – Ideally 25 to 40 data points would allow for a smooth transition, the 3 point map used in this model is an approximation as this is a directional study.
2. KERS System inertia and deceleration time constant – To calculate torque input to the CVT from the flywheel and calculate angular deceleration based on actual flywheel speed. This is a spec in the design of the KERS system that determines the discharge rate
3. CVT Torque and Speed Ratio Maps – To obtain the torque output from the CVT before factoring in clutch friction
4. Clutch Efficiency ratio - To obtain torque at the KERS System output factoring in clutch losses

The pseudo code for the control logic is as below:

1. Flywheel speed is taken as the input signal and based on the CVT speed ratios 3 speed bands can be defined.
2. Using event based logic, conditions are set to obtain net speed change available in the system at that time instant.
3. The net change in speed estimated is then multiplied with the deceleration time constant and moment of inertia to obtain the angular acceleration and the Torque as input to the CVT
4. The torque multiplied with the torque ratio for the respective speed band gives the actual torque at the output of the CVT
5. Using the clutch friction factor, the actual KERS torque out can be estimated.
6. If the torque request for is very high, the rate of discharge of flywheel energy is very high. If the flywheel discharges its stored energy before the controls can command the clutch disengagement, it will go below the threshold SOC. An upper limit can be specified after iteration to understand the optimal working range for the flywheel based on torque requests.
7. This becomes the new control criterion and is used to engage / disengage the KERS clutches.

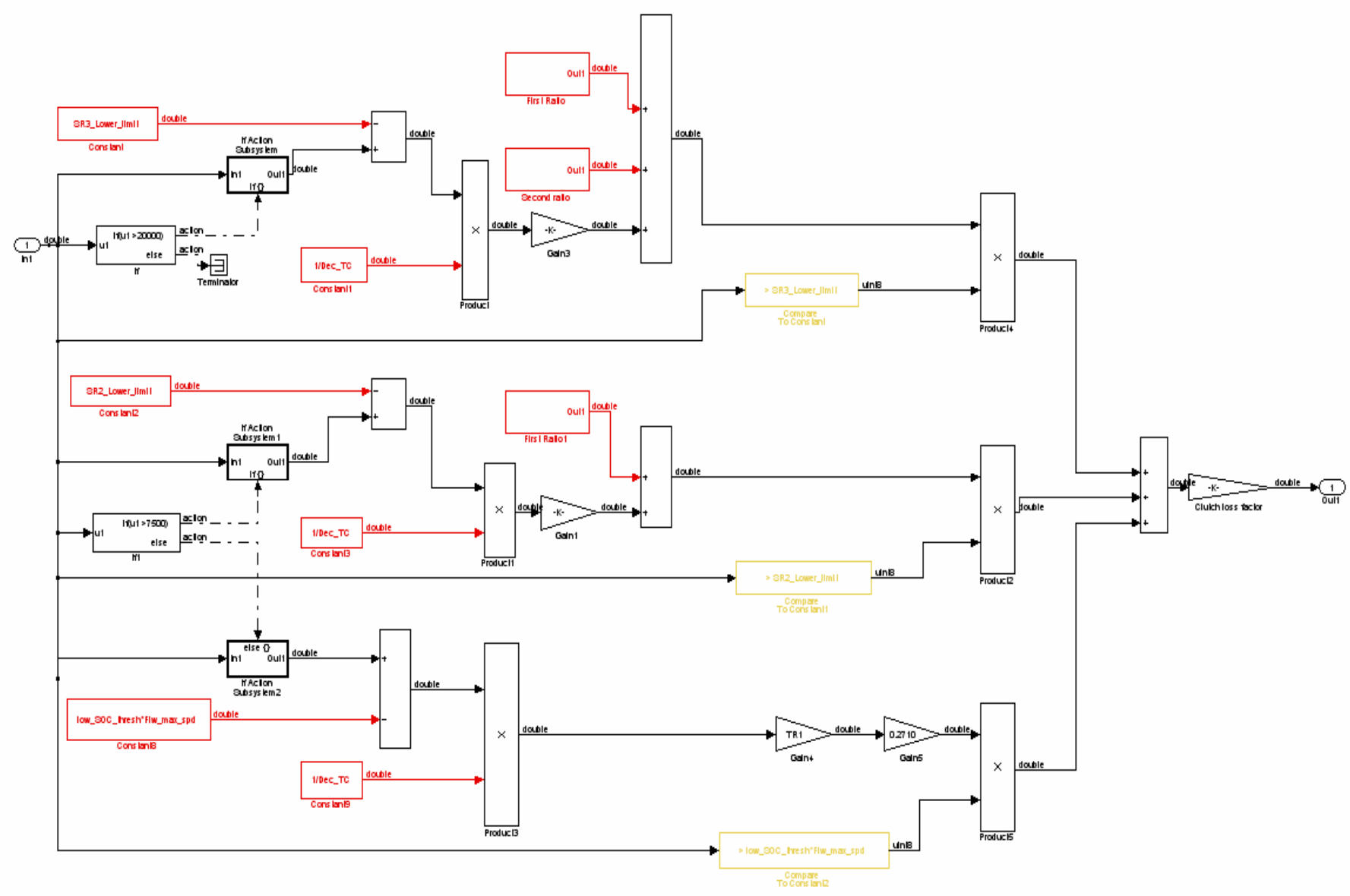

7.17.1 Flywheel Torque Estimator

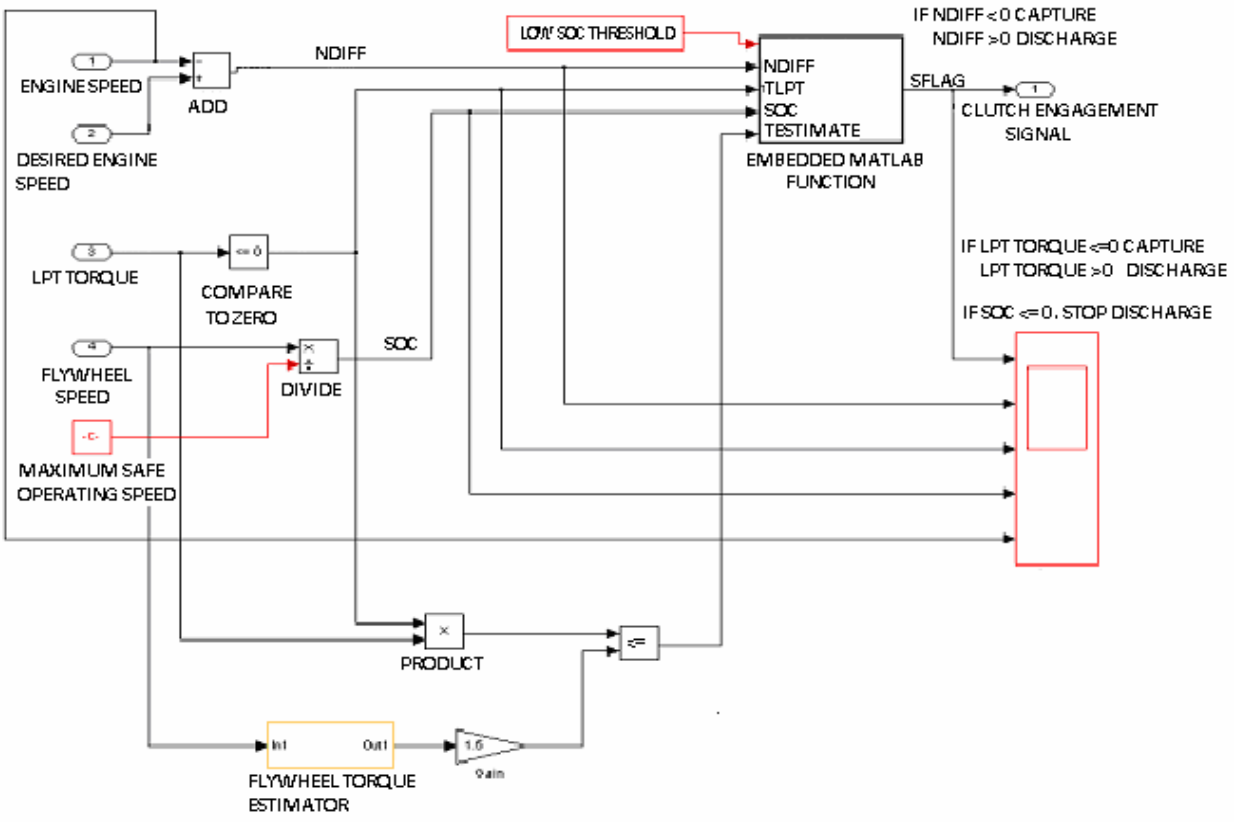

7.17.2 KERS controls with Flywheel Torque Estimator system

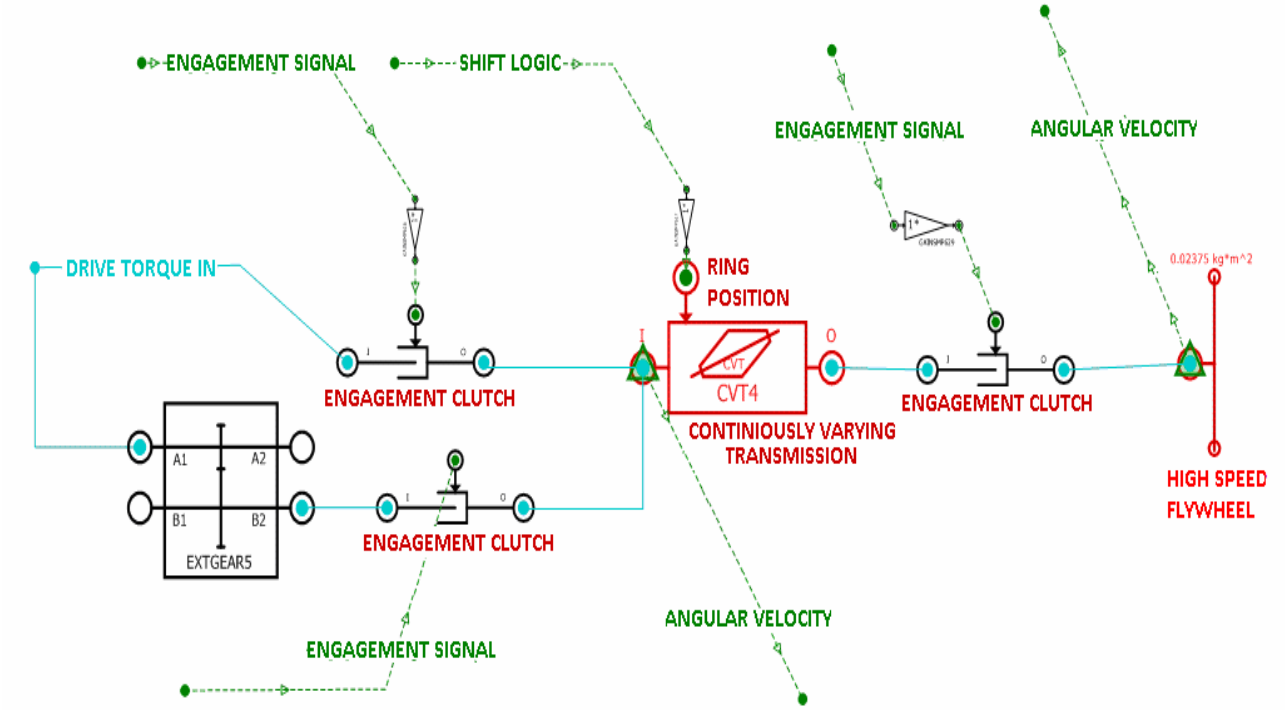

7.18 Proposed VPD / implementation solution

We can propose simple solution to change the direction of torque at the input.

1. Reverse idler gear.
2. Reverse engagement clutch.

The idler gear would be connected to a clutch which would receive the engagement and disengagement signals from the new control strategy. The reverse idler gear can be allowed to freewheel and as it has inertia will expect losses to the energy that is possible to be stored in the flywheel during the regular cycle, but this would allow us to harness the energy loss in the reverse cycle to allow for the net increase in fuel efficiency. In order to use the idler system we have to modify the machine level controls to interpret the direction of shaft rotation and be able to engage the reverse engagement clutch. This can be done by modifying the existing clutch engagement pressure to subsystem to compare the values of the angular rotation to zero and based on the result decide which clutch to engage. There will always be one clutch that is disengaged at any point during the work cycle. The fig 7.19 illustrates the schematic for the clutch pressure system with this change.

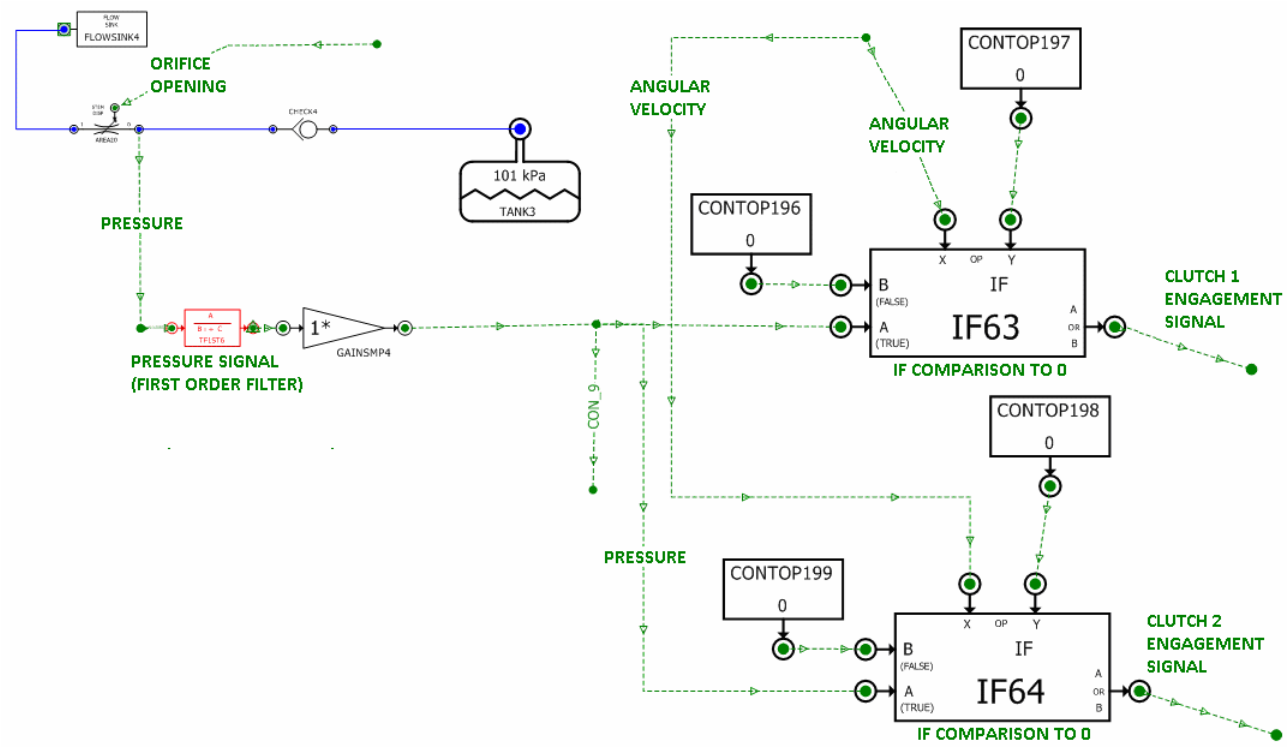

7.19 Proposed VPD solution – Clutch engagement

8. CONCLUSIONS AND FUTURE WORK

The Kinetic Energy Recovery System shows a significant improvement in machine performance when evaluated at different locations along the drivetrain. This system improves productivity (tons per hour), in the range of 5 to 18%. A substantial reduction in fuel consumption (liters per hour), in the range of 2 to 5%, is seen when it is modeled in the lower powertrain. There is also a significant improvement in fuel efficiency (tons per liter), in the range of 5 - 10%, when the KERS is placed after the transmission. The optimum location for the KERS as per VPD is at the output of the transmission. Based on the predictions with VPD, the KERS at this location on the drivetrain will improve fuel efficiency (tons per liter of fuel consumed) by 10%, reduce the fuel consumed (liters per hour) by 4% and improve productivity (tons per hour) by 5% when compared to the same machine with no KERS.

The model in here is a concept evaluation model and must undergo a lot more testing and validation before it can predict with accuracy in future simulations. There is work to be undertaken in the following areas:

1. Obtaining well sampled data points for the CVT maps and the shift point maps.
2. Set up a series of tests like speed sweeps with ramp up ramp down commands and verify the test data with the model with the same commands and inputs.
3. Proposed changes in the controls have to be evaluated and tested with various test scenarios before it can be used for future predictions.
4. Care to be taken to schedule the clutches to operate in tandem, because of high frequency content that the physics based components cannot respond to. Proper signal filtering is required before the model is to be run.

CITED LITERATURE

[1] Cetinkunt, S.: “Mechatronics”, John Wiley & Sons Inc., 2007.

[2] Ingram, R.: “Hydraulics and Powertrain Training Course”. Caterpillar Inc., 2011

[3] Ehsani, M., et al: “Modern Electric, Hybrid Electric, And Fuel Cell Vehicles, Fundamentals, Theory, and Design”, PPCRC Press, 2010

[4] Cornell, S.: “Dynasty Hydraulics Training Course”, Caterpillar Inc., 2008

[5] Vroeman, B.: “Component Control for the Zero Inertia Powertrain” 2001

[6] Actipower Inc : “White paper 112 : Understanding Flywheel Energy Storage: Does High-Speed Really Imply a Better Design” ,2008

[7] Croce, F: “Optimal Design of Powertrain and Hydraulic Implement Systems for Construction Equipment Applications” 2010

[8] Fuda Machinery Inc. website: www.fudamachinery.com

[9] Gale Banks Engineering Inc. website: www.bankspower.com

[10] Tamor, M.A.: “Control System and Control Method for a Hybrid Electric Vehicle Powertrain”, U.S. 6,746,366 B2, June 8, 2004.

[11] AutoRepairHelp Inc. website: www.auto-repair-help.com

[12] Monarch Bearing Company Inc. website: www.monarchbearing.com

[13] CAT performance handbook, 38th Edition. Caterpillar Inc 2008

[14] Flybrid Systems LLP. website: www.flybrid.com

[15] Fluid Power Handbook & Directory – 1998/1999

[16] Burr, A.H.; “Mechanical Analysis and Design”, Elsevier, New York, 1982

[17] Yamaguchi, K., et al.: “Hybrid Vehicle”, U.S. 6,488,608 B2, December 3, 2002.

[18] Kimura, T., et al.: “Charging/Discharging Control Method for Secondary Battery”, U.S. 6,573,687 B2, June 3, 2003.

[19] Shen, S., and Veldpaus, F.E.: “Analysis and Control of a Flywheel Hybrid Vehicular Powertrain”, IEEE Transaction on Control Systems Technology, Vol. 12, No. 5, pp. 645-660, 2004.

[20] Schlurmann, J., and Schroder, D.: “Compensation of Dynamic Torques and Flywheel Start in a CVT Based Hybrid Powertrain”, Proceedings of IEEE International conference on Control Applications, pp. 2456-2461, October 2006.

[21] Diego-Ayala, U., et al.: “A Simple Mechanical Transmission System for Hybrid Vehicles Incorporating a Flywheel”, IET HEVC, pp.1-8, 2008.

[22] Cross, D., and, Brockbank, C.: “Mechanical Hybrid System Comprising a Flywheel and CVT for Motorsport and Mainstream Automotive Applications”,SAE World Congress & Exhibition, 09PFL-0922, 2009.

[23] Katrasnik, T., et al.: “Analysis of Energy Conversion Efficiency in Parallel and Series Hybrid Powertrains”, IEEE Transactions on Vehicular Technology, Vol. 56, No.6, pp. 3649-3659, 2007.

[24] Jang, S., et al.: “A Study on Regenerative Braking for a parallel Hybrid Electric Vehicle”, KSME International Journal, Vol. 15, No. 11, pp.1490-1498, 2001.

[25] Katrasnik, T.: “Analytical Method to Evaluate Fuel Consumption of Hybrid Electric Vehicles at Balanced Energy Content of the Electric Storage Devices” Journal of Applied Energy, Vol. 87, pp. 3330-3339, 2010.

[26] Flynn, M.M., et al.: “Performance Testing of a Vehicular Flywheel Energy System”, SAE Advanced Hybrid Vehicle Powertrains, pp. 119-126, 2005.

[27] He, L., et al.: “A Novel Continuously Variable Transmission Flywheel Hybrid Electric Powertrain”, IEEE Vehicle Power and Propulsion Conference, Harbin, September, 2008.

[28] Jain, et al.: “A text Book of Engineering Chemistry”-, Dhanapatrai Publications, New Delhi.

[29] Hui,S., et al.: “ Control Strategy of Hydraulic/Electric Synergy System in Heavy Hybrid Vehicles”, Energy Conversion and Management, Vol. 52, pp. 668-674, 2011

[30] Mathews, J.C., et al.: “Development and Implementation of a control System for Parallel Hybrid Powertrain”, IEEE Vehicle Power and Propulsion Conference, pp.1-6, 2006.

[31] Lei, Z., et al.: “Development of Hybrid Powertrain Controller for a PSHEV”, IEEE Vehicular Electronics and Safety, pp.222-227, Beijing, 2006.

[32] Borhan, H.A. et al.: “Predictive Energy Management of a Power-Split Hybrid Electric Vehicle”, American Control conference, pp. 3970-3976, June 2009.

[33] Kirk, D.E.: “Optimal Control Theory, an Introduction”, New York, Dover Publications Inc., 1998.

[34] Grammatico, S., et al.: “A Series-Parallel Hybrid Electric Powertrain for Industrial Vehicles”, IEEE, Vehicle Power and Propulsion Conference, pp. 1-6, 2010.

Annexure A

Truck Loading Plots

KERS at Transmission Input

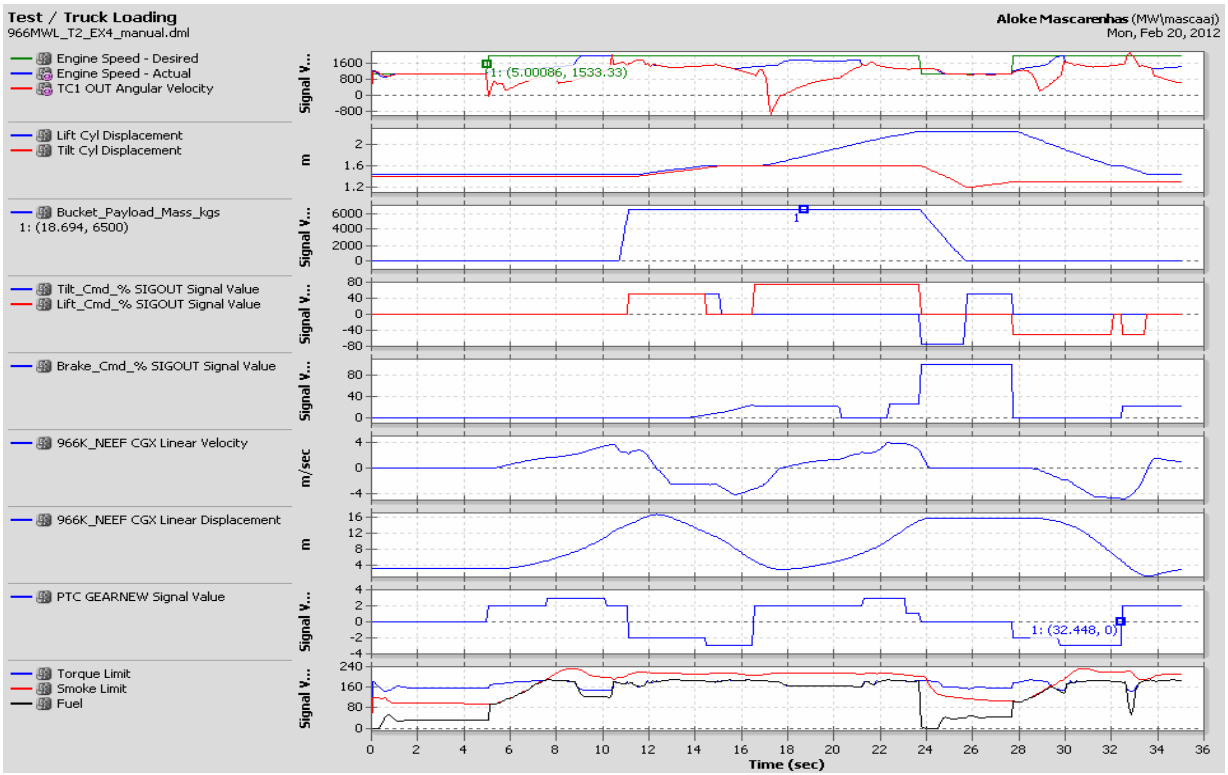

Truck Loading Cycle

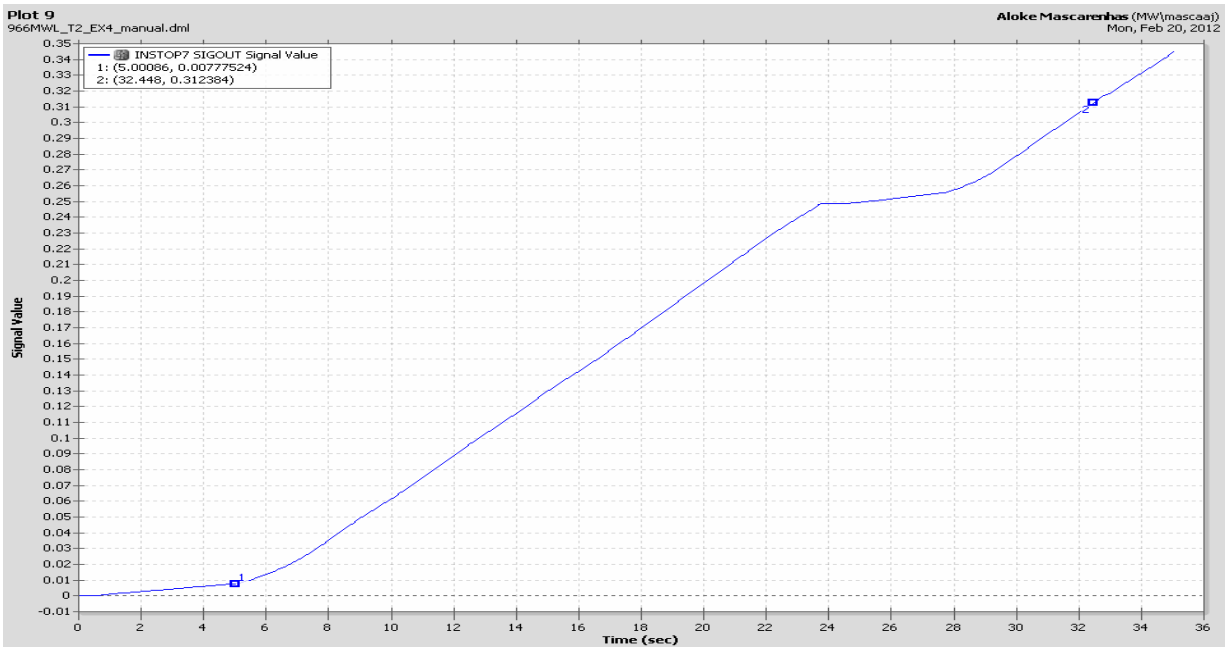

Fueling Plot

Annexure A (contd …)

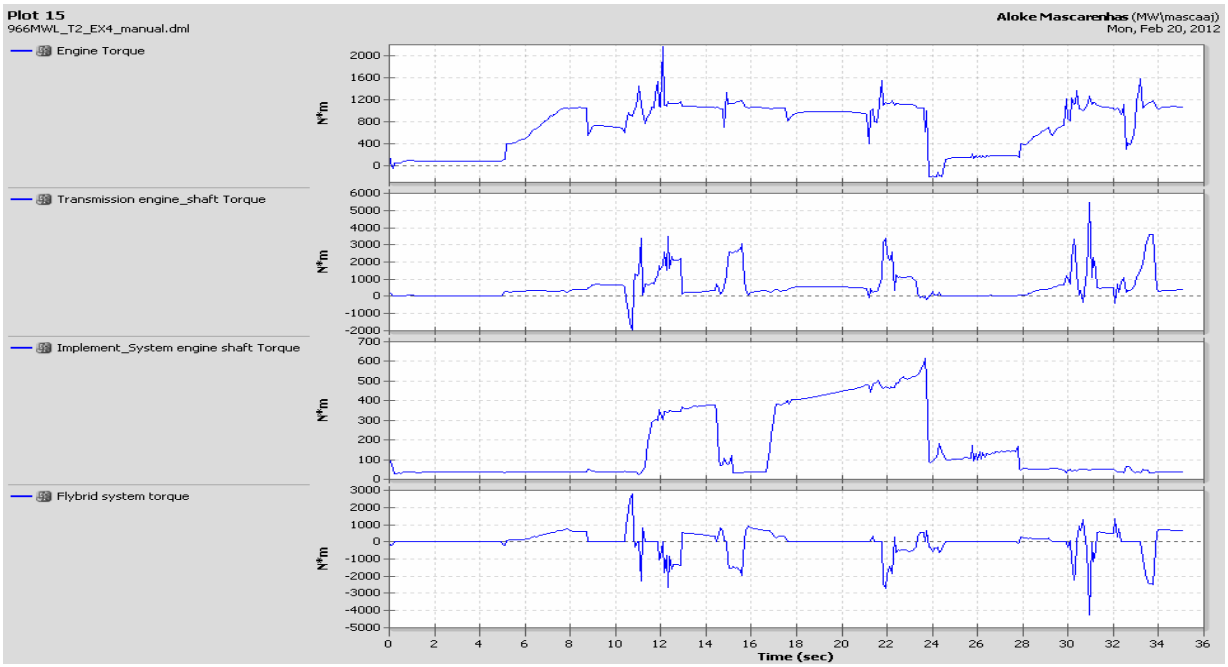

Torque Plot

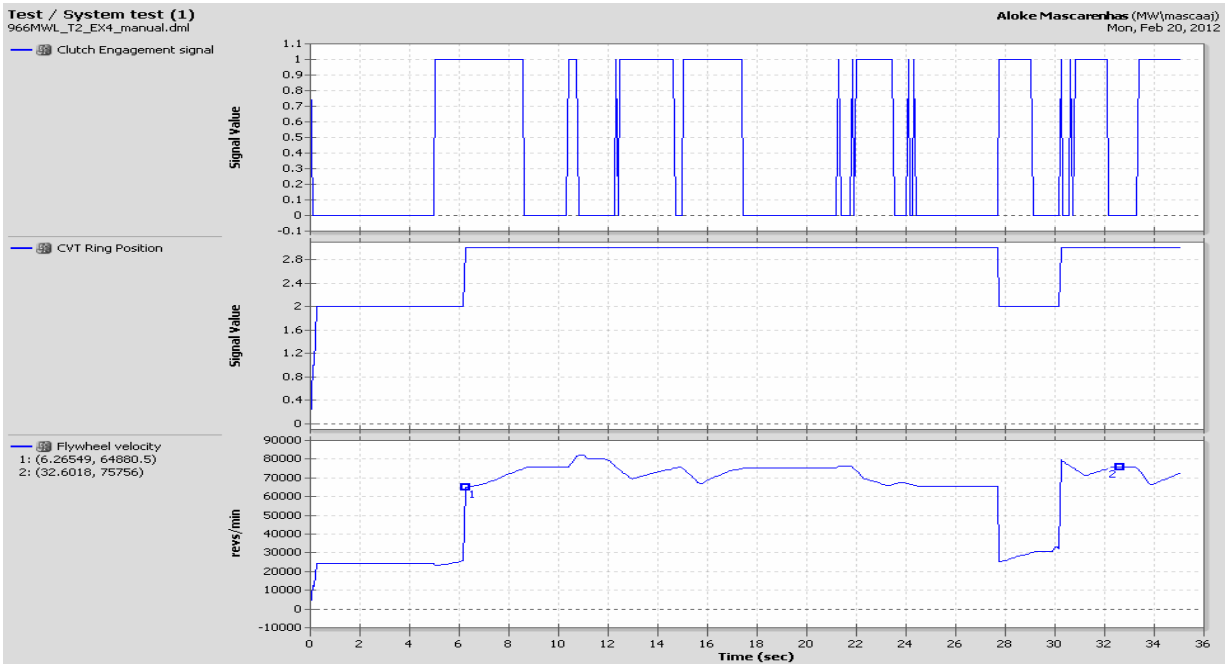

Active KERS parameters plot

Transmission output

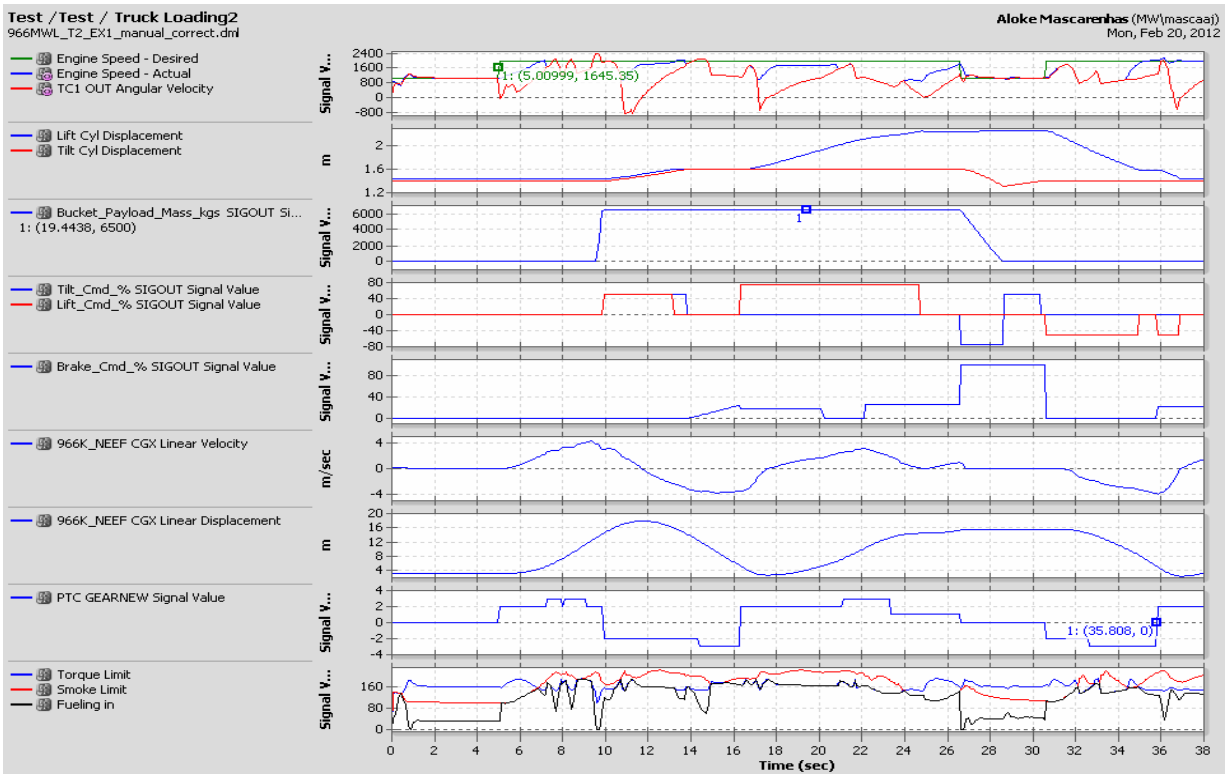

Truck Loading Cycle

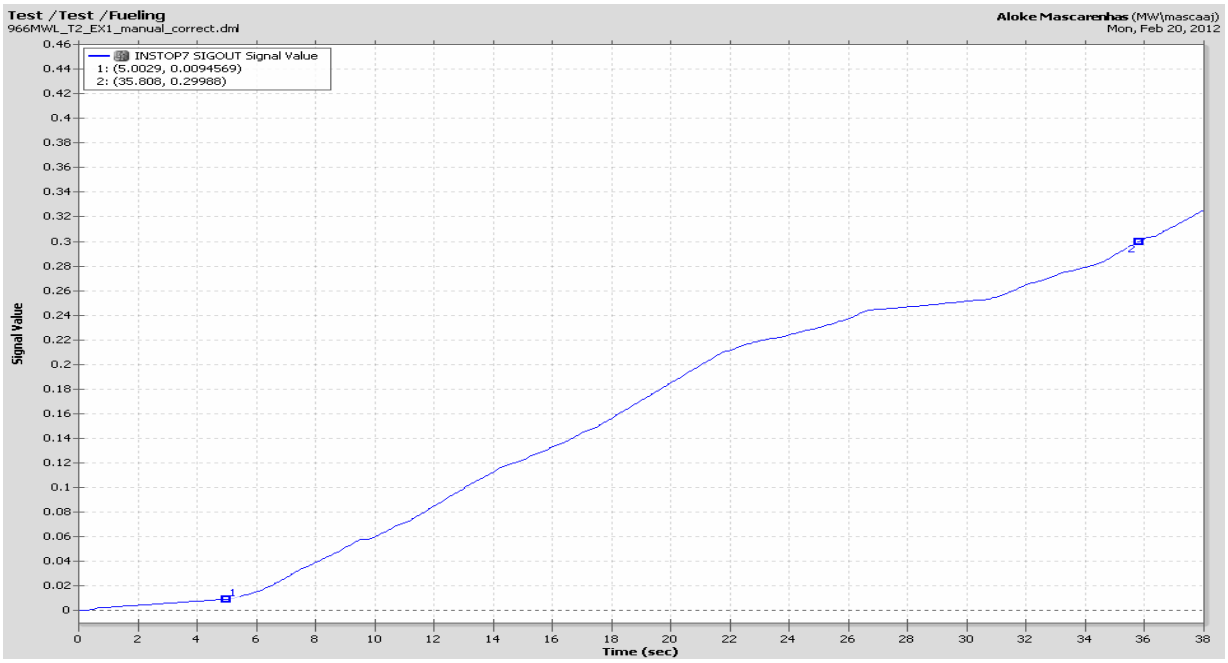

Fueling Plot

Annexure A (contd …)

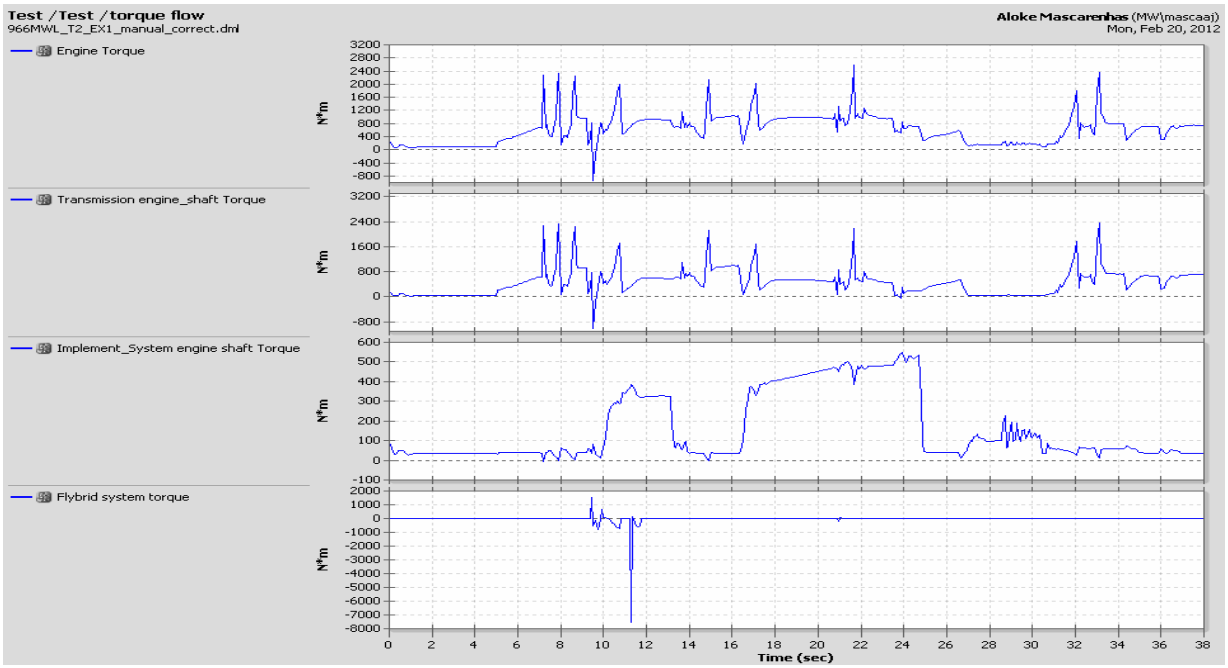

Torque Plot

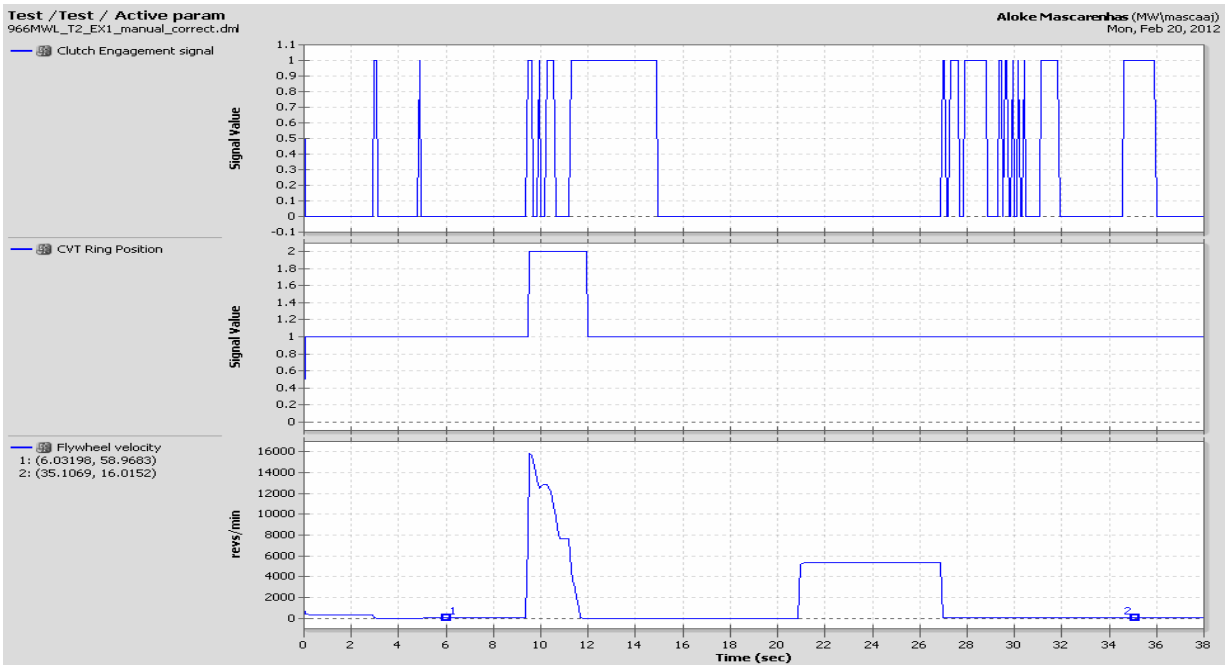

Active KERS parameters plot

Lower Powertrain

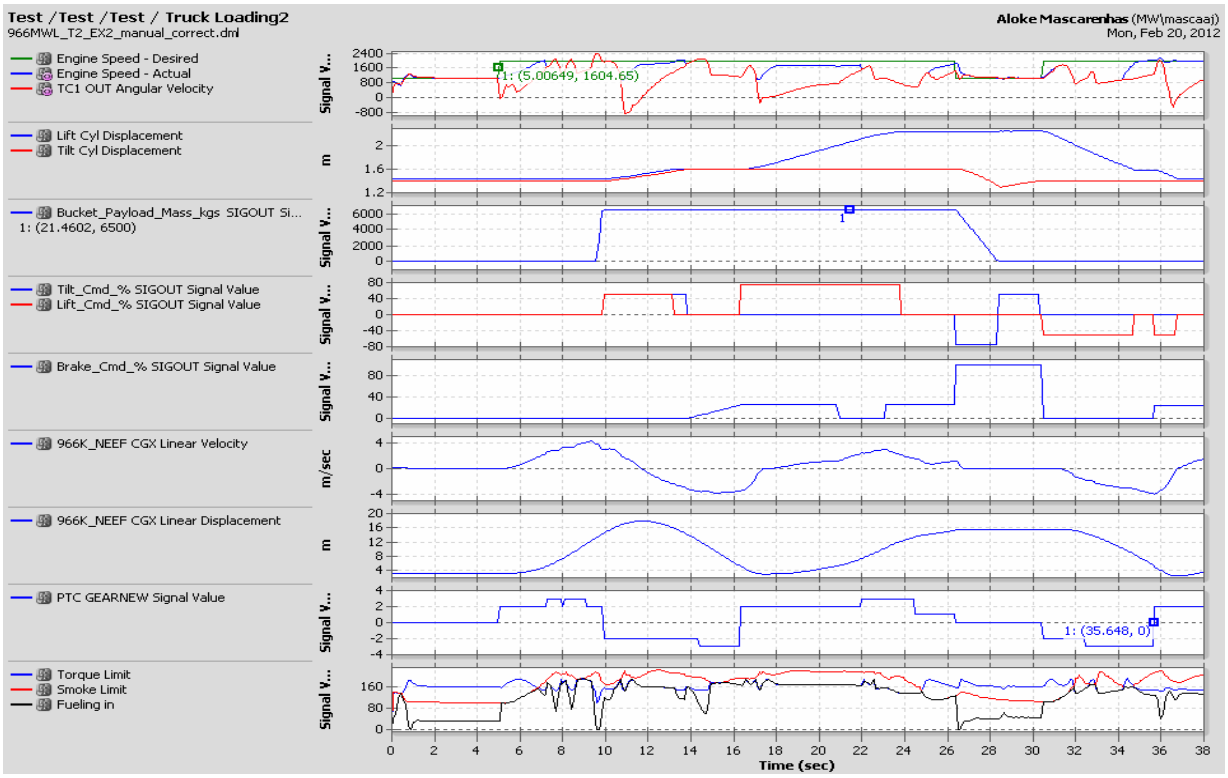

Truck Loading Cycle

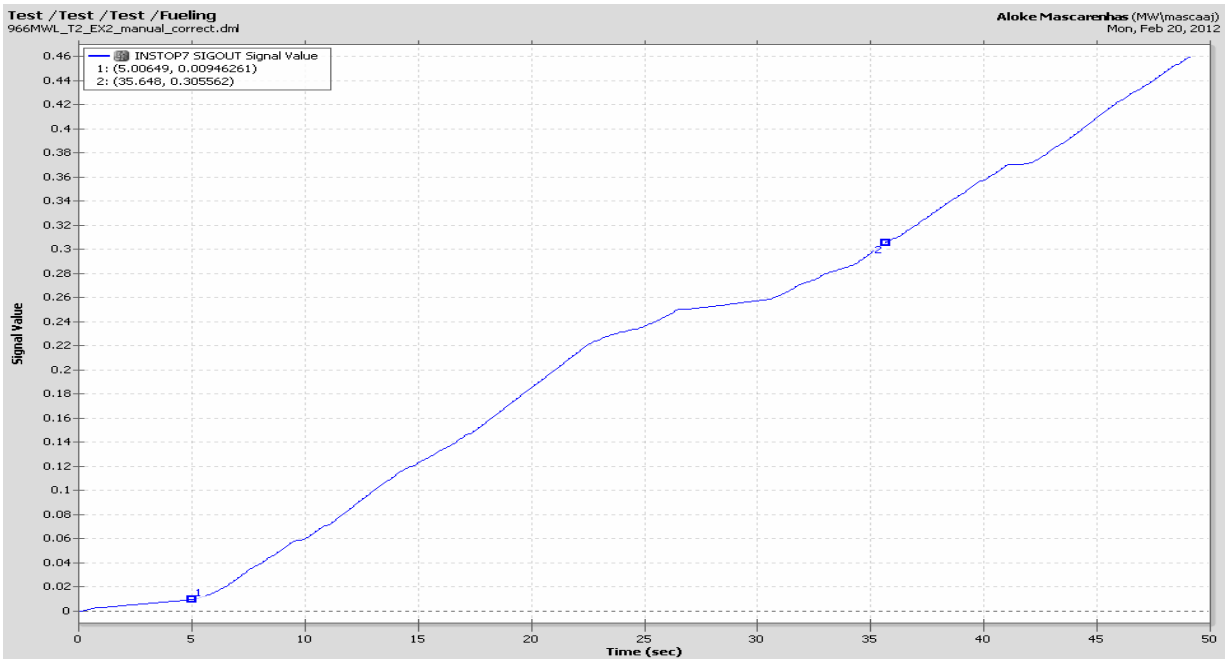

Fueling Plot

Annexure A (contd …)

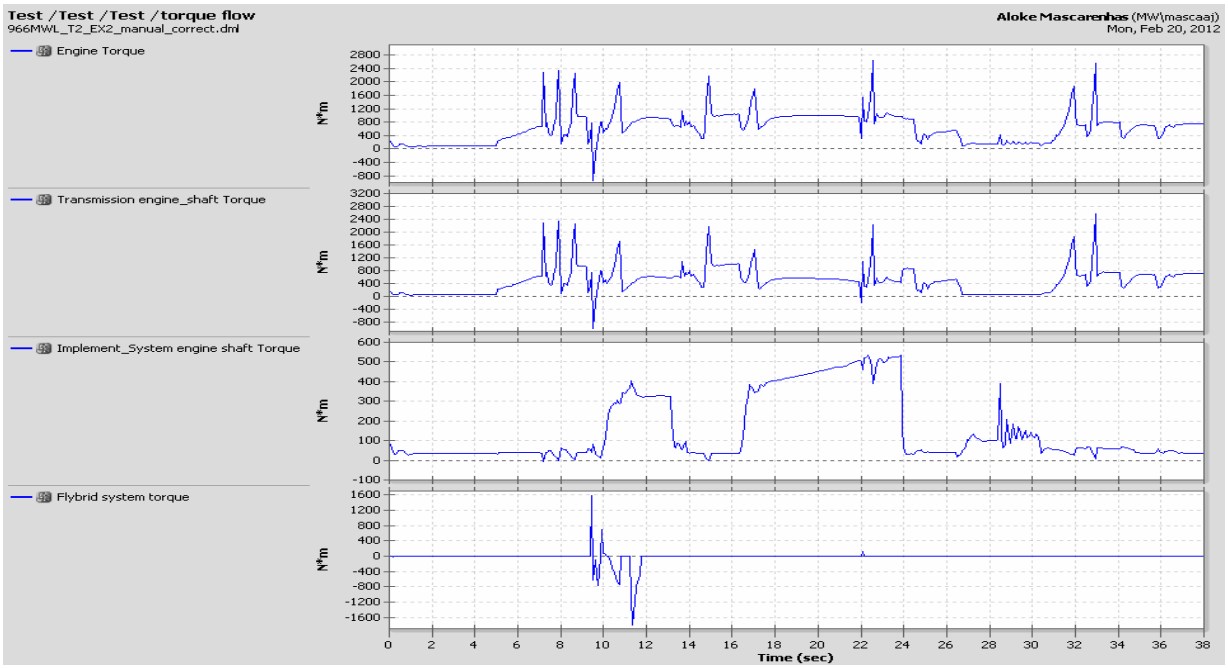

Torque Plot

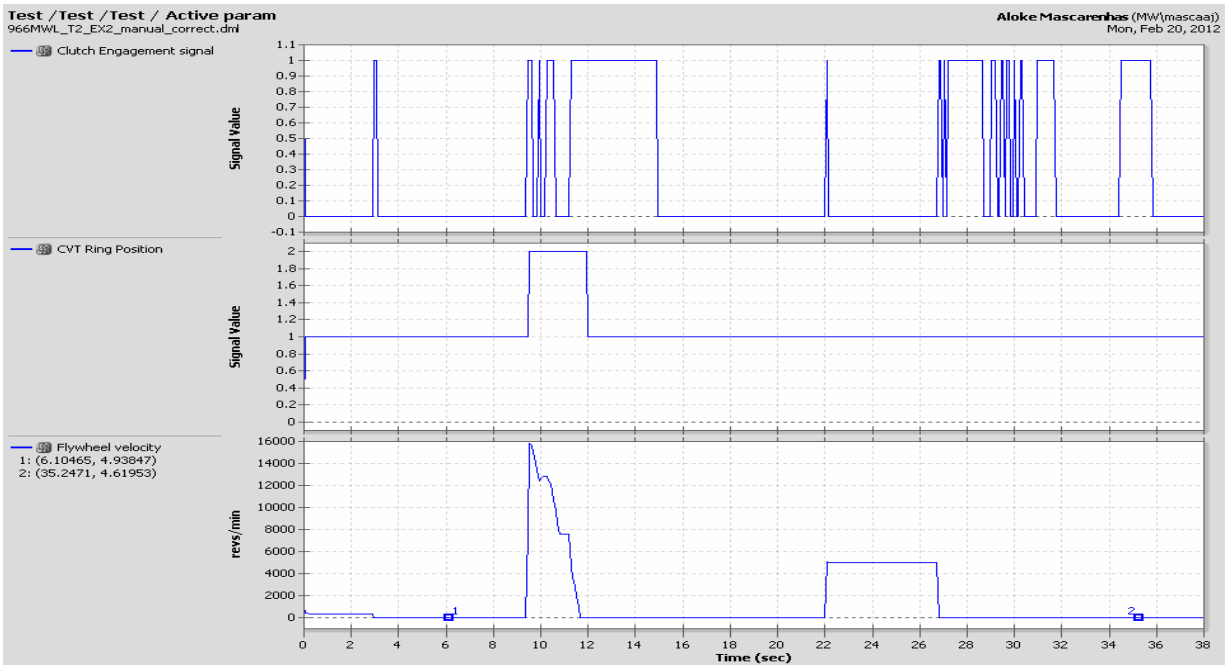

Active KERS parameters plot

ANNEXURE B – Machine specs

Engine		
Engine Model	Cat® C11 ACERT™	
Gross Power – SAE J1995	213 kW	286 hp
Net Power – ISO 9249	195 kW	262 hp

- Caterpillar engine with ACERT™ Technology – EPA Tier III, EU Stage III Compliant

Buckets		
Bucket Capacities	3.4-4.2 m³	4.5-5.5 yd³

Weights		
Operating Weight	23 698 kg	52,254 lb

- For 4.25 m³ (5.5 yd³) general purpose bucket with BOCE

Operating Specifications		
Static Tipping Load, Full Turn	15 474 kg	34,120 lb

- For 4.25 m³ (5.5 yd³) general purpose bucket with BOCE

Operating Specifications

Bucket		General Purpose Buckets					
		Teeth	Teeth and Segments	Bolt-On Edges	Teeth	Teeth and Segments	Bolt-On Edges
Rated Bucket Capacity (§)	m³ yd³	3.50 4.50	3.65 4.75	3.65 4.75	3.65 4.75	3.80 5.00	3.80 5.00
Struck Capacity (§)	m³ yd³	2.96 3.88	3.10 4.06	3.10 4.06	3.12 4.08	3.27 4.27	3.27 4.27
Width (§)	mm ft/in	3145 10'4"	3145 10'4"	3059 10'0"	3145 10'4"	3145 10'4"	3059 10'0"
Dump Clearance at Full Lift and 45° Discharge (§)	mm ft/in	3005 9'10"	3005 9'10"	3154 10'4"	2968 9'9"	2968 9'9"	3119 10'3"
Reach at Full Lift and 45° Discharge (§)	mm ft/in	1389 4'7"	1389 4'7"	1247 4'1"	1411 4'8"	1411 4'8"	1270 4'2"
Reach with Lift Arm Horizontal and Bucket Level (§)	mm ft/in	2857 9'4"	2857 9'4"	2652 8'8"	2900 9'6"	2900 9'6"	2695 8'10"
Digging Depth (§)	mm in	78 3.07	108 4.25	108 4.25	78 3.07	108 4.25	108 4.25
Overall Length	mm ft/in	8995 29'6"	8995 29'6"	8770 28'9"	9038 29'8"	9038 29'8"	8813 28'11"
Overall Height with Bucket at Full Raise	mm ft/in	5775 18'11"	5775 18'11"	5775 18'11"	5814 19'1"	5814 19'1"	5814 19'1"
Loader Clearance Circle with Bucket in Carry Position (§)	mm ft/in	14 733 48'4"	14 733 48'4"	14 528 47'8"	14 756 48'5"	14 756 48'5"	14 550 47'9"
Static Tipping Load Straight *	kg lb	17 763 39,167	17 401 38,369	17 585 38,775	17 649 38,916	17 290 38,124	17 475 38,532
Static Tipping Load Full 37° Turn	kg lb	15 824 34,892	15 480 34,133	15 665 34,541	15 717 34,656	15 375 33,902	15 560 34,310
Breakout Force ** (§)	kN lb	216 48,600	200 45,000	202 45,450	208 46,800	193 43,425	195 43,875
Operating Weight * (§)	kg lb	23 520 51,862	23 672 52,197	23 532 51,888	23 576 51,985	23 728 52,320	23 588 52,012

Annexure B (contd …)

Dimensions

All dimensions are approximate.

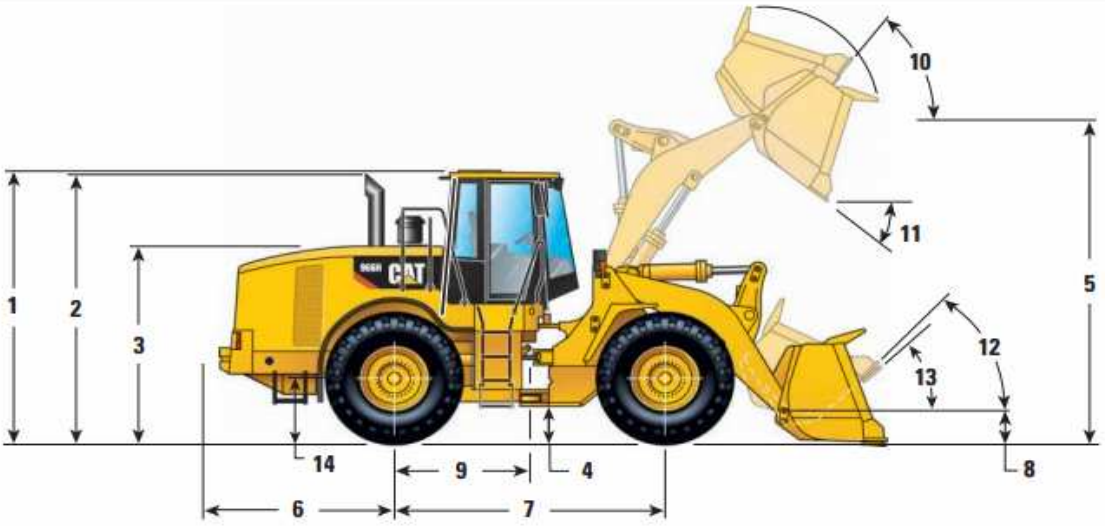

1	Height to top of ROPS	3600 mm (11'10")
2	Height to top of exhaust pipe	3552 mm (11'8")
3	Height to top of hood	2678 mm (8'9")
4	Ground clearance with 26.5R25 L-4 Firestone (see tire chart for other tires)	496 mm (1'8")
5	B-Pin height	4224 mm (13'10")
6	Center line of rear axle to edge of counterweight	2461 mm (8'1")
7	Wheelbase	3450 mm (11'4")
8	B-Pin height @ carry	507 mm (1'8")
9	Center line of rear axle to hitch	1725 mm (5'8")
10	Rack back @ maximum lift	60.8
11	Dump angle @ maximum lift	45
12	Rack back @ carry	47.4
13	Rack back @ ground	41.8
14	Height to center line of axle	815 mm (2'8")

Courtesy : Caterpillar Inc.

ANNEXURE C - FLYBRID SPECS

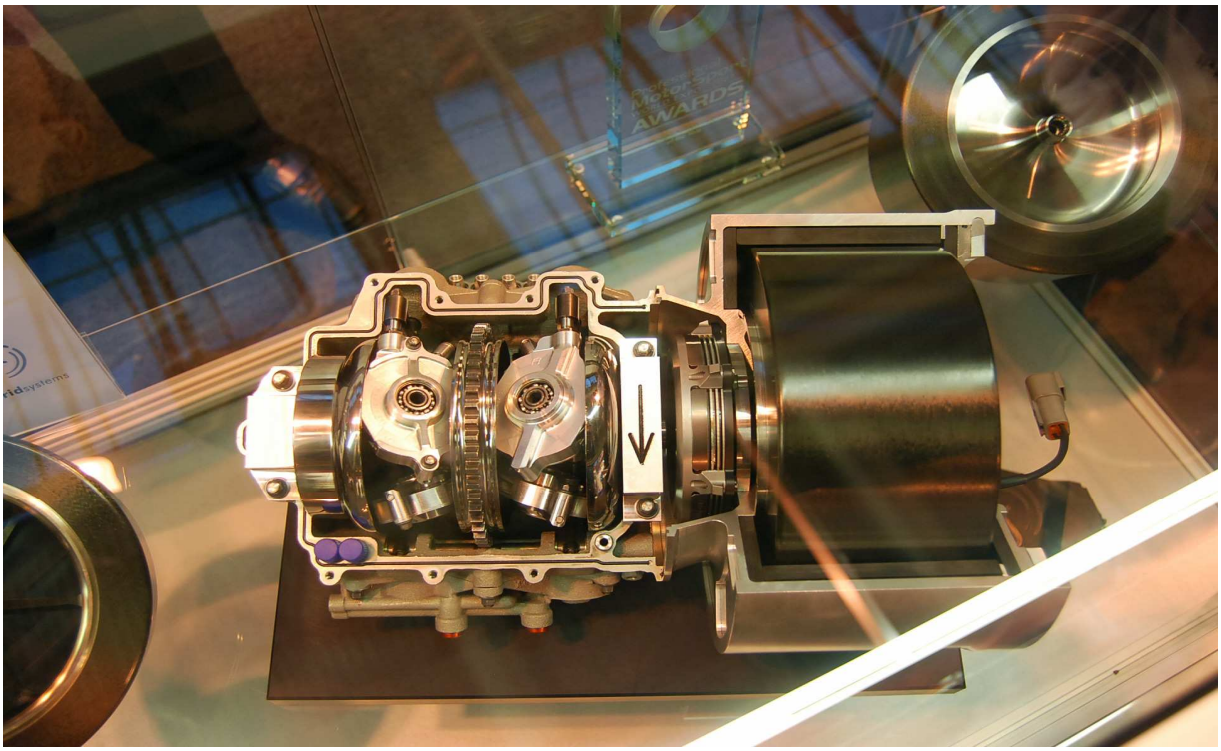

Flybrid KERS System - Crossection

The Flybrid System

Motorsport System Proposal

flybridsystems

• Power	60 kW
• Storage	480 kJ usable
• Life	20,000 km between rebuilds
• Weight	28 kg complete
• Volume	15 litres
• Efficiency	70% round trip
• Heat rejection	3kW
• Flywheel specification	5 kg @ 65,000 RPM
• Control system	Flybrid KCU with CAN link

Flybrid KERS System specs

Courtesy : Flybrid Systems LLP.

VITA

PERSONAL INFORMATION

Full name: Aloke J Mascarenhas

E-mail address: alokejm@gmail.com

ACADEMIC BACKGROUND

Master of Science: University of Illinois at Chicago, 2012

Bachelors of Engineering: Vishveshvaraya Technological University, 2007

ACAMDEMIC/RESEARCH EXPERIENCE

Teaching Assistant: University of Illinois at Chicago, 2011

PROFESSIONAL BACKGROUND

Oilgear Towler Polyhydron Ltd.: Intern, Belgaum, India 2006-2007

Cipla Ltd: Maintenance Engineer, Goa, India 2007

OMP Components Pvt. Ltd.: Product design and development Engineer, Goa, India 2007-2010

LANGUAGES

English, French, Hindi